

**DEVELOPMENT OF MODELS FOR SERIES AND PARALLEL
FAN VARIABLE AIR VOLUME TERMINAL UNITS**

A Thesis

by

JAMES C. FURR JR.

Submitted to the Office of Graduate Studies of
Texas A&M University
in partial fulfillment of the requirements for the degree of

MASTER OF SCIENCE

May 2006

Major Subject: Mechanical Engineering

**DEVELOPMENT OF MODELS FOR SERIES AND PARALLEL
FAN VARIABLE AIR VOLUME TERMINAL UNITS**

A Thesis

by

JAMES C. FURR JR.

Submitted to the Office of Graduate Studies of
Texas A&M University
in partial fulfillment of the requirements for the degree of

MASTER OF SCIENCE

Approved by:

Chair of Committee,
Committee Members,

Head of Department,

Dennis O'Neal
John Bryant
Warren Heffington
Dennis O'Neal

May 2006

Major Subject: Mechanical Engineering

ABSTRACT

Development of Models for Series and Parallel Fan
Variable Air Volume Terminal Units. (May 2006)
James C. Furr Jr., B.S., Texas A&M University
Chair of Advisory Committee: Dr. Dennis O'Neal

Empirical models of airflow output and power consumption were developed for series and parallel fan powered variable air volume terminal units at typical design pressure conditions. A testing procedure and experimental setup were developed to test sets of terminal units from three different manufacturers. Each set consisted of two series and two parallel units, each with 8 in. (203 mm) and 12 in. (304 mm) primary air inlets, for a total of four units in each set. Generalized models were developed for the series and parallel units, with coefficients varying by size and manufacturer. Statistical modeling utilized SAS software (2002).

Fan power and airflow data were collected at downstream static pressures over a range from 0.1 to 0.5 in. w.g. (25 to 125 Pa) for the parallel terminal units. Downstream static pressure was held constant at 0.25 in. w.g. (62 Pa) for the series units. Upstream static pressures of all variable air volume (VAV) terminal units ranged from 0.1 to 2.0 in. w.g. (25 to 498 Pa). Data were collected at four different primary air damper positions. Data were also collected at four different terminal unit fan speeds, controlled by a silicon controlled rectifier (SCR). The models utilized the RMS voltage entering the terminal unit fan, the 'rake' sensor velocity pressure, and the downstream static pressure. In addition to the terminal unit airflow and power models, a model was developed to quantify air leakage in parallel terminal units, when the unit fan was off.

In all but two of the VAV terminal units, the resulting models of airflow and power had R^2 values greater than 0.90. In the two exceptions, there appeared to be manufacturing defects: either excessive air leakage or a faulty SCR that limited the effectiveness of the airflow and power models to capture the variation in the data.

ACKNOWLEDGMENTS

This work was a part of a project funded by ASHRAE. I would like to thank this group for their financial support.

I would like to thank my advisor, Dr. Dennis O’Neal, and committee members, Dr. John Bryant and Dr. Warren Heffington. Dr. O’Neal has provided valuable guidance on this research and given me academic and career advice since before I started graduate school. Dr. Bryant provided advice during the course of my experimentation and Dr. Heffington also generously agreed to serve on my committee.

I would like to thank Mike Davis and Kelly Milligan at the Energy Systems Lab. Their advice was very helpful while I was working through technical difficulties in constructing some of the test apparatus. Aaron Hervey provided assistance during the testing of the terminal units. Having an extra pair of hands when installing a terminal unit into the test setup was quite ‘handy.’

Last of all, I send my heartfelt appreciation and love to my Mom and Dad. It would have been impossible to reach the achievements that I have, without their unfaltering encouragement and support. Thank you.

TABLE OF CONTENTS

	Page
ABSTRACT.....	iii
ACKNOWLEDGMENTS.....	iv
TABLE OF CONTENTS.....	v
LIST OF TABLES	vii
LIST OF FIGURES.....	viii
NOMENCLATURE.....	xi
CHAPTER	
I INTRODUCTION.....	1
II LITERATURE REVIEW	9
III EXPERIMENTAL APPARATUS.....	13
3.1 VAV Fan Powered Terminal Units.....	13
3.2 Airflow Measurement	20
3.3 Power Measurement.....	27
3.4 Data Acquisition System.....	28
IV EXPERIMENTAL PROCEDURE	29
4.1 Method of Experimentation	29
4.2 Method of Statistical Analysis	32
V RESULTS AND MODELS FOR PARALLEL FAN POWERED VAV	
TERMINAL UNITS	35
5.1 Parallel Terminal Unit Leakage Model.....	36
5.2 Parallel Terminal Unit Airflow Model.....	43
5.3 Parallel Terminal Unit Fan Power Model	51
VI RESULTS AND MODELS FOR SERIES FAN POWERED VAV	
TERMINAL UNITS	55
6.1 Series Terminal Unit Airflow Model	55
6.2 Series Power Model	61
VII SUMMARY AND CONCLUSIONS.....	65
REFERENCES.....	69

	Page
APPENDIX A: EXPERIMENTAL DATA AND ANALYSIS.....	71
A.1 Parallel Fan Terminal Units	71
A.2 Series Fan Terminal Units.....	78
APPENDIX B: FAN PULSATION PROBLEM	85
APPENDIX C: CONVERSION OF PRIMARY AIR TO RAKE PRESSURE	88
APPENDIX D: VERIFICATION ON TEST APPARATUS	90
VITA.	91

LIST OF TABLES

	Page
Table 3-1: General Specifications for Terminal Units	14
Table 3-2: Specifications of Series Terminal Units	19
Table 3-3: Specifications of Parallel Terminal Units	20
Table 3-4: Pressure Transducer Sizing.....	23
Table 4-1: Test Variable Levels	31
Table 5-1: Model Coefficients for Parallel Leakage Model.....	43
Table 5-2: Model Coefficients for Parallel Terminal Unit Airflow Model, for terminal units with gravity-operated backdraft damper.....	50
Table 5-3: Model Coefficients for Parallel Terminal Unit Airflow Model, for terminal units with primary air-operated backdraft damper	50
Table 5-4: Model Coefficients for Parallel Terminal Unit Fan Power Model	54
Table 6-1: Airflow Model Coefficients for Series Terminal Units	60
Table 6-2: Airflow Model Coefficients for Series Terminal Unit S12B.....	61
Table 6-3: Model Coefficients for Series Fan Power Model	64
Table C-1: Coefficients for Rake Sensor Approximation.....	89

LIST OF FIGURES

	Page
Figure 1-1: A Typical Variable Air Volume System (adapted from Chen and Demster 1996)	2
Figure 1-2: Series VAV Fan Powered Terminal Unit.....	4
Figure 1-3: Parallel VAV Fan Powered Terminal Unit	5
Figure 1-4: Idealized Voltage Sine Wave Resulting from SCR Operation.....	6
Figure 3-1: Example of (a) Butterfly Damper and (b) Opposing-Blade Damper	14
Figure 3-2: Terminal Unit with Gravity Operated Backdraft Damper.....	15
Figure 3-3: Terminal Unit with Air-Operated Backdraft Damper	16
Figure 3-4: Schematic of Group A Parallel Terminal Units, plan view.....	17
Figure 3-5: Schematic of Group B Parallel Terminal Units, plan view	17
Figure 3-6: Schematic of Group C Parallel Terminal Units, plan view	18
Figure 3-7: Schematic of Groups A and B Series Terminal Units, plan view	18
Figure 3-8: Schematic of Group C Series Terminal Units, plan view	19
Figure 3-9: Schematic of Experimental Test Setup	21
Figure 3-10: Schematic of Low Pass Filter	24
Figure 3-11: Example of a Typical Pressure Signal (a)Before and (b)After Low-Pass Filter.....	25
Figure 3-12: Volumetric Balance of Terminal Unit.....	26
Figure 3-13: Schematic of Voltage Divider Circuit	27
Figure 5-1: Typical Parallel VAV Fan Powered Terminal Unit	36
Figure 5-2: Parallel Terminal Unit with Air-Operated Backdraft Damper	37
Figure 5-3: Parallel Terminal Unit with Gravity Operated Backdraft Damper	38
Figure 5-4: Schematic of Group A Parallel Terminal Units, plan view.....	38
Figure 5-5: Schematic of Group C Parallel Terminal Units, plan view	39
Figure 5-6: Schematic of Group B Parallel Terminal Units, plan view	39
Figure 5-7: Air Leakage for 8 in. (203 mm) Inlet Parallel Terminal Units.....	40

Figure 5-8: Air Leakage for 12 in. (304 mm) Inlet Parallel Terminal Units.....	40
Figure 5-9: Residuals Plot for Parallel Terminal Unit P8C	42
Figure 5-10: Effect of SCR Voltage on Fan RPM for Parallel Terminal Unit P8A	45
Figure 5-11: Effect of SCR Voltage on Fan RPM for Parallel Terminal Unit P12B.....	46
Figure 5-12: Fan Airflow for Parallel Terminal Unit P8B.....	47
Figure 5-13: Fan Airflow for Parallel Terminal Unit P8A.....	48
Figure 5-14: Fan Airflow for Parallel Terminal Unit P12A.....	48
Figure 5-15: Fan Power for Parallel Terminal Unit P12A	52
Figure 5-16: Fan Power for Parallel Terminal Unit P8A	53
Figure 6-1: Typical Series VAV Fan Powered Terminal Unit.....	56
Figure 6-2: Fan Airflow for Series Terminal Unit S12C	58
Figure 6-3: Fan Airflow for Series Terminal Unit S12B	59
Figure 6-4: Fan Power for Series Terminal Unit S8A	62
Figure 6-5: Fan Power for Series Terminal Unit S12B.....	63
Figure A-1: Residuals Plot for Parallel Terminal Unit P8B.....	71
Figure A-2: Fan Airflow for Parallel Terminal Unit P8A.....	72
Figure A-3: Fan Airflow for Parallel Terminal Unit P12A.....	72
Figure A-4: Fan Airflow for Parallel Terminal Unit P8B	73
Figure A-5: Fan Airflow for Parallel Terminal Unit P12B.....	73
Figure A-6: Fan Airflow for Parallel Terminal Unit P8C.....	74
Figure A-7: Fan Airflow for Parallel Terminal Unit P12C.....	74
Figure A-8: Fan Power for Parallel Terminal Unit P8A	75
Figure A-9: Fan Power for Parallel Terminal Unit P12A	75
Figure A-10: Fan Power for Parallel Terminal Unit P8B	76
Figure A-11: Fan Power for Parallel Terminal Unit P12B	76
Figure A-12: Fan Power for Parallel Terminal Unit P8C	77
Figure A-13: Fan Power for Parallel Terminal Unit P12C	77
Figure A-14: Fan Airflow for Series Terminal Unit S8A	78
Figure A-15: Fan Airflow for Series Terminal Unit S12A	79

Figure A-16: Fan Airflow for Series Terminal Unit S8B	79
Figure A-17: Fan Airflow for Series Terminal Unit S12B	80
Figure A-18: Fan Airflow for Series Terminal Unit S8C	80
Figure A-19: Fan Airflow for Series Terminal Unit S12C	81
Figure A-20: Fan Power for Series Terminal Unit S8A.....	81
Figure A-21: Fan Power for Series Terminal Unit S12A.....	82
Figure A-22: Fan Power for Series Terminal Unit S8B.....	82
Figure A-23: Fan Power for Series Terminal Unit S12B.....	83
Figure A-24: Fan Power for Series Terminal Unit S8C.....	83
Figure A-25: Fan Power for Series Terminal Unit S12C.....	84
Figure B-1: Downstream Static Pressure During Pressure Fluctuations.....	86
Figure B-2: Fan Motor Speed During Pressure Fluctuations	86
Figure C-1: Linear Approximation between Primary Airflow and Rake Pressure	88

NOMENCLATURE

AHU	Air Handling Unit
C	Capacitance
CAV	Constant Air Volume
DAQ	Data Acquisition
f	frequency of pressure fluctuations
f_B	half-power frequency
$ H(f) $	Magnitude of output signal from low pass filter
HVAC	Heating, Ventilation, & Air Conditioning
I_{RMS}	RMS value of current
P_{down}	Downstream static pressure
P_{rake}	Pressure across ‘rake’ flow sensor
P_{unit}	Static pressure inside terminal unit
P_{up}	Upstream static pressure
$Power_{fan}$	Power consumption of terminal unit fan
Q_{fan}	Amount of airflow through terminal unit fan
$Q_{induced}$	Amount of airflow induced from plenum
$Q_{leakage}$	Amount of airflow leaking from a terminal unit
Q_{out}	Amount of parallel terminal unit airflow output
$Q_{primary}$	Amount of primary airflow
R	Resistance
RMS	Root Mean Square
SCR.....	Silicon Controlled Rectifier
V	RMS average of SCR voltage output; used as an independent variable in models
V_{DAQ}	Voltage entering DAQ card
V_{fan}	Voltage entering terminal unit fan

V_{RMS}	RMS value of voltage
VAV.....	Variable Air Volume
VSD	Variable Speed Drive

CHAPTER I

INTRODUCTION

The 1970's energy crisis changed the way Americans thought about oil, the environment, and energy conservation. This period led to the birth of several energy efficiency improvements, one of these being variable air volume (VAV) air distribution systems. It has become quite popular for commercial and institutional applications, and is widely accepted for maintaining occupant comfort and reducing energy use (Chen and Demster 1996).

VAV systems maintain comfort conditions by varying the volume of air that is delivered to a space. In contrast, a constant air volume (CAV) system maintains comfort conditions by changing the temperature of a constant amount of air being supplied to a zone. A VAV system (Figure 1-1) will often consist of a central air handling unit (AHU), where air is cooled to 55 °F (13 °C) by cooling coils (Wendes 1994). This air, referred to as primary air, is sent through a single-duct supply system to VAV terminal units by the supply fan. Each terminal unit is ducted to supply diffusers, usually serving two or more offices or an open area.

There is a variety of styles for VAV terminal units. The simplest terminal units are not much more than a box with a damper to vary the amount of primary air supplied to the zone. More complex styles include terminal units that have a port to induce plenum air and mix it with the primary airstream, and units with fans to improve zone circulation. A single AHU is often ducted to a system of VAV terminals of the same type, but some designs may require a mixed system (Wendes 1994).

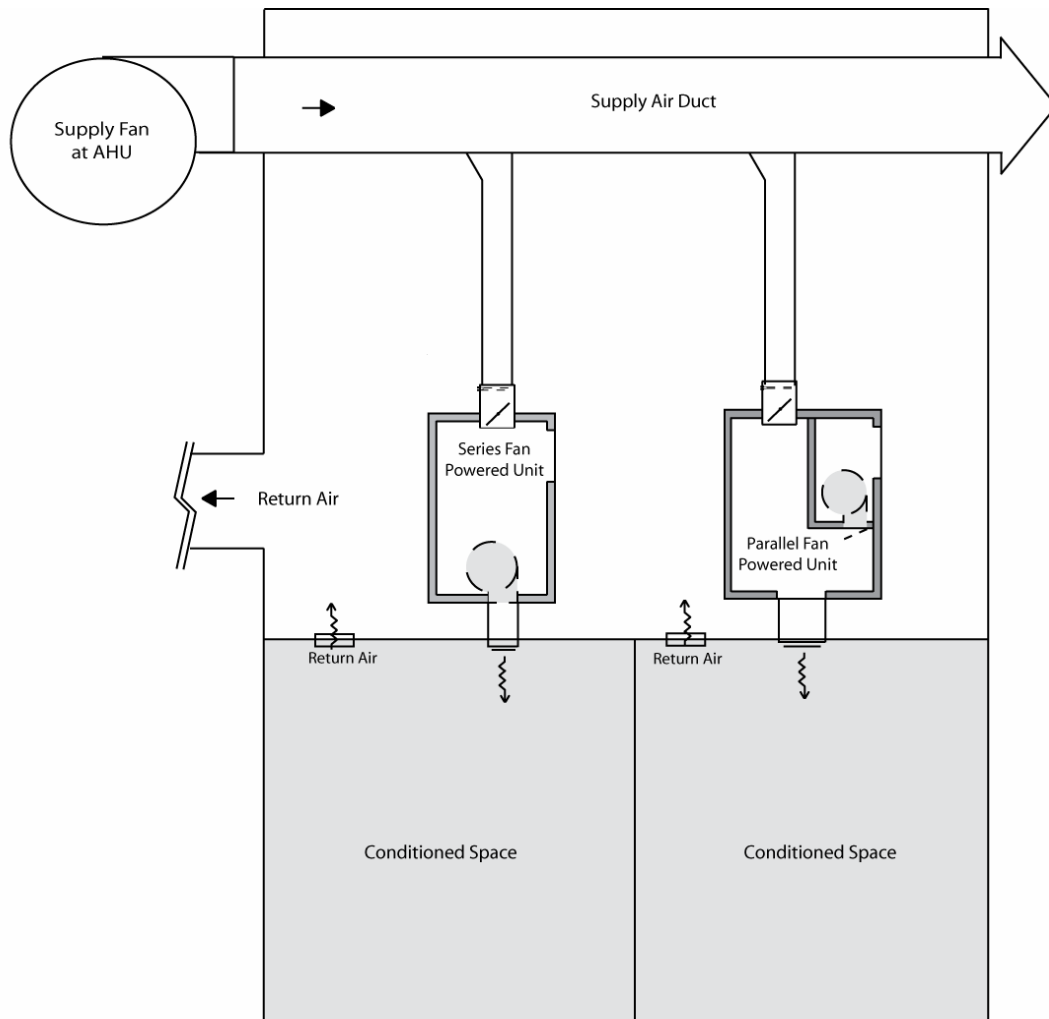


Figure 1-1: A Typical Variable Air Volume System (adapted from Chen and Demster 1996)

All VAV terminal units are equipped with controllers that adjust the unit's damper to augment the amount of cool primary air being delivered to a space in response to a signal from a room thermostat. However, it is possible for changes in the system supply static pressure to affect the amount of air traveling past the terminal unit damper, resulting in control instability. To solve this problem, some units include an air velocity sensor placed within the primary airstream, allowing the controller to maintain a consistent volume of airflow to the zone depending on the temperature setpoint. The

style of this 'rake' sensor is quite similar among manufacturers of VAV units. They are designed to take a multiple point average of velocity pressures across the primary air inlet. Pneumatic lines transmit this pressure from the sensor to a pressure transducer at the controller on the terminal unit.

VAV terminal units that include a fan to improve circulation within a zone are called fan powered terminal units. These terminal units can draw in warm air from the plenum space and mix it with primary air from the central AHU. This process is considered energy efficient because it takes advantage of the warmer plenum air, instead of relying on hot water or electric reheat, for heating needs (Wendes 1994).

There are two configurations for fan powered terminal units. The fan can be in the path of the primary airflow and will always be on (Figure 1-2). This configuration is a series terminal unit. The controller will modulate the terminal unit damper in response to the control signals from the thermostat and air velocity sensor. The fans on these terminal units output a constant amount of air that does not vary with load because the downstream pressure is constant (Alexander and Int-Hout 1998). As a result, when the primary air damper closes, more plenum air is induced and recirculated into the space. When the signal from the air velocity sensor indicates that the primary airflow has reached a predetermined minimum (because of ventilation requirements), the damper will not close any more. If the space is still too cold, electric or hot water reheat can be used to meet the thermostat setpoint.

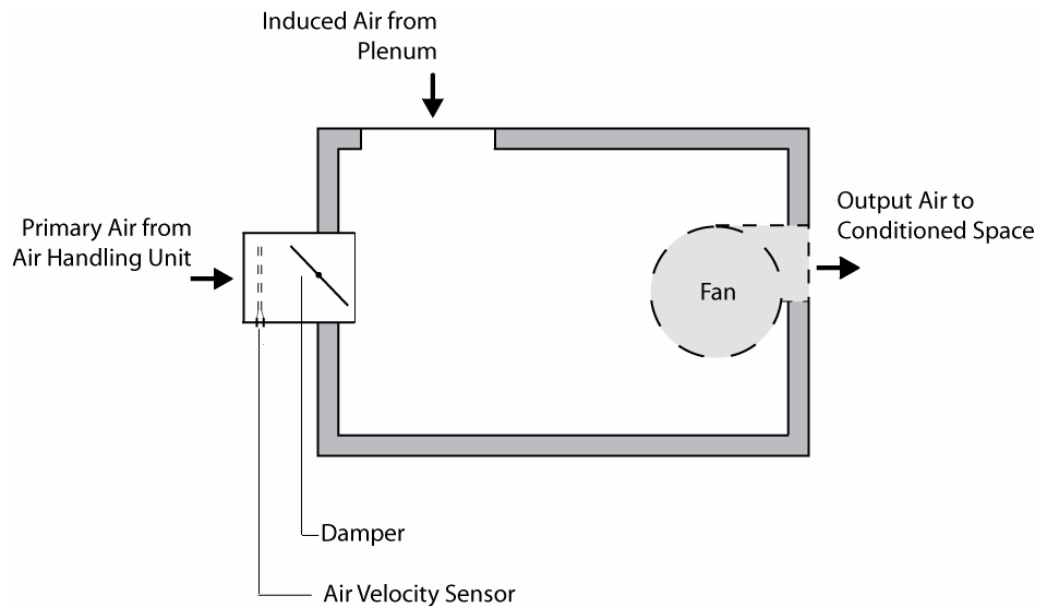


Figure 1-2: Series VAV Fan Powered Terminal Unit

When the fan is outside the primary airflow, the configuration is called a parallel terminal unit (Figure 1-3). The fan for a parallel terminal unit cycles on and off. During periods of maximum cooling, the fan is off. A backdraft damper prevents cold air from blowing backwards through the fan. The terminal unit damper modulates the airflow to maintain the temperature setpoint. When the primary airflow drops below a specific amount, the controller turns on the fan. At this point, the terminal unit mixes primary air with air being drawn in from the plenum. Depending on the control scheme, the controller can continue to reduce primary air to the conditioned space by adjusting the damper. Electric or hot water reheat can also be used in this instance.

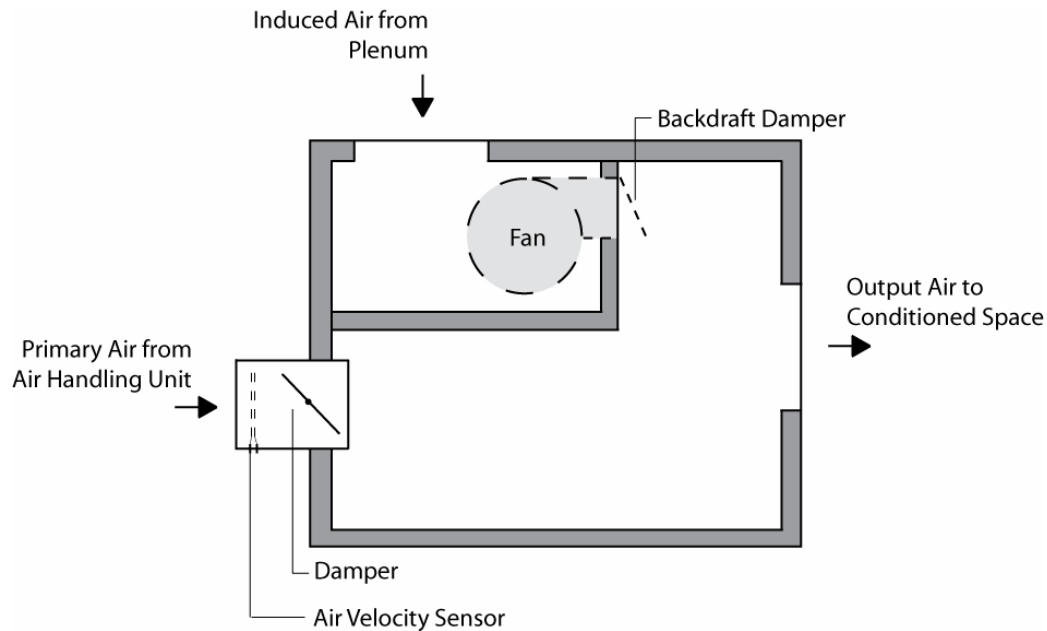


Figure 1-3: Parallel VAV Fan Powered Terminal Unit

In the field, the fan on a VAV terminal unit often must be fine tuned, referred to as test & balancing, to alter the airflow output for the specific space's needs. For these cases, the fan in both series and parallel fan powered terminal units is equipped with a speed controller known as a silicon-controlled rectifier (SCR). This device utilizes a triac, a semiconductor electronic circuit, to alter the input AC voltage going to the fan motor. After the voltage sine wave crosses zero the SCR holds the voltage off the motor for a specified time (Figure 1-4). The triac then turns on, allowing the voltage to pass. The process continues at the other zero crossing. This process chops the sine wave twice every period and slows the motor speed. The amount of time that the SCR holds the voltage is determined by a setscrew located on the SCR. For a typical unit in the field, this SCR would be adjusted only once as the VAV system was being initially balanced and then would not change.

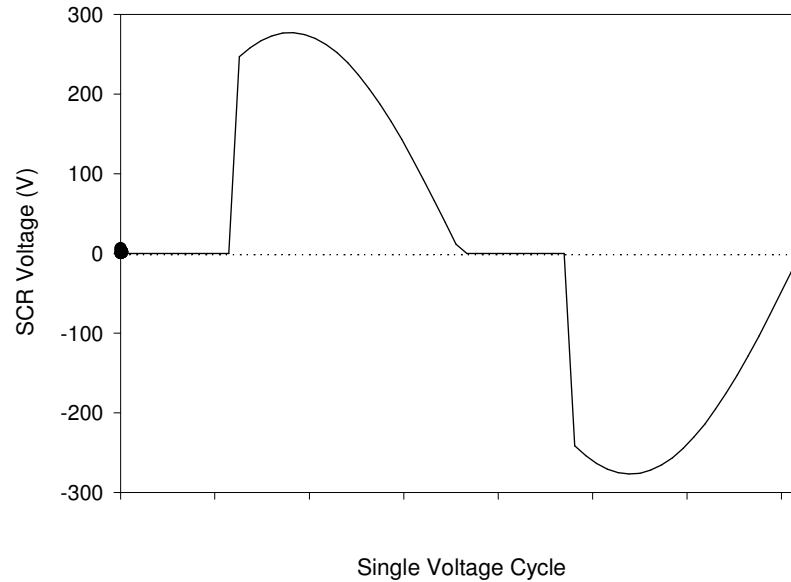


Figure 1-4: Idealized Voltage Sine Wave Resulting from SCR Operation

Several authors, from both academic and industry settings, believe that from an energy standpoint the parallel units are more energy efficient than the series because the series fan does not cycle like the parallel does (Wendes 1994, Chen and Demster 1996, Elleson 1993). This thinking has influenced current energy codes and shows a preference for parallel over series terminal units. For example, when following the energy cost budget method in ASHRAE Standard 90.1(2004), parallel fan powered terminal units are prescribed to be used for VAV systems. Series terminal units are not mentioned. In design guidelines published by the California Energy Commission, Hydeman et al. (2003) states that “series fan powered terminal units should be avoided, with the exception of a few specific applications...” These conclusions are supported with reference to the low combined efficiencies of the small terminal unit fans and motors. However, the standard treats the energy use of the terminal units separately from the supply fans rather than treating them as a system. Although the fans on series VAV terminal units are in constant operation, there is potential for energy savings

because the static pressure of the supply fan can be set lower than with parallel terminal unit systems.

Alexander and Int-Hout (1998) point out that series terminal units “have significantly lower inlet static pressure requirements than conventional VAV systems.” A configuration with all series terminal units allows the main air handling unit to maintain a lower static pressure upstream of the terminal units, allowing energy savings at the main supply fan. The lower supply static pressure also reduces the amount of duct leakage. A parallel system in heating mode requires that the main supply fan maintain a higher duct static pressure to prevent air from the parallel terminal units from blowing backwards through the ductwork. This additional energy must be considered when comparing parallel and series systems.

Some of the literature reviewed indicated that despite the requirement for higher supply static pressure, parallel systems are still more energy efficient than series systems. Elleson (1993) and Kolderup et al. (2003) used computer simulations to compare energy use between the two fan powered systems. Both studies showed parallel systems using less energy than series systems. However, their computer simulations’ approximations of fan powered terminal units did not properly account for the effects of all of the variables acting on the terminal unit. The deficiencies in these analyses are discussed in Chapter II.

The terminal unit fan performance is the primary factor influencing the air output and power consumption of the unit. However, the position of the primary air damper, the box geometry, the SCR setting, and the style and location of the parallel backdraft damper are variables that previous computer simulations did not consider. Empirical models can be used to accurately characterize these variables. Little literature was found on the development of empirical models of VAV terminal units. Khoo et al. (1998) developed some models for simple VAV terminal units without fans. However, there has not been any work in the development of characterizations for individual fan powered terminal units.

The primary goal for this research was the development of empirical models of energy consumption and airflow output for series and parallel fan powered terminal units at typical design pressure conditions. An experimental setup was developed and used to test fan powered terminal units from three manufacturers. An experimental protocol was developed and used for all tests. Statistical analyses of experimental data were performed and used to develop generalized models that can be applied to different manufacturers' terminal units. The empirical models were developed for a variety of manufacturers and sizes, for both series and parallel units to obtain representative sample of VAV terminal units in the field. In addition to the models of airflow output and energy consumption, a model was developed to characterize the air leakage that occurred in the parallel terminal units when unit fan was off.

This research helped characterize the performance of both parallel and series fan terminal units. The models resulting from this study of the individual terminal units can be combined to model a VAV system, to compare energy use of systems with the two styles of VAV terminal units.

This thesis has seven chapters. Chapter II is a review of applicable research literature, concerning VAV systems and fan powered units. Chapters III and IV provide details of the experimental apparatus and procedure. Chapters V and VI provide the results of the experimentation and statistical modeling for the parallel and series terminal units, respectively. Chapter VII summarizes the results and presents conclusions from this research study. A complete set of results are presented in the appendices.

CHAPTER II

LITERATURE REVIEW

It has been widely accepted in the HVAC industry that VAV systems are an energy efficient method for providing air conditioning in commercial and institutional buildings. During the years that VAV systems began to gain popularity, Inoue and Matsumoto (1979) concluded that a VAV system could reduce supply fan power consumption by 40% compared to a dual duct constant air volume (CAV) or a terminal reheat CAV system. These conclusions were based on computer simulations in HASP/ACLD 7101 (1971), a Japanese nationally developed HVAC simulation tool, and confirmed by a field study on a building in Tokyo.

Sekhar (1997) had similar conclusions based on a set of computer simulations on two buildings. Sekhar quantified energy savings for buildings located in a hot and humid environment. He concluded that between 10 and 20 % combined fan and cooling energy could be saved by employing a VAV system. However, in his study and that by Inoue and Matsumoto (1979), the VAV systems consisted of damper-only operated VAV terminal units and did not include fan powered terminal units. For any system that did utilize fan powered terminal units, some of the energy savings of a VAV system would be forfeited to the terminal fans.

Ardehali and Smith (1996) conducted a simulation that did make the comparison between CAV systems and VAV systems using fan powered terminal units. The simulation, utilizing the TRACE (1993) program, modeled a commercial building in Des Moines, Iowa. The building was selected to represent a 'typical' existing office building. The results of the simulations indicated that a fan powered VAV system could result in energy savings, providing a 40% reduction in utility costs compared to a CAV system.

All of these studies indicated that VAV systems were a significant improvement over CAV systems. Because they have been proven to be the most energy efficient

method for air distribution, the current challenge is to improve VAV systems. Proper application of parallel and series fan VAV systems has become an important issue in today's HVAC industry. The general disagreement concerning the energy differences between systems of these two VAV terminal units has led to several investigations into the overall power consumption of the two systems.

Elleson (1993) conducted a field study of cold air distribution systems with series and parallel fan powered mixing terminal units in two separate buildings. Cold air distribution systems use reduced temperature supply air, typically at 45 °F (7.2 °C), which requires less primary air delivered to conditioned space than a higher temperature system, resulting in supply fan energy savings. Field data were compared to the results from computer simulations of alternative air distribution systems for each building. Although the focus of the paper was to provide evidence supporting cold air distribution systems, the results from the simulations provided a comparison between series and parallel systems for both cold air and conventional air distribution systems. For both cold air and conventional systems, the results showed that the total fan power consumption, combining the power of the supply fan and terminal units' fans, was greater for series terminal unit systems. This conclusion was based from results of simulations on one of the two buildings studied. The simulations included a reduced supply static pressure for series units of 0.25 in. w.g. (62 Pa) less than the parallel units' design static pressure.

An energy study sponsored by the California Energy Commission included a comparison of parallel and series terminal units operating in perimeter zones (Kolderup et al. 2003). The study was based on running a simulation with DOE 2.2 (1998) and took into account the reduced static pressure of the main supply fan in series systems. The main supply fan static pressure was reduced from 4.0 to 3.67 in. w.g. (996 to 914 Pa) for the series systems. The findings concluded that, for the case studied, a parallel system would have 9% less energy costs than a series system. The bulk of the energy savings was in the difference in total power consumption of the fans. The explanation given for the energy difference was that since the series fans were in constant operation,

and they were less efficient than the larger primary supply fan, a series system had greater energy consumption than a parallel system. However, the study only simulated a single building in California. A building located in a cooler climate could expect larger reheat requirements, in which the parallel terminal unit fans would be required to operate longer hours, and use more energy.

The studies by Elleson (1993) and Kolderup et al. (2003) use the built-in functions of their HVAC simulation software to model the fan powered terminal units. These built-in functions approximate the terminal units, ignoring some variables (U.S. Department of Energy 1982). The effect of the SCR on power consumption is ignored. Other design differences, such as the type of primary air or backdraft dampers are also not included. As a result, these built in functions do not fully describe the characteristics of typical fan powered terminal units.

There is no experimental evidence to support the computer simulations by Elleson (1993) and Kolderup et al. (2003) who claim that parallel VAV systems are more energy efficient than a series system. There is a need to develop a better understanding of systems using parallel and series fan powered VAV terminal units. To model the system properly, it is important to be able to characterize the individual units. To date, there has been little work in this area. Khoo et al. (1998) developed non-linear models for three VAV terminal units. They focused on standard VAV terminal units without fans. The empirical models approximated the pressure drop across the entire unit as a function of damper position. Because of the non-linear relationship between pressure drop and the position of the damper, logarithmic functions were used to express this relationship. This study concluded that the damper-only approximations of VAV terminal units used in some HVAC simulation packages were not accurate representations of VAV terminal units. The work by Khoo et al. (1998) was the only research found on modeling VAV terminal units.

The literature review indicated that the development of models for fan powered terminal units is an area that has not been thoroughly investigated. These empirical

models could allow for a better understanding of the system operation and, in the end, allow for energy conscious decisions to be made in implementing these systems.

CHAPTER III

EXPERIMENTAL APPARATUS

The primary goal of this research was to develop an empirical model for energy consumption and airflow output for series and parallel fan powered VAV terminal units. This goal was achieved in two phases: the acquisition of experimental data, and the statistical analysis to develop the models. This section describes the experimental apparatus, which included the VAV terminal units, the equipment to measure airflow, the equipment to measure power, and the data acquisition system.

3.1 VAV FAN POWERED TERMINAL UNITS

A set of fan powered terminal units was obtained from three manufacturers. These sets consisted of series and parallel units, each with 8 in. (203 mm) and 12 in. (304 mm) primary air inlets, resulting in a total of four units from each manufacturer. These terminal units provided a ‘snapshot’ of fan powered terminal units typically installed in the field.

A naming convention of groups A, B, and C was used to differentiate between the three manufacturers. Units were identified as S (series) or P (parallel), followed by the inlet size in inches, and then the manufacturer identification. For example, the 8 in. (203 mm) series terminal unit from manufacturer B was terminal unit S8B.

The terminal units were selected so that the units in one set would be similar in airflow output to those in the other two sets. Specifications were given to the manufacturers to meet this criterion (Table 3-1). All of the unit fans were powered with single phase, 277 AC voltage. However, there were small differences between the terminal units. These included the rated power of the terminal unit fan, the style of the primary airflow damper, and the style of the backdraft damper. These differences in the box design resulted in different unit performances across the three manufacturers.

Table 3-1: General Specifications for Terminal Units

Terminal Unit	Maximum Fan Airflow CFM (m ³ /s)	Maximum Terminal Unit Output CFM (m ³ /s)
8 in. (203 mm) Series	700 (0.330)	700 (0.330)
12 in. (304 mm) Series	1500 (0.708)	1500(0.708)
8 in. (203 mm) Parallel	500 (0.236)	700 (0.330)
12 in. (304 mm) Parallel	1050 (0.496)	1500 (0.708)

In the series terminal units the primary air inlet had a butterfly damper, with a single rotated blade, or an opposing-blade style, where two blades operated in unison (Figure 3-1). Series group C used the opposing-blade dampers. Series groups A and B were equipped with butterfly dampers. In all of the parallel units, the butterfly style primary air damper was used.

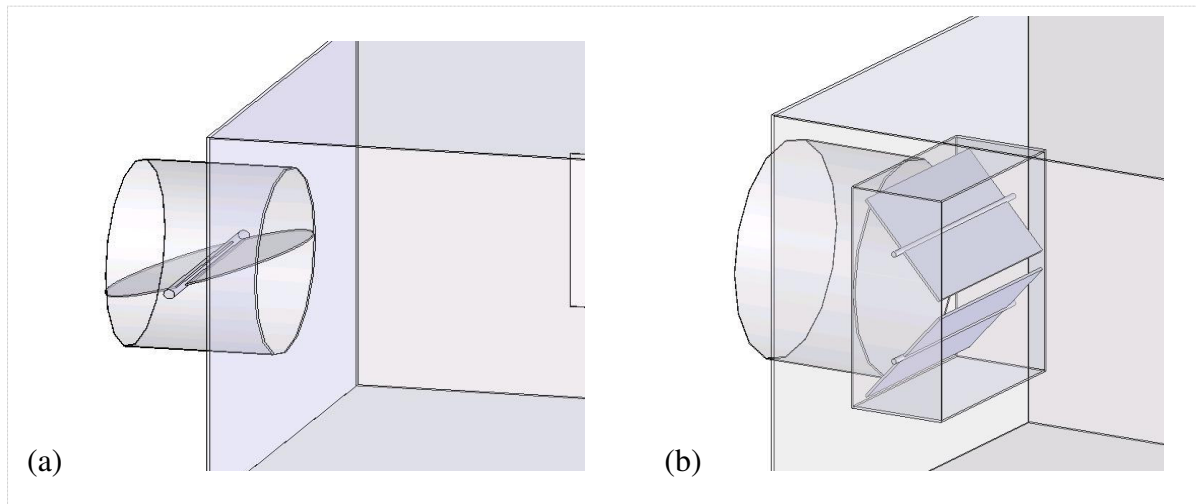


Figure 3-1: Example of (a) Butterfly Damper and (b) Opposing-Blade Damper

A major difference between the parallel terminal units was the style of the backdraft damper used. Parallel groups B and C used a gravity-operated damper (Figure 3-2). During cooling mode, when the fan was off, the damper naturally closed. Approximately 1/8 in. (3.18 mm) thick foam along the edges of the damper formed a loose seal when it closed. The pressure inside the terminal unit would assist in pushing the damper closed against this foam. When the fan turned on, the damper opened due to the output pressure of the fan.

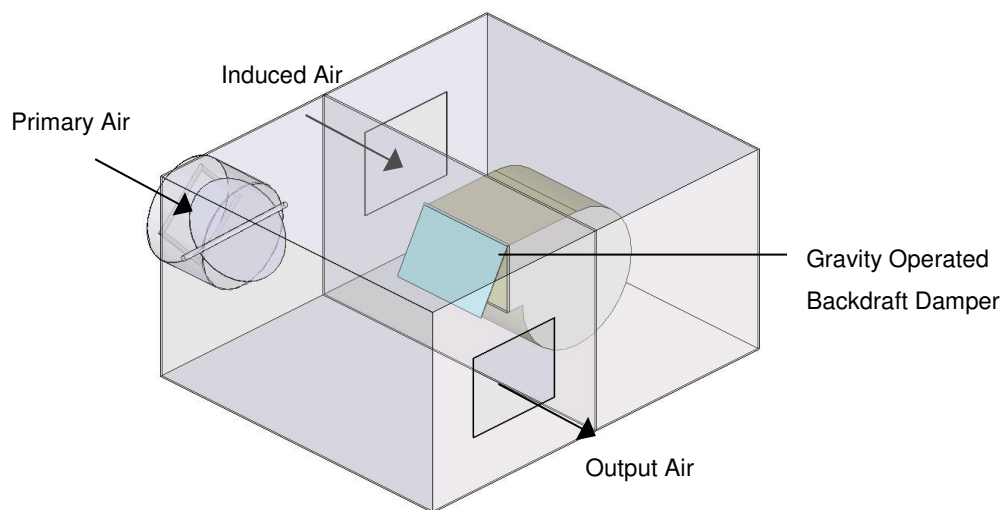


Figure 3-2: Terminal Unit with Gravity Operated Backdraft Damper

Parallel group A utilized a primary-air operated damper (Figure 3-3). An extension attached to the damper was in the primary airstream. When the fan was off during cooling mode, the primary air pushed against the damper extension to push the damper closed. When the fan turned on, the damper opened due to the output airflow of the fan. Unlike parallel groups B and C, the parallel terminal units from group A did not have the foam seal along the backdraft damper edges.

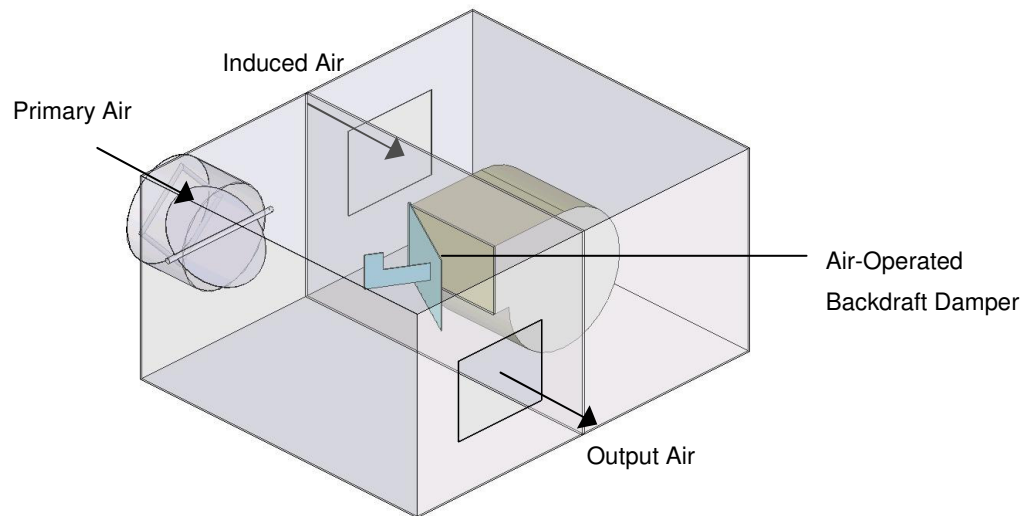


Figure 3-3: Terminal Unit with Air-Operated Backdraft Damper

Other significant differences among the parallel terminal units were the location of some box features, such as the plenum air inlet and the backdraft damper. Figure 3-4 through Figure 3-6 are schematics of the parallel units, showing these differences. Parallel groups A and C had backdraft dampers located in the primary airstream, as opposed to parallel group B, where the terminal unit fan was oriented facing the unit outlet. Parallel groups A and B had the induced air port located parallel to the primary inlet. In parallel group C, the induced air port was located on the side of the terminal unit.

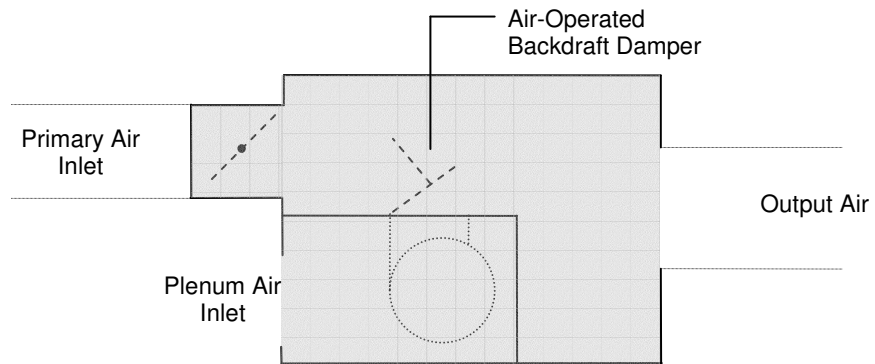


Figure 3-4: Schematic of Group A Parallel Terminal Units, plan view

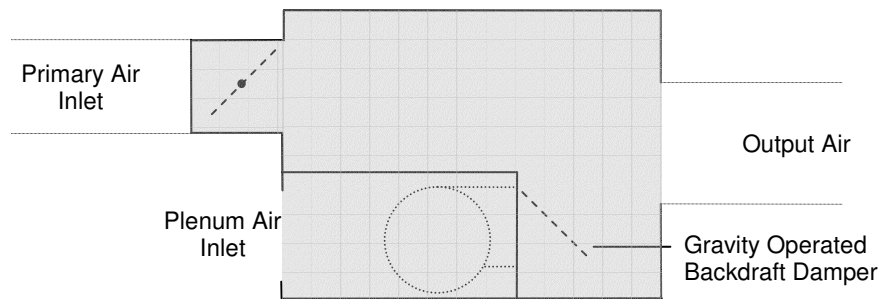


Figure 3-5: Schematic of Group B Parallel Terminal Units, plan view

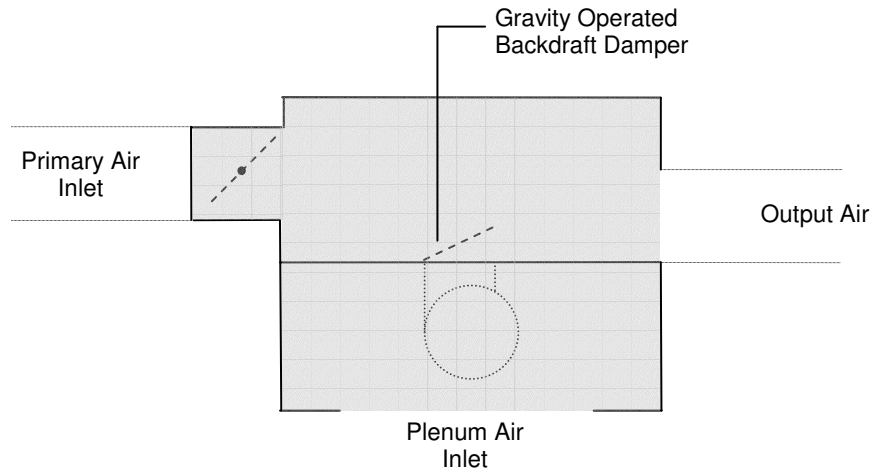


Figure 3-6: Schematic of Group C Parallel Terminal Units, plan view

Apart from the style of primary airflow damper, the design configuration difference among the series terminal units was the placement of the induced air inlet (Figure 3-7 and Figure 3-8). Series groups A and B were very similar in that the induced air port was parallel to the primary air port. Series group C had the induced air port located on the side of the box.



Figure 3-7: Schematic of Groups A and B Series Terminal Units, plan view

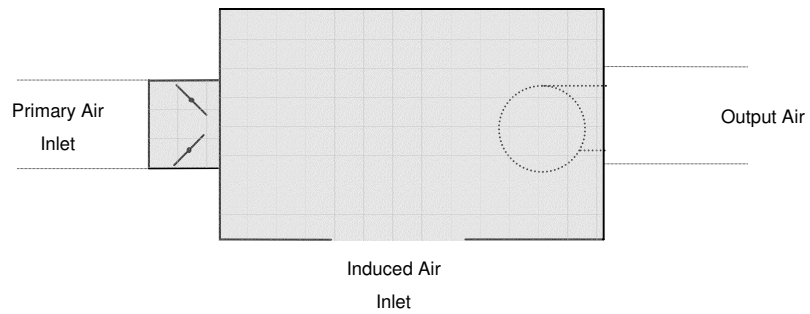


Figure 3-8: Schematic of Group C Series Terminal Units, plan view

Table 3-2 and Table 3-3 summarize the specifications for each of the series and parallel fan powered VAV units tested.

Table 3-2: Specifications of Series Terminal Units

Size	Terminal Unit	Fan Rated hp (W)	Primary Air Damper type	Location of Induced Air Port
8 in. (203 mm)	S8A	¼ (187)	Butterfly	Parallel to Primary Inlet
	S8B	¼ (187)	Butterfly	Parallel to Primary Inlet
	S8C	¼ (187)	Opposing Blade	Side
12 in. (304 mm)	S12A	½ (373)	Butterfly	Parallel to Primary Inlet
	S12B	⅓ (249)	Butterfly	Parallel to Primary Inlet
	S12C	½ (373)	Opposing Blade	Side

Table 3-3: Specifications of Parallel Terminal Units

Size	Terminal Unit	Fan Rated hp (W)	Primary Air Damper Type	Backdraft damper style	Location of Backdraft Damper
8 in. (203 mm)	P8A	$\frac{1}{10}$ (75)	Butterfly	Primary Airflow Operated	In primary airstream
	P8B	$\frac{1}{6}$ (124)	Butterfly	Gravity Operated	Out of primary airstream
	P8C	$\frac{1}{4}$ (187)	Butterfly	Gravity Operated	In primary airstream
12 in. (304 mm)	P12A	$\frac{1}{2}$ (373)	Butterfly	Primary Airflow Operated	In primary airstream
	P12B	$\frac{1}{4}$ (187)	Butterfly	Gravity Operated	Out of primary airstream
	P12C	$\frac{1}{2}$ (373)	Butterfly	Gravity Operated	In primary airstream

3.2 AIRFLOW MEASUREMENT

All experiments were conducted at the Riverside Campus facilities of the Energy Systems Laboratory at Texas A&M University. The experimental setup was located in an open, unconditioned area of the lab where the space temperature varied from 70 °F (24 °C) to 95 °F (35 °C), depending on the time of year. The relative humidity varied from 23% to 52%.

The experimental test setup (Figure 3-9) was constructed in accordance with the guidelines for testing fan powered terminal units as specified in ANSI/ASHRAE Standard 130 (1996). A 10 hp (7.5 kW) blower provided primary air to the terminal unit. A 7.5 hp (5.6 kW) assist blower was used to control the output static pressure of the terminal unit. Both blowers were controlled by variable speed drives (VSD's), allowing the upstream and downstream static pressures to be varied. For typical system installations in the field, VAV terminal units are supplied with primary air at 55 °F (13 °C). For this study, unconditioned lab air was used as the primary air. Unconditioned air was used because the research was primarily concerned with airflow and fan power consumption. The mixing of primary airflow and induced air was not analyzed.

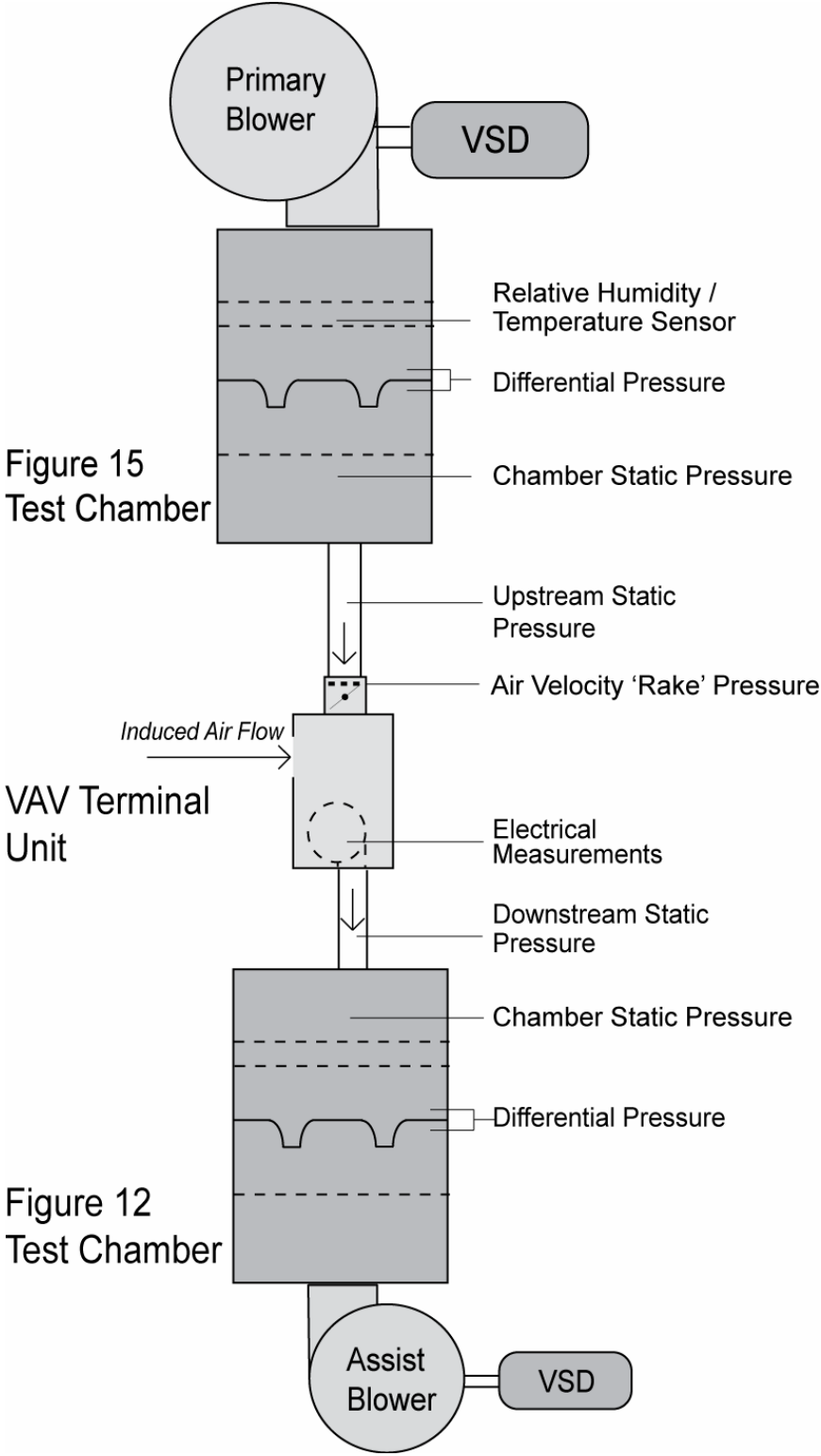


Figure 3-9: Schematic of Experimental Test Setup

During a test, air was drawn in by the primary blower and into the Figure 15 airflow test chamber¹. Here, the air temperature and relative humidity were measured and used to calculate air density. This humidity and temperature transmitter had an accuracy of $\pm 2\%$ RH and ± 0.7 °F (± 0.4 °C).

The air then went into the chamber through a set of flow nozzles. Static pressure was measured near the chamber exhaust. The differential pressure across the nozzles, chamber static pressure, and air density were used to determine the primary airflow rate.

The air from the airflow chamber was then ducted through a sheet metal round duct to the primary port on the VAV terminal unit being tested. The VAV unit mixed this air with induced air that was freely drawn in from the lab. The air from the output port of the VAV terminal unit was ducted through a sheet metal rectangular duct to a Figure 12 airflow test chamber². Like the Figure 15 chamber, the differential pressure across the airflow nozzles, a chamber static pressure, and air density were used to find the airflow rate. When calculating airflow through the Figure 12 chamber, it was assumed that the density of the air was the same as the calculation taken at the Figure 15 chamber. Temperature in the Figure 12 chamber could be up to 2 °F (1.2 °C) higher than the measurement taken at the Figure 15 chamber due to heat gains through the terminal unit fan. However, the effect on density calculations due to this slight change in temperature was less than 1%. For example, using a psychometric chart, the density of air at 70°F (21°C) & 60 %RH is 0.0738 lb/ft³ (1.18 kg/m³). The density of air at 75°F (24°C) & 50 %RH is 0.0731 lb/ft³ (1.17 kg/m³). This 5 °F (2.8°C) difference results in a density difference of 0.958%.

Temperature, humidity, and pressure measurements at each airflow chamber were used to calculate the airflow from equations provided in ANSI/AMCA 210-99 (1999). Because of the changes in temperature and humidity on various days that the tests were conducted, the volumetric airflow quantities were converted to an airflow at density of 0.075 lb/ft³ (1.20 kg/m³) to allow for comparison between terminal units.

¹ Figure 15 airflow chamber built in accordance to ANSI/AMCA Standard 210 (1999).

² Figure 12 airflow chamber built in accordance to ANSI/AMCA Standard 210 (1999).

The upstream and downstream static pressures, P_{up} and P_{down} , are two important variables in the characterization of the VAV units. The measurement locations for these values were specified in ANSI/ASHRAE Standard 130 (1996). The upstream static pressure was an average of four taps, 90° apart, located 1.5 equivalent diameters upstream of the VAV terminal unit. The downstream static pressure was an average of four taps, 90° apart, located 2.5 equivalent diameters downstream of the VAV terminal unit.

The upstream and downstream static pressures, the differential pressures across the flow nozzles, the chamber static pressures, and the rake sensor pressure were measured using pressure transducers that output an electrical current proportional to the differential pressure applied to it. Terminating resistors provided a voltage from these output electrical currents that the data acquisition system (DAQ) could measure. The accuracy of each of the transducers was $\pm 0.25\%$ of their full-scale output. The transducers were sized as specified in Table 3-4.

Table 3-4: Pressure Transducer Sizing

Point Name	Transducer Size
Differential Pressure Across Nozzles, Fig 12	0-6 in. w.g.(0 – 1.5 kPa)
Differential Pressure Across Nozzles, Fig 15	0-6 in. w.g. (0-1.5 kPa)
Chamber Static Pressure, Fig 12	0-10 in. w.g. (0-2.5 kPa)
Chamber Static Pressure, Fig 15	0-10 in. w.g. (0-2.5 kPa)
Upstream Static Pressure	0-2 in. w.g. (0-0.5 kPa)
Downstream Static Pressure	0-2 in. w.g. (0-0.5 kPa)
Rake Sensor Pressure	0-2 in. w.g. (0-0.5 kPa)

After some initial experimentation, it was discovered that the upstream and downstream static pressures and both differential nozzle pressure transducers were sensitive to pulsations from the test setup primary blower, which was seen as noise at the

same frequency that the blower was operating. It was decided that a low pass filter (Figure 3-10) could filter out this noise. Because all measurements were taken at steady state, the data acquisition responsiveness was not important. Equations (3.1) and (3.2) define the operation of a low-pass RC filter. $|H(f)|$ is the magnitude of the output signal of the filter, for a specific input frequency. The half-power frequency, f_B , is the frequency of the input signal that is attenuated by 0.707. All frequencies higher than this are reduced by a factor, according to Eq. (3.1). For example, in each filter, R was 199 Ω and C was 1000 μF , resulting in f_B equal to 0.800 Hz. Any input signals with noise at 60 Hz would be reduced 98%. A graphical example is provided in Figure 3-11, showing how these filters significantly reduced the noise being picked up by the transducers.

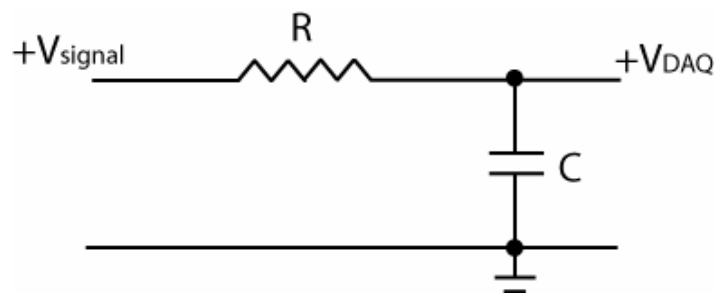


Figure 3-10: Schematic of Low Pass Filter

$$|H(f)| = \frac{1}{\sqrt{1+(f/f_B)^2}} \quad (3.1)$$

$$f_B = \frac{1}{2\pi RC} \quad (3.2)$$

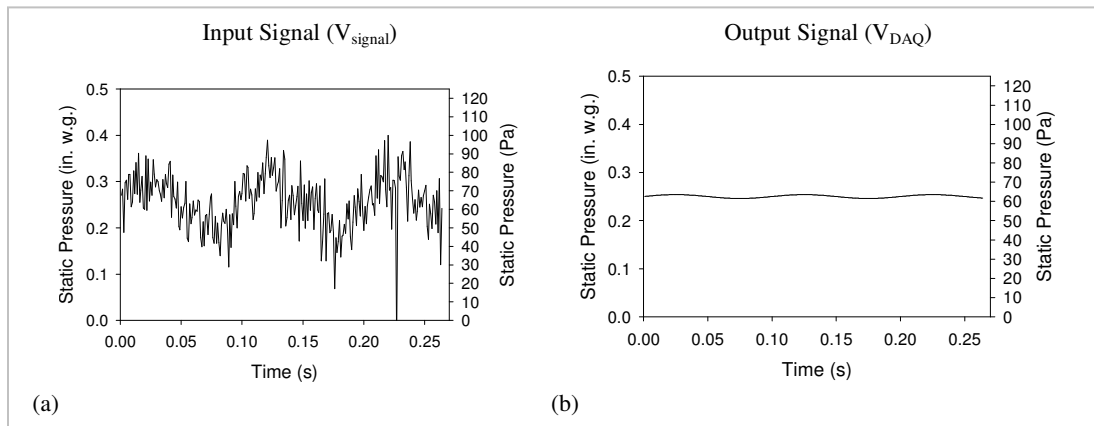


Figure 3-11: Example of a Typical Pressure Signal (a) Before and (b) After Low-Pass Filter

The accuracy of the chamber nozzle differential pressures was an important factor in determining the airflow. High accuracies of the upstream and downstream static pressures were also desired, because of their inclusion in the empirical models. Because the low pass filters did not completely eliminate the noise to the transducers (Appendix B), these pressures were averaged from 2000 points over 20 seconds during the data acquisition. This provided steady state values of the pressures ranging from 0.25 to 2.0 in. w.g. (62 to 498 Pa), with standard deviations averaging 0.01 in w.g. (2.5 Pa).

A sensitivity analysis of the equations used to calculate airflow showed that the accuracy of the temperature/relative humidity, chamber pressures, and the rake pressure were not as important. These values were averaged from 200 points taken in a two second interval, in order to reduce computing time.

In this test setup, the Figure 15 chamber measured the amount of primary airflow, Q_{primary} , and the Figure 12 chamber measured terminal unit output, Q_{out} (Figure 3-12). Assuming equal air densities, a mass balance (Eq. 3.3) based on volumetric flow was derived. In series units, Q_{induced} was the amount of airflow induced through the induced air port. For parallel units, Q_{induced} was the amount of airflow through the

terminal unit fan. Q_{leakage} was the amount of air leaking along the sheet metal seams of the unit, and along the backdraft damper when the fan was off in parallel units. For this equation, the direction of air leakage is out of the terminal unit.

$$Q_{\text{primary}} + Q_{\text{induced}} = Q_{\text{out}} + Q_{\text{leakage}} \quad (3.3)$$

In calculating Q_{induced} for both series and parallel units, it was assumed that Q_{leakage} was small in value, relative to the other terms. Q_{induced} was then calculated as the difference between Q_{out} and Q_{primary} . This was done because it was difficult to measure the air leakage directly. During testing, it was determined that assuming negligible air leakage was accurate for all of the terminal units, except one. This exception is discussed in the results section of this paper.

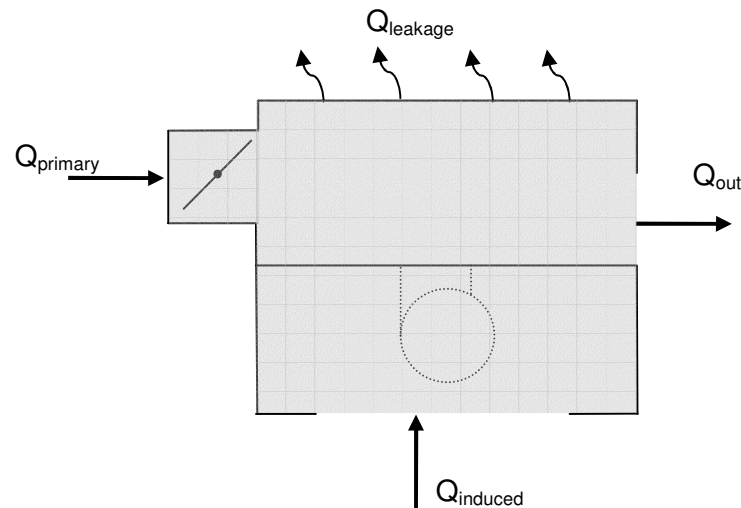


Figure 3-12: Volumetric Balance of Terminal Unit

The two airflow chambers were connected in series, without a terminal unit, in order to verify that the two provided similar results for airflow measurements (Appendix D).

3.3 POWER MEASUREMENT

The data for instantaneous current and voltage entering the VAV terminal unit fan motor were obtained at 1320 Hz and saved for a duration of six seconds, allowing for current and voltage waveforms to be produced. The current was measured using a 5 Amp current transducer installed on the 277 V wire entering the fan. This transducer had a full-scale accuracy of $\pm 1\%$.

The voltage was measured at the +277 V wire between the output of the SCR and the fan motor. However, the maximum voltage that the data acquisition card could handle was 10 V. A voltage divider circuit (Figure 3-13), was used to scale the voltage. In this case, R_1 was 987 k Ω and R_2 was 9.88 k Ω . V_{fan} was the voltage at the fan motor. V_{DAQ} was the voltage sent to the DAQ card.

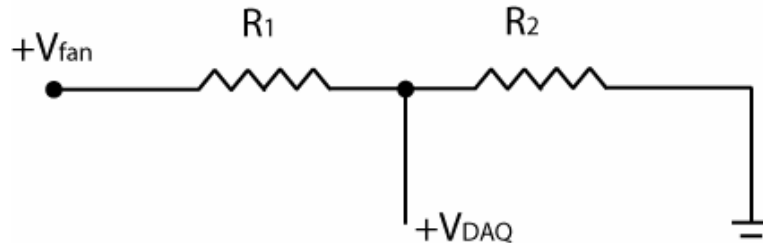


Figure 3-13: Schematic of Voltage Divider Circuit

For a voltage divider circuit, the signal received at the DAQ card is related to the voltage powering the fan, R_1 and R_2 by:

$$V_{DAQ} = V_{fan} \frac{R_2}{R_1 + R_2} \quad (3.4)$$

During data collection, the voltage and current data were obtained at 1320 Hz for six seconds, resulting in 360 voltage/current cycles. RMS of current and voltage were calculated for each cycle, and then averaged across the 360 cycles. Power was determined using V_{RMS} and I_{RMS} .

3.4 DATA ACQUISITION SYSTEM

A computer data acquisition system was used to obtain, process, and store data. This system consisted of a PC, two separate DAQ cards, and the termination blocks for all signal wires.

An eight channel, sixteen-bit sample-and-hold data card was used to measure instantaneous current and voltage. The simultaneous sample and hold prevented any introduction of error due to phase shift between the voltage and current signals. The elimination of phase shift allowed for accurate determination of the power factor for the VAV unit fans. The analog inputs had a resolution of 16 bits.

The other data acquisition card was an eight channel card, with two analog outputs to control the VSD's on the test setup assist blowers. The resolution of the analog inputs on this card was 12 bits.

CHAPTER IV

EXPERIMENTAL PROCEDURE

Empirical models of energy consumption and airflow output for series and parallel fan powered terminal units required collection and statistical analysis of experimental data on the units. This section provides the details of the experimental procedure used in the data acquisition, and the methodology applied during the statistical analysis of the data.

4.1 METHOD OF EXPERIMENTATION

For the testing of the VAV terminal units, a factorial design was employed. In this case, there were two separate dependent variables that were of interest: Q_{out} , the airflow through the fan, and $Power_{fan}$, the power consumption of the terminal unit fan. The independent variables were:

1. P_{up} : The static pressure upstream of the terminal unit. In the field, this variable is affected by the system supply air fan at the air-handling unit, and by damper changes in other terminal units.
2. P_{down} : The static pressure downstream of the terminal unit. This value is considered a constant design variable for series terminal units. In parallel terminal units, it can vary as the damper continues to modulate after the fan has been turned on.
3. The speed of the terminal unit fan. This speed is controlled by the SCR, which alters the voltage supplied to the fan motor. For the models, an RMS average of the voltage was obtained and used as the independent variable.

4. The position of the terminal unit's damper. The controller sends signals to a damper actuator that adjusts the damper, to meet the temperature set point for the zone.
5. Q_{primary} or P_{rake} : The control pressure from the flow sensor, P_{rake} , has a linear response with changes in the primary airflow, Q_{primary} . These variables are not actually independent, because they are directly affected by the position of the damper and the upstream static pressure. However, they are easier to quantify than the position of the damper, and are better understood by those in the industry.

Before testing a unit, each of the independent variables was assigned a set of specific values, statistically known as 'levels', to be tested. The number of levels for each of the variables and their values are shown in Table 4-1. Many levels for the variables were determined by using their maximum and minimum values, and equally spacing the other values between these two. For example, in terminal unit P8B an RMS voltage of 271 V was measured at the maximum SCR speed setting; an RMS value of 145 V was measured at the minimum SCR speed setting. From this, the resulting levels for SCR voltage were 271 V, 209 V, 169 V, and 145 V.

The values for the levels differed across VAV terminal units because the maximum and minimum values for certain variables differed across units. The maximum and minimum values for the SCR voltage were determined by adjusting the SCR setscrew completely in both directions. The maximum value for the damper setting was defined as when the damper was horizontal, or fully open; the minimum was defined when the damper was closed. The levels for downstream static pressure were defined according to Table 4-1. The levels for upstream static pressure varied depending on the test being run.

Table 4-1: Test Variable Levels

Independent Variable	Parallel Unit Testing		Series Unit Testing	
	# of Levels	Values	# of Levels	Values
Upstream Static Pressure	3	varied from 0.3 to 2 in. w.g. (75 to 498 Pa)	6	varied from 0.25 to 2 in. w.g. (62 to 498 Pa)
Downstream Static Pressure	3	0.1, 0.25, 0.5 in. w.g (25, 62, 125 Pa)	1	0.25 in. w.g. (62 Pa)
SCR Voltage (Fan Speed)	4	Equally spaced	4	Equally spaced
Damper Position	4	Equally spaced	4	Equally spaced

The characterization of a terminal unit consisted of several tests. These tests were conducted for each combination of damper and SCR settings. In every test, data for every combination of upstream and downstream static pressure levels were obtained. This process is a full-factorial design because data points for all combinations of independent variables were obtained. The sequence of these tests usually consisted of running the tests for all of the SCR speeds at a single damper position, adjusting the damper to the next position, and continuing the sequence.

Before starting a test, the damper and SCR were manually adjusted to the desired positions, according to the test being run. Throughout the test, the damper and SCR would remain in the same position. During the test, the data acquisition program allowed the user to adjust the VSD's on the upstream and downstream blowers to meet desired conditions for a test point. The downstream static pressure was fixed at 0.25 in. w.g. (62 Pa) for the series terminal units. The parallel terminal units were tested with the discharge static pressure varied from 0.10 in. w.g. (25 Pa) to 0.50 in. w.g. (125 Pa).

The upstream static pressure was first adjusted to the smaller of the following: the point where the primary airflow was approximately 5% greater than the terminal unit's specified maximum or 2 in. w.g. (498 Pa). This pressure was designated as the maximum level for upstream static pressure variable. In series units, the minimum upstream static pressure was selected to be 0.10 in. w.g. (25 Pa). Testing was done by

equally spacing data points between these maximum and minimum upstream static pressures while maintaining a constant downstream static throughout the test.

For the parallel units, the maximum level for the upstream static pressure had the same definition as that for the series. However, in determining the minimum, it could never be lower than the downstream static pressure because primary air would flow backwards in that case. Therefore, each test had three minimum level upstream static pressures, one for each downstream static pressure level. These minimums were selected to be approximately 0.25 in. w.g (60 Pa) greater than the corresponding downstream static pressure, except in cases that this caused insufficient primary airflow (due to damper position). For each downstream static pressure, a third point was obtained for the upstream static pressure approximately halfway between the corresponding minimum and maximum. This procedure resulted in three data points for each downstream static pressure level, and nine points per test.

The upstream and downstream blowers were manually adjusted to the desired conditions for a specific data point. After static pressures settled into a steady state (5-10 sec.) the data acquisition was begun. The data acquisition program acquired all of the data, calculated air density, airflow and fan power, and then output to an Excel spreadsheet. After testing was completed, the data from these spreadsheets were applied in statistical analysis to create the models.

4.2 METHOD OF STATISTICAL ANALYSIS

For the statistical analysis, SAS software (2002) was used. The goal of the statistics was to obtain an accurate model, while maintaining simplicity of the model. To begin the analysis, variables were identified that were expected to be significant in explaining fan airflow and power. The models were then developed, with consideration to these variables.

Models were developed in a method very similar to the forward stepwise regression method (Mickey et al. 2004, Neter et al. 1996). In this method, a linear model was regressed using the most statistically influential independent variable. This

determination was made using the F statistic. The F statistic is commonly used to determine the degree of influence a variable may have on the dependent variable (Neter et al. 1996). The variable with the largest F statistic was added first. This method of adding terms to the model was continued until no other variables added were significant, defined as when the variables' F statistic was below 4.0 (Neter et al. 1996).

Between each step, models were compared against each other according to their adjusted coefficient of determination, R^2_{adj} values. The R^2_{adj} statistic is similar to the R^2 statistic. The R^2 statistic is a value between 0 and 1.0 used to express how well the model explains the variance in the data. An R^2 of 1.0 means the model perfectly fits all of the data. However, when using a forward stepwise procedure as described above, the R^2 statistic will always increase as you increase the number of terms in the model and will become 1.0 when the number of terms equals the number of data points. This could produce an unnecessarily complex model and may not be very useful in describing the response of a VAV terminal unit. The R^2_{adj} statistic allows for a way to justify the improvement from adding terms to create a more complex model. If adding another term to a model doesn't sufficiently increase the R^2 statistic, the R^2_{adj} statistic will decrease from its value in the simpler model.

The resulting model was checked for linearity (to check the validity of the linear regression), equal variances (to ensure that the model's error terms were approximately equal for the range of the dependent variable's values), and normality (to check the assumption of a normal distribution of error) (Neter et al. 1996). These tests were conducted by visually inspecting the residual plots of the final model. The residual plots were inspected for the residuals to fall within a horizontal band, centered at zero, with no systematic tendencies to be positive or negative. All of these tests were conducted to ensure that the linear model did a sufficient job of capturing the variance in the data.

The data analysis was conducted separately for the parallel units and series units. Because of the significant differences in their configuration, it was not necessarily expected that the models for the two would be similar. In developing the models for the parallel units, several variables were considered: the SCR voltage, P_{rake} , P_{down} , P_{up} , and

Q_{primary} . The models for all of the parallel terminal units were compared against each other. Any differences in terms included in the airflow or power models were investigated in an effort to create a single form model that would be applicable to all of the terminal units. The same analysis was done for the series terminal units. The variables considered for these models were the SCR voltage, P_{rake} , P_{up} , and Q_{primary} .

The assumptions made are typical in model regressions: an approximately linear relationship between the response variable and predictors, errors are independent & random, and the error has constant variance (Montgomery et al. 2001). The models were checked to ensure minimal interaction effects between variables. From this it was decided not to use Q_{primary} and P_{rake} in the same model because there is a direct linear relationship between the two (P_{rake} is used to measure Q_{primary}). A model that included both variables would be unnecessarily complex because the effect of primary airflow should only be represented by a single term in a model.

CHAPTER V

RESULTS AND MODELS FOR PARALLEL FAN POWERED VAV TERMINAL UNITS

Experimental data were collected for six parallel fan powered VAV terminal units. This section discusses the results for the data on these units. Three models were developed for each parallel terminal unit. The first model estimated performance when the terminal unit fan was off. After initial testing, it was discovered that some air leakage occurred when the fan was off. This model quantified that leakage. The second and third models estimated performance when the terminal unit was in heating mode, and the terminal unit fan was on. The second model quantified the amount of fan air and the third quantified the power draw of the fan as a function of several variables that influence the performance of the terminal unit. Each model is described in this chapter.

One goal of this research was to develop a generalized approach for the models of these terminal units. A single model was required to be applicable to terminal units of different sizes and manufacturers. Because each of the terminal units was designed differently, the experimental results were not consistent for the same rated size terminal unit among the different manufacturers. Thus, the models tended to maintain the same form, but used different coefficients for the different sizes and manufacturers. There were some exceptions to this rule and they are discussed in this chapter.

When creating the models, the statistically significant variables were analyzed with respect to the applicable dynamics. The leakage model utilized an estimate of the internal terminal unit pressure to determine its leakage. The other models basically recreated the fan curves of the fan but included the effect of any extraneous variables, such as the interaction effects of primary air on the backdraft damper, within the terminal unit.

Presented below are three sections, one for each model. In each section, a discussion of the dynamics that act on the terminal unit is presented, followed by an analysis of the data obtained relating to these dynamics. Concluding each section is the statistically developed model and a discussion regarding its statistical validity.

5.1 PARALLEL TERMINAL UNIT LEAKAGE MODEL

During the cooling mode, the terminal unit fan was off and the backdraft damper was supposed to prevent any air from traveling backwards through the fan. In this instance, the output airflow downstream of the terminal unit should have been equal to the primary airflow. However, it was discovered that leakage occurred along the backdraft damper and along the sheet metal seams of the terminal unit. The leakage model was used to quantify the amount of air leakage from the terminal units.

The primary factor that should have influenced air leakage was the pressure inside the terminal unit. The static pressure inside the terminal unit was not measured. Examination of the units showed that there was no physical obstruction at the outlet of the terminal units (Figure 5-1). It was assumed that the static pressure inside the terminal units was very close in value to the downstream static pressure. Therefore, the downstream static pressure was used as a proxy for the pressure inside the box and was expected to be the most significant variable in the leakage model.

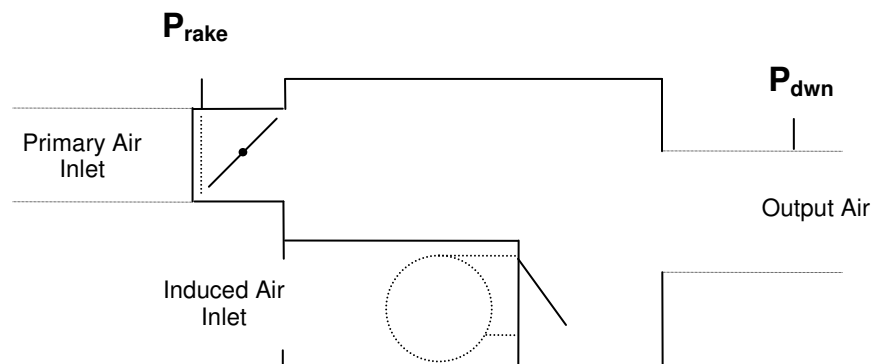


Figure 5-1: Typical Parallel VAV Fan Powered Terminal Unit

Air leakage occurred along either the sheet metal seams of the terminal units or along the edges of the backdraft damper. The leakage along the seams was affected primarily by the static pressure inside the terminal unit. However, accounting for the leakage along the backdraft damper was somewhat more complex. Internal static pressure would be a factor but additionally, the primary air velocity across the damper was expected to have an influence. In the terminal units from group A, the backdraft damper included an extension that was designed to push the damper closed as primary air pushed against it (Figure 5-2). It was expected that a change in primary air would have an effect on the operation of this damper. In the terminal units from groups B and C, the backdraft dampers were gravity operated, and primary air velocity was expected to have a lesser effect, or possibly no effect on leakage (Figure 5-3).

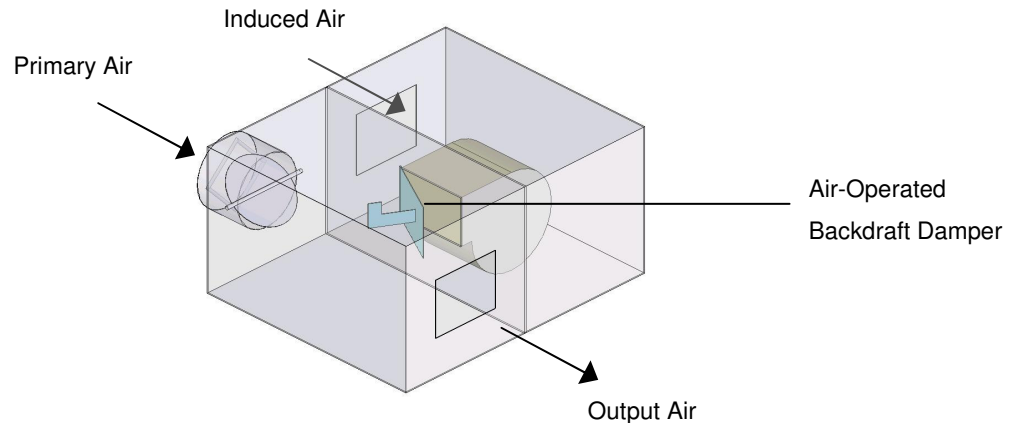


Figure 5-2: Parallel Terminal Unit with Air-Operated Backdraft Damper

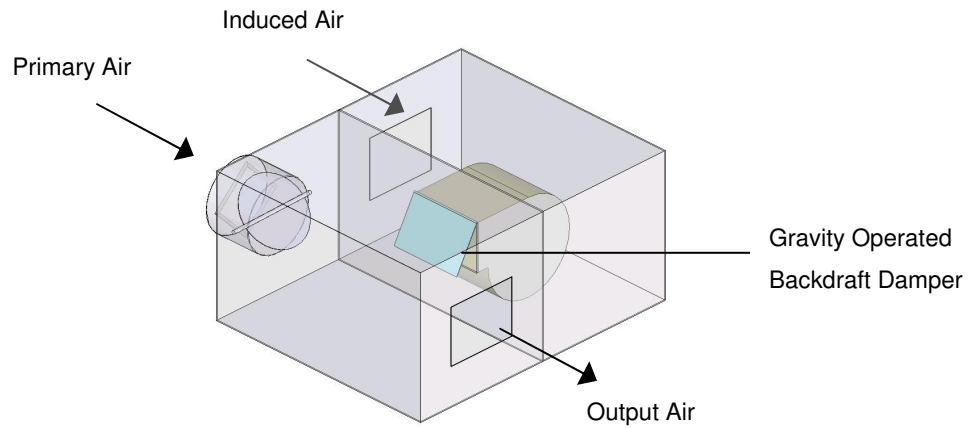


Figure 5-3: Parallel Terminal Unit with Gravity Operated Backdraft Damper

The location of the backdraft damper within the terminal unit differed by manufacturer. Groups A and C placed the damper in the path of the primary airflow (Figure 5-4 and Figure 5-5). The dampers on the terminal units from group B were not directly in the primary airstream (Figure 5-6). Because of the variety of damper design and location, it was expected that the primary airflow velocity's effect on overall air leakage would differ by manufacturer.

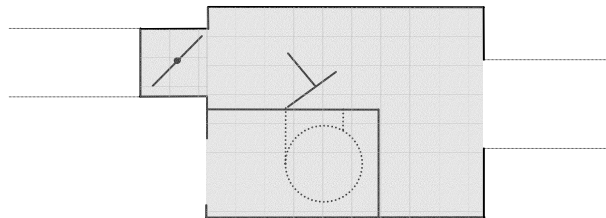


Figure 5-4: Schematic of Group A Parallel Terminal Units, plan view

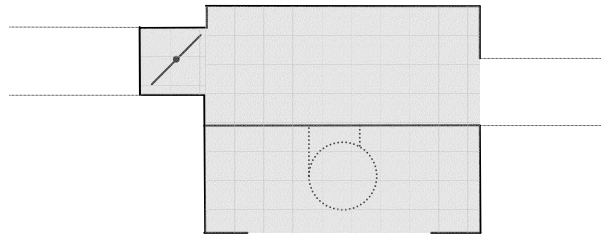


Figure 5-5: Schematic of Group C Parallel Terminal Units, plan view

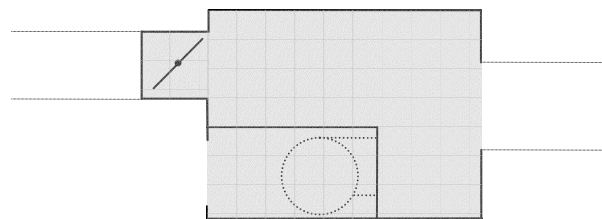


Figure 5-6: Schematic of Group B Parallel Terminal Units, plan view

5.1.1 Data Analysis

Initial analysis of the data reaffirmed that the downstream static pressure played a significant role in air leakage. Air leakage increased with an increase in downstream static pressure for the 8 in. (203 mm) and 12 in. (304 mm) units (Figure 5-7 and Figure 5-8). The response between air leakage and downstream static pressure was very similar among the six terminal units. However, there appears to be more scatter in the data for some, such as terminal unit P8A. This scatter prompted consideration for using primary airflow velocity as another explanatory variable in the air leakage model.

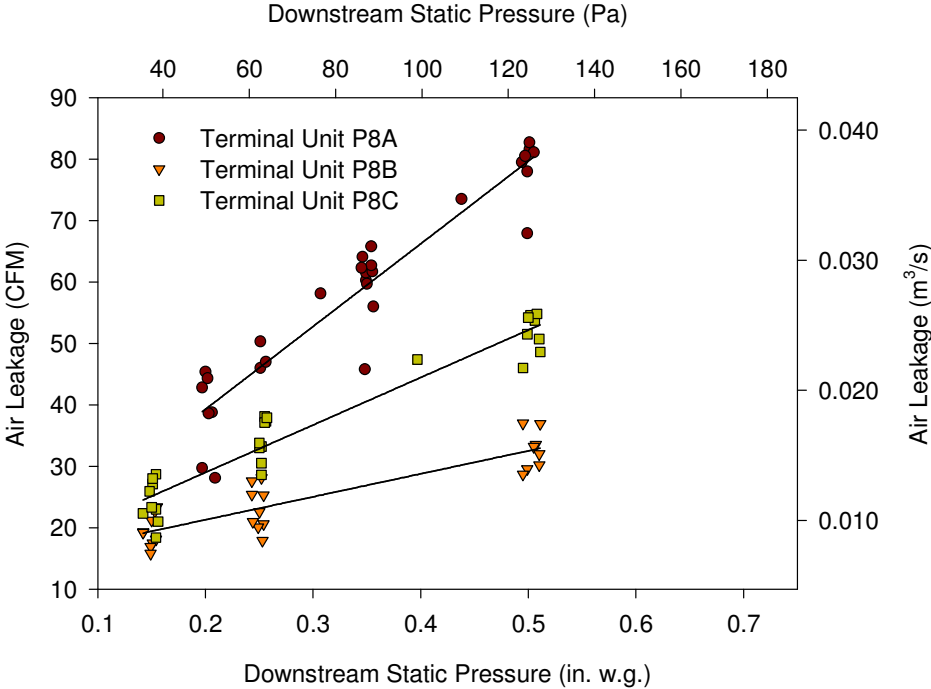


Figure 5-7: Air Leakage for 8 in. (203 mm) Inlet Parallel Terminal Units

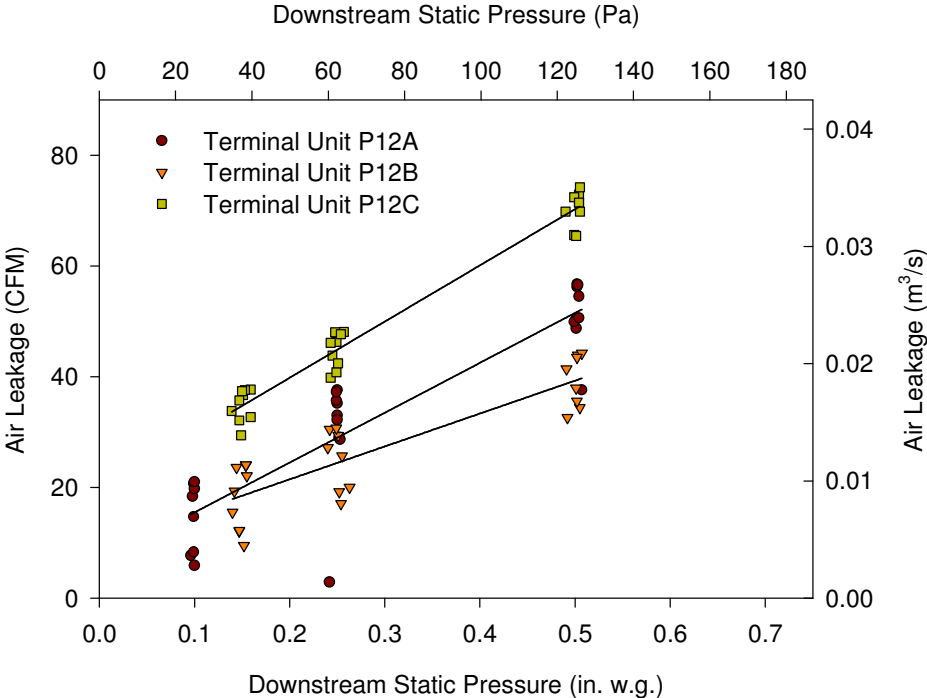


Figure 5-8: Air Leakage for 12 in. (304 mm) Inlet Parallel Terminal Units

According to each of the manufacturers, the pressure at the rake sensor was approximately linear with the amount of primary air entering the terminal unit. Thus, the variable P_{rake} was used to approximate the influence of primary air velocity.

In developing the leakage model for parallel terminal unit P8C, a model with only P_{down} as a variable was initially created. The R^2_{adj} statistic for this model was 0.9167. To graphically show the significance of the variable P_{rake} , some plots of the model residuals were created. Analysis of Figure 5-9 showed that the residuals for the model had an inverse relationship with P_{rake} , because the slope of the line is negative. The errors in the first model could be reduced by incorporating P_{rake} in the model. Another model with P_{down} and P_{rake} as explanatory variables was developed. This model had an R^2_{adj} value of 0.9702, an improvement over the first model. This analysis was conducted for all of the parallel terminal units, resulting in similar results for on the all the terminal units from groups A and C. Because of the consistent results among these terminal units, it would indicate that the amount of primary airflow does play a statistically significant role in the air leakage from the terminal unit.

Similar analysis was conducted for parallel terminal unit P8B, with the backdraft damper out of the primary airstream. The P_{rake} term failed the F-statistic test ($F=1.3 < 4.0$), did not improve the R^2_{adj} statistic from 0.767, and was not included in the model. From the plot of residuals (Appendix A), no statistical relationship could be inferred. This analysis supports the discussion from the introduction to this section. Because the backdraft damper in the B terminal units was not directly in the primary airstream, the velocity of this air should not play a significant role in the model of air leakage.

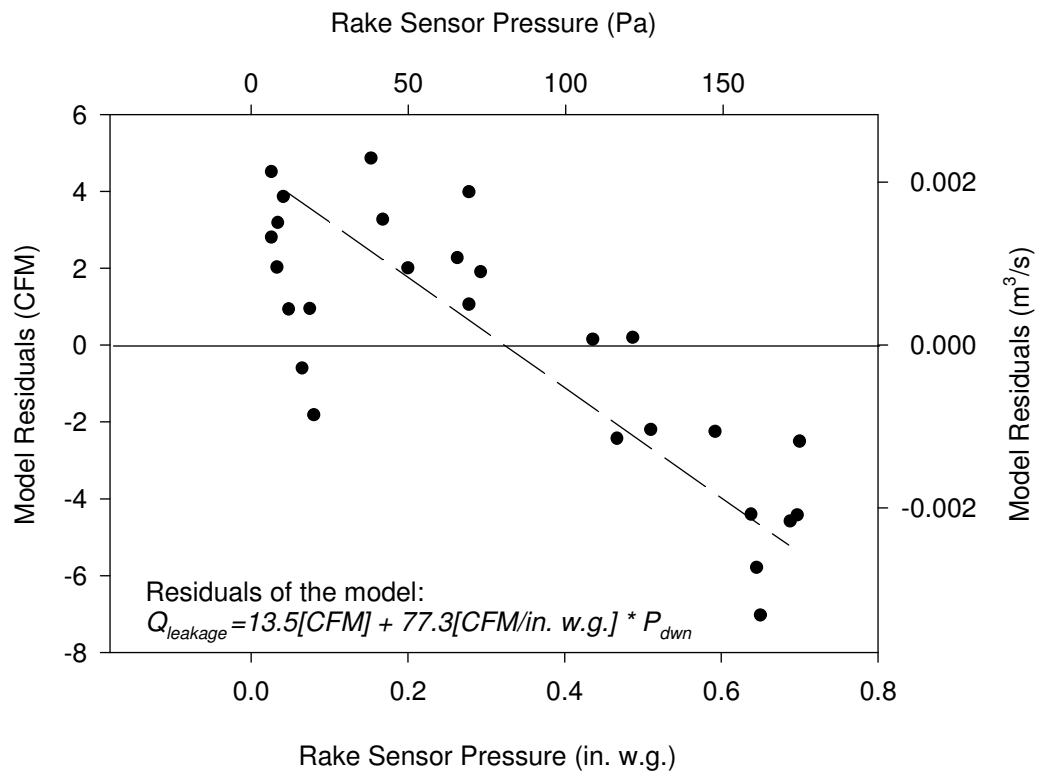


Figure 5-9: Residuals Plot for Parallel Terminal Unit P8C

However, the P12B terminal unit, with the backdraft damper out of the primary airstream, did not respond in the same way. The addition of the P_{rake} variable (with an F stat of 87.6) increased the R^2_{adj} statistic from 0.7398 to 0.9454. This indicated that there was a relationship between the P_{rake} variable and the residuals from the first model, and that P_{rake} should be included in the model. It is possible that although these two units had the same configuration, the larger terminal unit had air dynamics acting on the backdraft damper that did not occur in the smaller terminal unit. More investigation would need to be conducted regarding the air dynamics within the terminal units.

5.1.2 Leakage Model

Eq. (5.1) is the model that was developed for quantifying the amount of air leakage in the parallel terminal units. Table 5-1 provides the coefficients for each of the

terminal units. In this model, the P_{down} term accounts for the effect of the internal terminal unit pressure on leakage, while P_{rake} accounts for the effects of primary air on the backdraft damper.

$$Q_{\text{leakage}} = C_1 + C_2 \cdot P_{\text{down}} + C_3 \cdot P_{\text{rake}} \quad (5.1)$$

Table 5-1: Model Coefficients for Parallel Leakage Model

Name	C_1 [CFM]	C_2 [$\text{CFM}/\text{in. w.g.}$]	C_3 [$\text{CFM}/\text{in. w.g.}$]	R^2_{adj}
P8A	16.47	138.1	-6.16	0.970
P8B	13.8	37.41	0	0.767
P8C	16.86	77.55	-10.76	0.970
P12A	14.4	97.94	-37.9	0.858
P12B	17.83	58.26	-27.16	0.945
P12C	22.30	100.83	-15.02	0.989

By comparing the R^2_{adj} statistics, it appears that this form for the leakage model explained 95% of the variation in data for four of the six boxes tested. However, it is apparent that 23% of the variation for leakage in terminal unit P8B was not explained by the variables that were measured in the tests. Further examination of the leakage in this unit would need to be conducted to better characterize this leakage.

5.2 PARALLEL TERMINAL UNIT AIRFLOW MODEL

This model quantified the amount of airflow going through a terminal unit fan during the heating mode when the fan was on. The fans on each of the terminal units were centrifugal, forward-curved style fans. In developing the model for these fans, they were expected to follow typical fan curves and the fan laws (ASHRAE 2001).

The SCR settings of the fans were a variable in the model that had to be quantified before applying the fan laws. Each SCR setting corresponded to a different fan speed. A fan curve could be applied to the fan for each of these speeds. Each of these fan curves was used to find airflow as a function of the pressure across the fan. In the development of the models, a simple experiment was conducted to determine the relationship between the SCR setting and the speed of the fan.

In examining the backdraft dampers for the parallel terminal units of group A, it could be reasoned that the velocity of primary airflow could have an effect on the output of the VAV fan. When the fan was off, the primary air pushed against the extension on the damper, forcing it closed. When the fan was on, the pressure from the fan pushed the damper open. However, the primary air continued to push on the damper. Any change in the velocity of the primary air would affect the damper, and most likely, the fan output. The model that was developed attempted to quantify this effect.

It is important to reiterate that the amount of air through the VAV fan was not directly measured. The value for fan air was determined by the difference in output air and primary air, which were each measured by separate airflow chambers. However, this method to determine fan air assumed that there was no air leakage. Every terminal unit tested had some air leakage along their seams. This leakage was never explicitly measured but upon examination never appeared to be significant except for parallel terminal unit P8A, which is discussed below.

5.2.1 Data Analysis

The variable with the strongest influence on fan airflow was the SCR voltage. The relationship between this voltage and the fan speed had to be determined. A simple test was performed on one fan to estimate a general relationship. A tachometer was instrumented to parallel terminal unit P8A. At several different voltage settings, the RPM of the fan was measured. During this testing, the upstream and downstream static pressures were maintained constant to eliminate the effects of pressure on the fan speed. A quadratic equation was fit to the data (Figure 5-10). The high R^2 value of 0.999

implies that the quadratic equation does a good job of explaining the variation of fan speed with SCR voltage.

This test was conducted on two other terminal units, parallel terminal units P12B and P8C, which resulted in R^2 values of 0.994 and 0.997, respectively. The coefficients were not the same for these units. The maximum speed for terminal unit P12C was higher than that for P8A, and the model coefficients differed (Figure 5-11). However, because of the high R^2 values for the variety of groups and sizes, it was assumed that a general quadratic relationship would remain true for all of the terminal units even if their coefficients differed. Because each airflow model would use different coefficients for the various units, this would not be a problem in the modeling.

According to the fan laws, there should be a linear relationship between airflow and fan speed (ASHRAE 2001). Because a quadratic equation had been used to show the relationship between SCR voltage and fan speed, it was assumed that a different equation of the same form could be used for the relationship between SCR voltage and airflow.

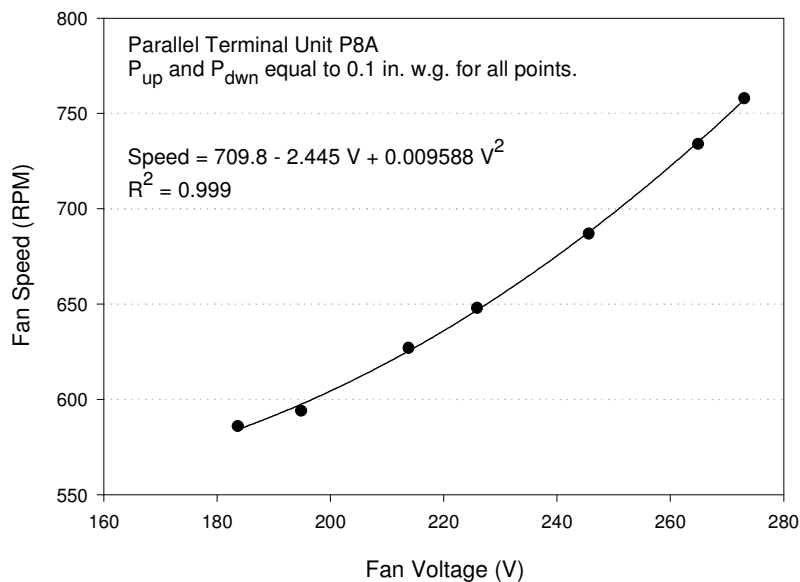


Figure 5-10: Effect of SCR Voltage on Fan RPM for Parallel Terminal Unit P8A

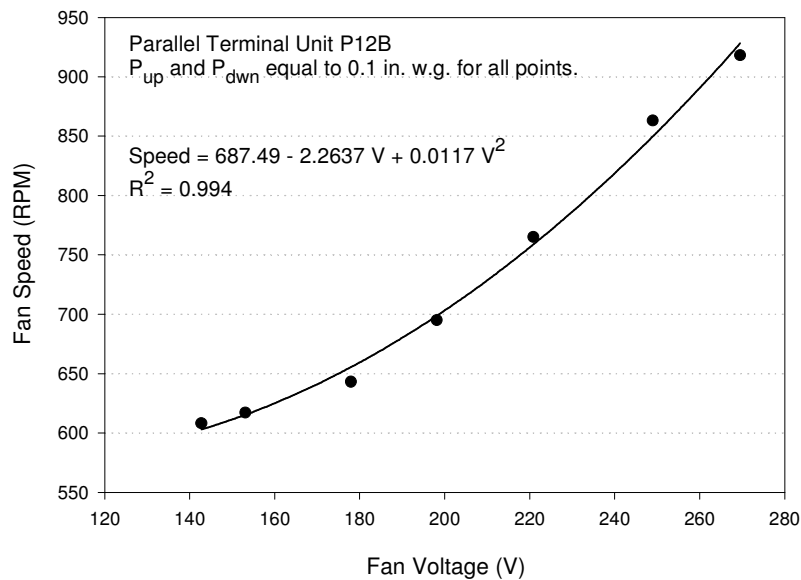


Figure 5-11: Effect of SCR Voltage on Fan RPM for Parallel Terminal Unit P12B

From an understanding of fan curves and the fan laws, it was known that the only other factor that should influence the fan output would be the pressure across the fan. For all parallel terminal units tested, the pressure on the front side of the fan was atmospheric. The pressure at the fan output was assumed to be approximated by the downstream static pressure. Therefore, this pressure would have the other significant influence on the terminal fan capacity. The results typical to the terminal units of groups B and C show the effect on fan airflow due to the downstream static pressure and the SCR voltage (Figure 5-12). Figures of the data for the other units can be found in Appendix A.

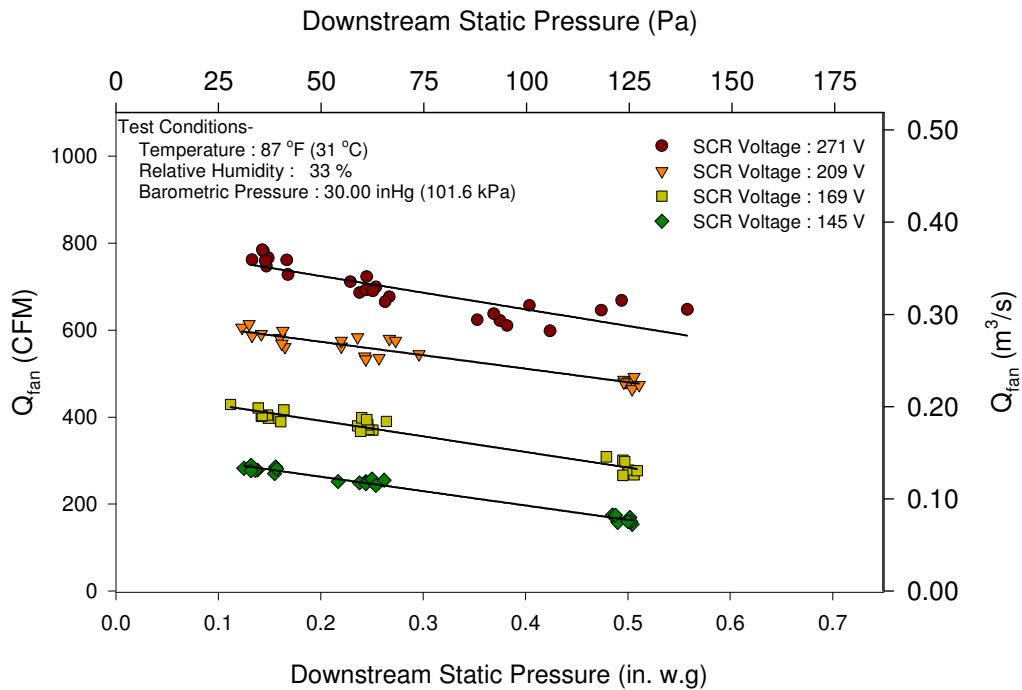


Figure 5-12: Fan Airflow for Parallel Terminal Unit P8B

The results from group A differed with that of groups B and C (Figure 5-13 and Figure 5-14). Two reasons possibly explain this difference in results. First, parallel terminal unit P8A appeared to have significant air leakage. Second, both terminal units had a different style backdraft damper that could have affected the fan performance. Both of these hypotheses are discussed below.

During testing, parallel terminal unit P8A leaked much more air than any of the other parallel terminal units did (Figure 5-7). Quantitatively, the coefficient, C_2 , of the leakage model was higher for P8A (Table 5-1). This part of the model estimates the leakage affected by the internal static pressure of the terminal unit. It would be expected that a terminal unit with greater leakage would have a model that gave more weight towards P_{down} . The leakage model for P8A displayed this characteristic, confirming the leakage that occurred when the unit fan was off.

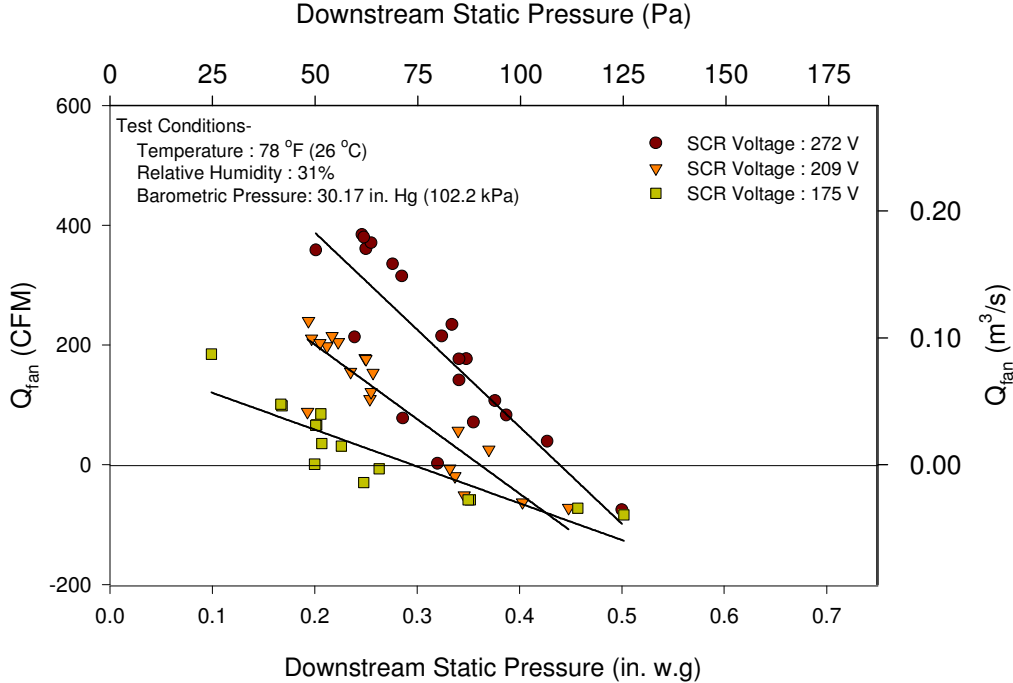


Figure 5-13: Fan Airflow for Parallel Terminal Unit P8A

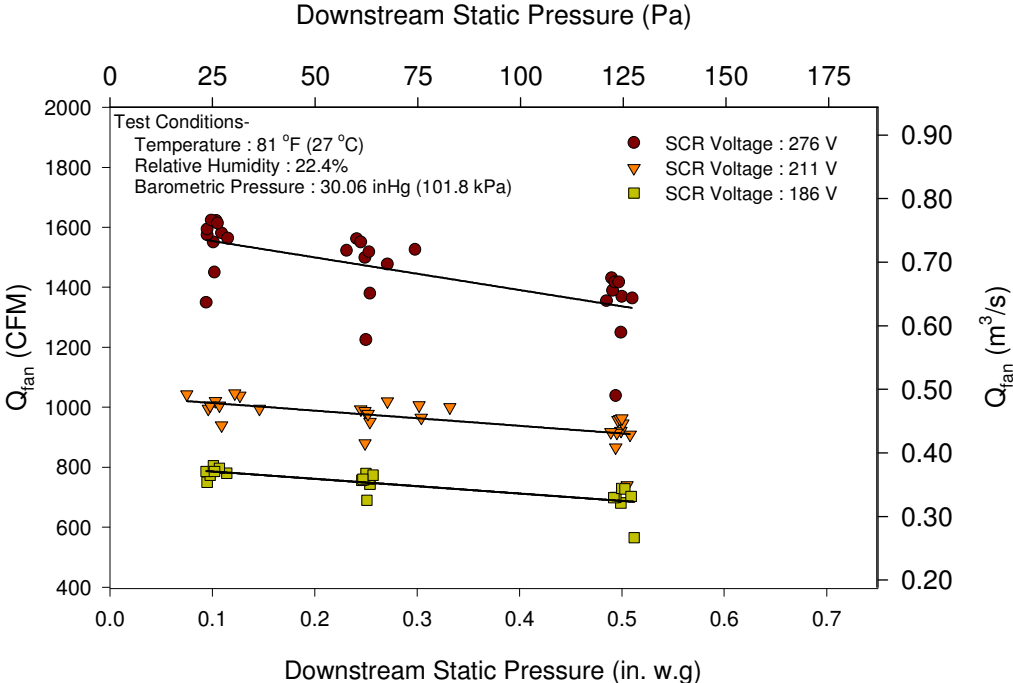


Figure 5-14: Fan Airflow for Parallel Terminal Unit P12A

At higher downstream static pressures, the P8A unit fan appears to have had a negative airflow (Figure 5-13). This is due to the faulty assumption that air leakage is zero, from Eq. (5.2). Recall that Q_{fan} was not directly measured; it was determined by taking the difference between Q_{out} and $Q_{primary}$ and assuming leakage to be negligible. The negative values on the figure show that the terminal unit was leaking more air along its seams than the fan was producing.

$$Q_{fan} = (Q_{out} - Q_{primary}) + Q_{leakage} \quad (5.2)$$

The second reason for the distinctive results from the parallel terminal units of group A was the style of the backdraft damper in the terminal units (Figure 5-2). These were the dampers that used an extension to allow primary air to force it closed. It was expected that while the fan was on, an increase in the amount of primary air would push the damper further closed, resulting in a decrease in output of the terminal unit fan. P_{rake} was added as an explanatory variable to the parallel airflow model to account for this effect of the backdraft damper. Only the terminal units from group A utilized this extra variable. Analysis of the F statistics for P_{rake} confirmed that it was an insignificant variable in the terminal units from groups B and C, which did not have that style backdraft damper.

5.2.2 *Airflow Model*

For the gravity-operated backdraft damper terminal units (Figure 5-5 and Figure 5-6) the airflow was not affected by the amount of primary air input to the terminal unit. The airflow model, Eq. (5.3), for these terminal units was a function of SCR voltage and downstream static pressure to include the effects the SCR setting and the pressure difference across the terminal unit fans. Table 5-2 provides the coefficients for the groups B and C parallel terminal units.

$$Q_{fan} = C_1 + C_2 \cdot V + C_3 \cdot V^2 + C_4 \cdot P_{dwn} \quad (5.3)$$

Table 5-2: Model Coefficients for Parallel Terminal Unit Airflow Model, for terminal units with gravity-operated backdraft damper

Name	C ₁ [CFM]	C ₂ [^{CFM} /V]	C ₃ [^{CFM} /V ²]	C ₄ [^{CFM} /in. w.g.]	R ² _{adj}
P8B	-988.5	11.85	-0.0197	-303.0	0.990
P8C	-1725	19.79	-0.0328	-564.4	0.991
P12B	-1143	13.56	-0.0131	-364.8	0.998
P12C	-2142.9	26.36	-0.0396	-1920.9	0.931

The airflow model for the primary air-operated backdraft damper terminal units (Figure 5-4), Eq. (5.4), had the same form as the airflow model already presented, except that P_{rake} was added as a variable to include the effect of primary air interacting with the backdraft damper. Table 5-3 provides the coefficients for the terminal units from group A which were the only units with that style backdraft damper.

$$Q_{fan} = C_1 + C_2 \cdot V + C_3 \cdot V^2 + C_4 \cdot P_{dwn} + C_5 \cdot P_{rake} \quad (5.4)$$

Table 5-3: Model Coefficients for Parallel Terminal Unit Airflow Model, for terminal units with primary air-operated backdraft damper

Name	C ₁ [CFM]	C ₂ [^{CFM} /V]	C ₃ [^{CFM} /V ²]	C ₄ [^{CFM} /in. w.g.]	C ₅ [^{CFM} /in. w.g.]	R ² _{adj}
P8A	-233.2	3.37	-0.023	-917.3	-229.1	0.808
P12A	-1567.3	16.98	-0.0199	-407.4	-360.2	0.978

Comparison of the R^2_{adj} for each of the models showed that the model for parallel terminal unit P8A had the lowest R^2_{adj} , implying that terminal unit P8A had the most scatter. This terminal unit also had the worst air leakage. At downstream static pressures above 0.3 in w.g. (75 Pa), the leakage was equal to or greater than the primary airflow output of the terminal unit. The leakage created an extra variation in the primary airflow model. Because of the other high values of R^2 (all above 0.90), it can be concluded that the parallel airflow model accurately captured the variation in the data, as long as the box construction prevented excessive air leakage.

5.3 PARALLEL TERMINAL UNIT FAN POWER MODEL

This model quantified the power consumption of a parallel terminal unit fan when it was on. As previously mentioned, the fans were expected to follow typical fan curves of a centrifugal, forward-curved style fan. The expected relationship between power and the fan air output was investigated first.

5.3.1 *Data Analysis*

Data analysis of the power curves for each of the terminal unit fans revealed a common characteristic. In each of the terminal units, except parallel terminal unit P8A, there appeared to be a nearly linear relationship between power and airflow (Figure 5-15). Appendix A shows the complete set of figures for the parallel terminal units.

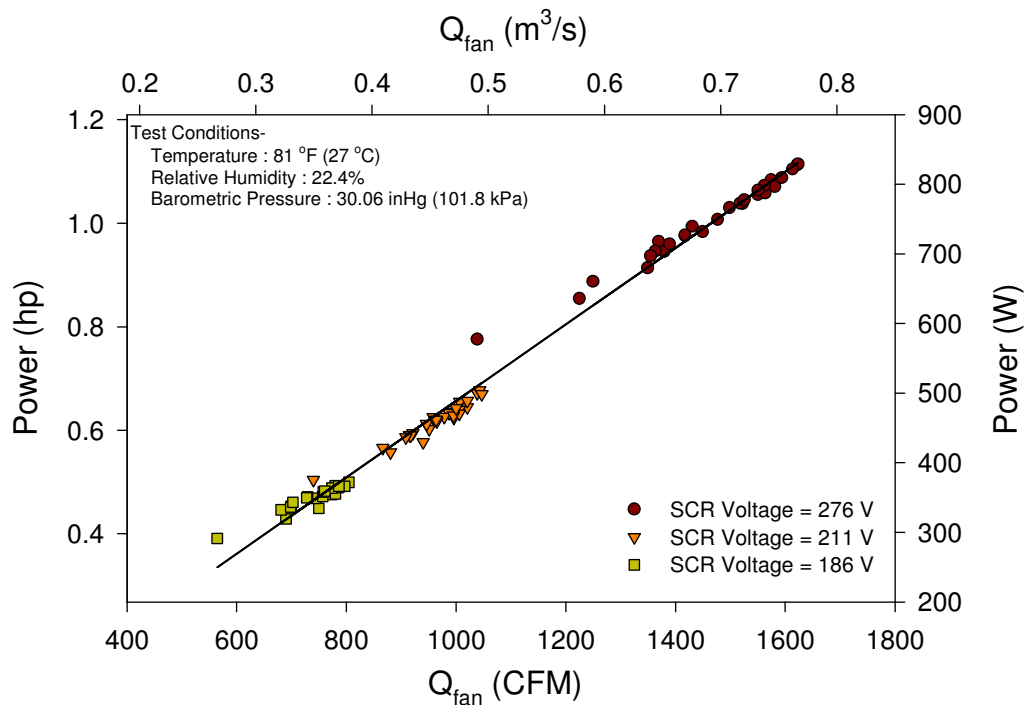


Figure 5-15: Fan Power for Parallel Terminal Unit P12A

The data for power versus fan airflow for terminal unit P8A showed a different relationship (Figure 5-16). There was an approximately linear relationship between the two variables. However, there appears to be another variable affecting the fan power. This can be explained by the no-leakage assumption.

Terminal units with minimal leakage, such as parallel terminal unit P12A (Figure 5-15), allow the direct relationship between fan capacity and power to be depicted in a single graph. However, because parallel terminal unit P8A has been shown to have significant leakage, Figure 5-16 does not depict the relationship between the fan airflow and power. Rather, it illustrates the relationship between $(Q_{fan} - Q_{leakage})$, and the fan power. It was expected that for this terminal unit the model for power would need to include a term to account for terminal unit leakage.

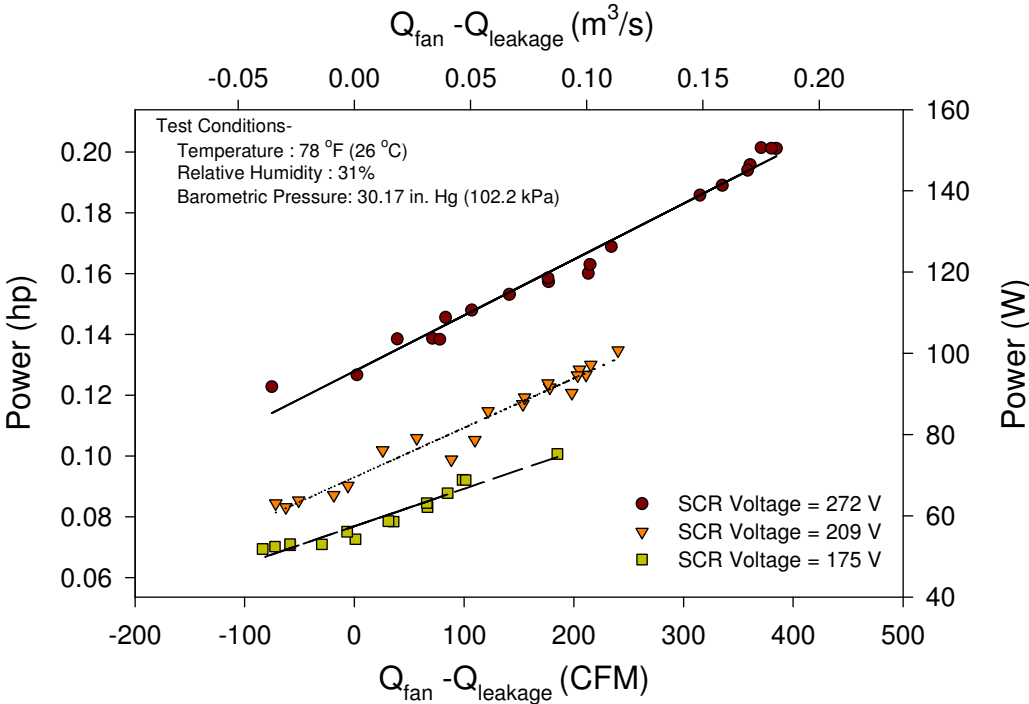


Figure 5-16: Fan Power for Parallel Terminal Unit P8A

5.3.2 Power Model

Because of the linear approximation between airflow and power for parallel terminal units, the model developed for power maintained the same form as the model for airflow.

Eq. (5.5) is the model that was developed for quantifying the power consumption of the fan in parallel terminal units. Table 5-4 provides the coefficients for each of the terminal units.

$$Power_{fan} = C_1 + C_2 \cdot V^2 + C_3 \cdot V + C_4 \cdot P_{dwn} + C_5 \cdot P_{rake} \tag{5.5}$$

Table 5-4: Model Coefficients for Parallel Terminal Unit Fan Power Model

Name	C_1 [W]	C_2 [W/v^2]	C_3 [W/v]	C_4 [$W/in. w.g.$]	C_5 [$W/in. w.g.$]	R^2_{adj}
P8A	5.86	0.000895	0.304	-89.3	-31.9	0.908
P8B	-258	-0.00600	3.65	-82.3	0	0.989
P8C	-363	-0.00880	5.18	-145	0	0.990
P12A	-631	-0.0039	6.22	-142	0	0.956
P12B	-403	-0.00515	5.15	-128.7	0	0.996
P12C	-622	-0.0159	9.48	-638	0	0.923

The R^2_{adj} statistics for all of the models were high (above 0.9) indicating a high correlation of power with respect to voltage, downstream static pressure, and the rake pressure for terminal unit P8A. The terminal unit with the lowest R^2 value was P8A, which was the unit that had the greatest air leakage. Like the airflow model, this leakage was a variable that the power model did not capture well.

CHAPTER VI

RESULTS AND MODELS FOR SERIES FAN POWERED VAV

TERMINAL UNITS

Experimental data were collected for six series fan powered VAV terminal units. This section discusses the results for these units. Airflow and power models were developed for each series unit as a function of several variables that influenced the performance of the terminal unit fans.

The goal during model development was to create generic models for the series terminal units. The models maintained the same forms but used different coefficients for the different sizes and manufacturers.

A separate section is provided for the airflow and power models. Each section presents the method used to develop the models. A number of variables were examined to determine which were statistically significant. Each section includes an analysis of the data, the final models for each terminal unit, and a discussion regarding the statistical significance of the models.

During the testing of series terminal unit S8A, some irregular pressure pulsations were observed downstream of the terminal unit fan. There was a concern that these pulsations would adversely affect the data and the models. An investigation into the cause of these pulsations was conducted and the results are discussed in Appendix B.

6.1 SERIES TERMINAL UNIT AIRFLOW MODEL

This model quantified the airflow delivered by the series terminal unit fan. Like the parallel terminal units, the fans on the series units used centrifugal, forward-curved style fans. These fans were expected to follow typical fan curves and fan laws (ASHRAE 2001). The SCR voltage, upstream static pressure, and rake sensor pressure

were all variables that would be expected to influence the capacity of the terminal unit fan.

SCR setting was a variable in the model that had to be quantified. Each SCR setting corresponded to a different fan speed. A fan curve would be applied to the fan for each of these speeds. Each fan curve could then be used to find airflow as a function of the internal box pressure. Developing these fan curves required characterizing the relationship between the SCR setting and the fan speed.

After this relationship was established, the other factors that were considered in the modeling of the air output of the fan were the pressures immediately upstream and downstream of the fan. Because the downstream static pressure was maintained at the same value for all tests, it was eliminated as an explanatory variable for the model. Another pressure that could influence the airflow output of the unit fan would be the pressure inside the terminal unit, immediately upstream of the fan, P_{unit} (Figure 6-1).

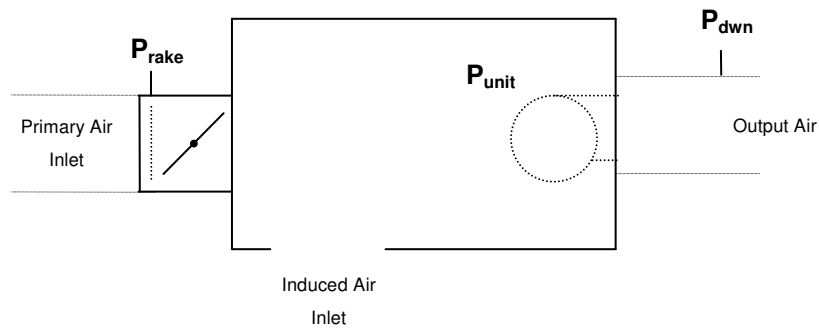


Figure 6-1: Typical Series VAV Fan Powered Terminal Unit

During normal operation, some air was always induced into the terminal unit. Thus, the static pressure within the series terminal unit was always sub-atmospheric but the exact pressure was not measured. In planning for the experiments, there did not appear to be a good way to instrument the terminal unit to measure this pressure accurately. After statistical analysis, it was determined that the pressure that

corresponded to the amount of primary air delivered to the terminal unit, P_{rake} , was a suitable variable to include in the model to estimate the influence of the internal terminal unit static pressure.

The resulting model for predicting the airflow in series terminal units was a function of the SCR voltage and the rake pressure.

6.1.1 Data Analysis

The variable with the strongest influence on fan airflow was the SCR voltage. The relationship between fan airflow and SCR voltage was discussed previously in the results section for the parallel terminal units (section 5.2.1). There was a quadratic relationship between the SCR voltage and fan speed for the parallel terminal units, leading to the assumption of a similar relationship between SCR voltage and airflow. Because the same motors and SCR's were used with the parallel and series terminal units, it was assumed that this relationship would remain the same for the series fans. It would have been preferred to test the series units' fans, to verify this assumption. However, given the nature of the terminal units a testing scheme would not be able to ensure a constant pressure difference across the fan, thus isolating the relationship between fan speed and SCR setting.

After the effect of fan voltage on airflow was determined, the data were analyzed to determine the effect of other variables on the model, such as P_{rake} , and P_{up} . Consistently, P_{rake} appeared to have the strongest influence when F statistics for the model were considered. For example, when an airflow model using V , V^2 , P_{rake} , and P_{up} was regressed for the series terminal unit S8C, the resulting F statistics for P_{rake} and P_{up} were 160 and 15, respectively. Because both F values were greater than 4.0 both variables should be used in the model. However, the model using only V , V^2 , and P_{rake} for the S8C terminal unit obtained an R^2_{adj} value of 0.989. This model was deemed sufficient and in an attempt to maintain model simplicity, the variable P_{up} was not included in the airflow models for the series units.

Five of the six series terminal units had very similar results (Figure 6-2), with terminal unit S12B being the exception. The gentle slopes of the lines indicate that airflow was only slightly dependent on P_{rake} . These results support the premise, found in literature (Alexander and Int-Hout 1998), that variations of upstream duct pressure, primary airflow, and damper position have little effect on the pressure inside a series terminal unit, resulting in fairly constant airflow. After a series terminal unit has been balanced for airflow, the air output of the series terminal unit should be relatively constant despite changes in the upstream conditions. The results from all the series units are presented in Appendix A.

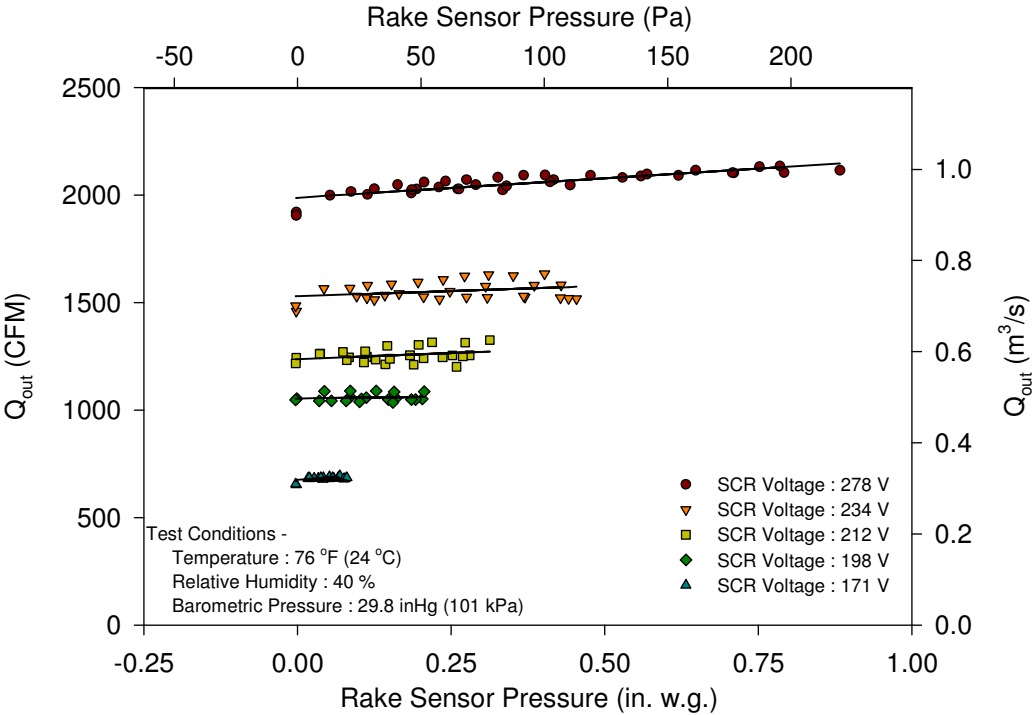


Figure 6-2: Fan Airflow for Series Terminal Unit S12C

The airflow results from series terminal unit S12B showed much more scatter than the results from the other terminal units (Figure 6-3). One hypothesis for this disparity would be a defective or malfunctioning SCR. The full range of SCR settings

on this unit only resulted in a difference of 30 V, as compared to the other terminal unit SCR's that had a difference of more than 100 V. Additionally, the scatter in the data for the individual SCR settings prevented a clear distinction to be made in airflow output for the different settings.

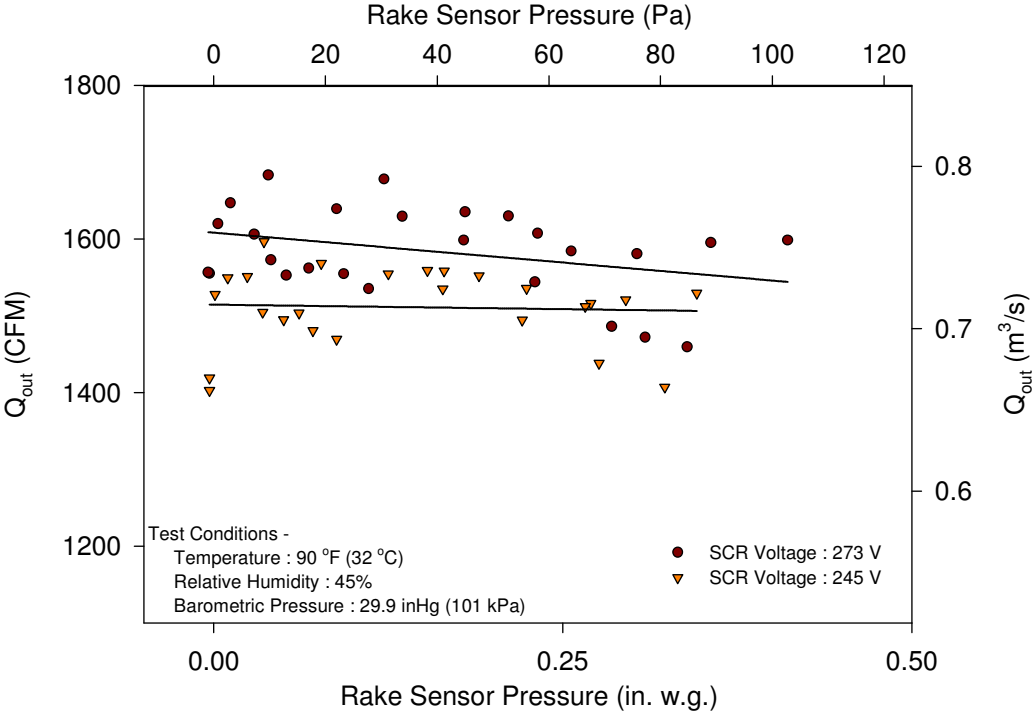


Figure 6-3: Fan Airflow for Series Terminal Unit S12B

Analysis of unit S12B showed that the quadratic relationship between the SCR voltage and fan output was not evident. After initially developing models that included V^2 and V , the F statistics were 0.04 and 0.22, respectively. A model developed using only V resulted in an F statistic of 34. Inclusion of the squared term was never significant. This was possibly due to the SCR not behaving as the ones in the other terminal units that were tested.

6.1.2 Airflow Model

The fan airflow model in series fan terminal units is shown in Eq (6.1). The coefficients for each unit are presented in

Table 6-1.

$$Q_{fan} = C_1 + C_2 \cdot V^2 + C_3 \cdot V + C_4 \cdot P_{rake} \quad (6.1)$$

Table 6-1: Airflow Model Coefficients for Series Terminal Units

Name	C ₁ [CFM]	C ₂ [^{CFM} / ^{V²}]	C ₃ [^{CFM} / ^V]	C ₄ [^{CFM} / ^{in. w.g.}]	R ² _{adj}
S8A	-1776	-0.0228	16.49	0.0036	0.989
S8B	-1705	-0.0254	18.15	-0.0448	0.994
S8C	-1310	-0.0183	13.94	0.0677	0.997
S12A	-778.5	0.0091	6.918	0.0394	0.993
S12C	-1903	-0.0105	16.78	0.0812	0.990

Eq. (6.2) is the model to characterize series terminal unit S12B, which was presumed to have a faulty or malfunctioning SCR. In this model, V captures the small effect that SCR setting has on the airflow output. P_{up} and P_{rake} were both included in this model, because their F values in the model were 88 and 83. Table 6-2 provides the coefficients for the model of this terminal unit.

$$Q_{fan} = C_5 + C_6 \cdot V + C_7 \cdot P_{up} + C_8 \cdot P_{rake} \quad (6.2)$$

Table 6-2: Airflow Model Coefficients for Series Terminal Unit S12B

Name	C_5 [CFM]	C_6 [$^{CFM}/\sqrt{V}$]	C_7 [$^{CFM}/in. w.g.$]	C_8 [$^{CFM}/in. w.g.$]	R^2_{adj}
S12B	925.7	2.68	-55.8	-293.2	0.688

The R^2_{adj} values equaling 0.99 in five of the six terminal units indicated that the model does a very good job in capturing the variation of fan airflow. The exception was series terminal unit S12B. In this case, it was not possible to develop a model that could adequately describe the response to the airflow variable. The model did not account for 31% of the variation in the data. The hypothesis for the poor results from this terminal unit was that the SCR was malfunctioning.

6.2 SERIES POWER MODEL

This model was developed to quantify the power consumption of a series terminal unit fan. The relationship between power and the fan air output for the series terminal units was similar to the linear response shown in the parallel units. The resulting model to predict power was a function of the SCR voltage and the rake sensor pressure.

6.2.1 Data Analysis

The analysis of the power data for the series terminal units provided similar results to that of the parallel terminal units. As with the parallel units, a linear relationship was observed between the fan airflow and power consumption. However, the graphs for the series units show more scatter than the parallel units do (Figure 6-4). The results for all series terminal units are provided in Appendix A. Due to the approximately linear relationship between power and fan airflow, the model for power used the same descriptive variables as the airflow model.

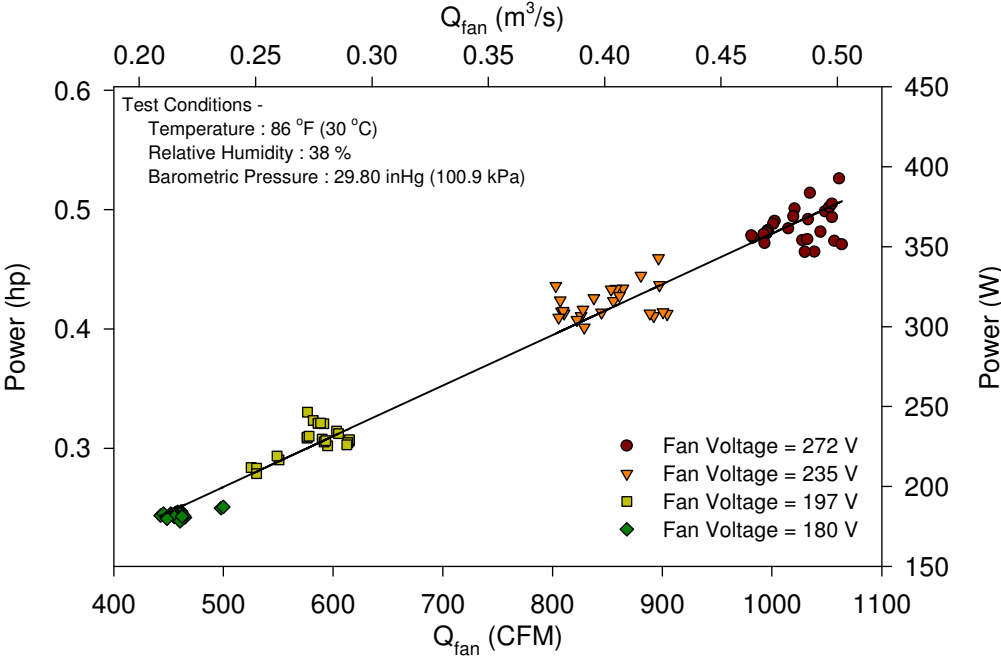


Figure 6-4: Fan Power for Series Terminal Unit S8A

As mentioned in the previous section, terminal unit S12B produced inconsistent data from the others, possibly because of a malfunctioning SCR. Those results provided little distinction in airflow output for the various SCR settings. In the analysis of the power data for this terminal unit (Figure 6-5), there is also little distinction in power for the various SCR settings.

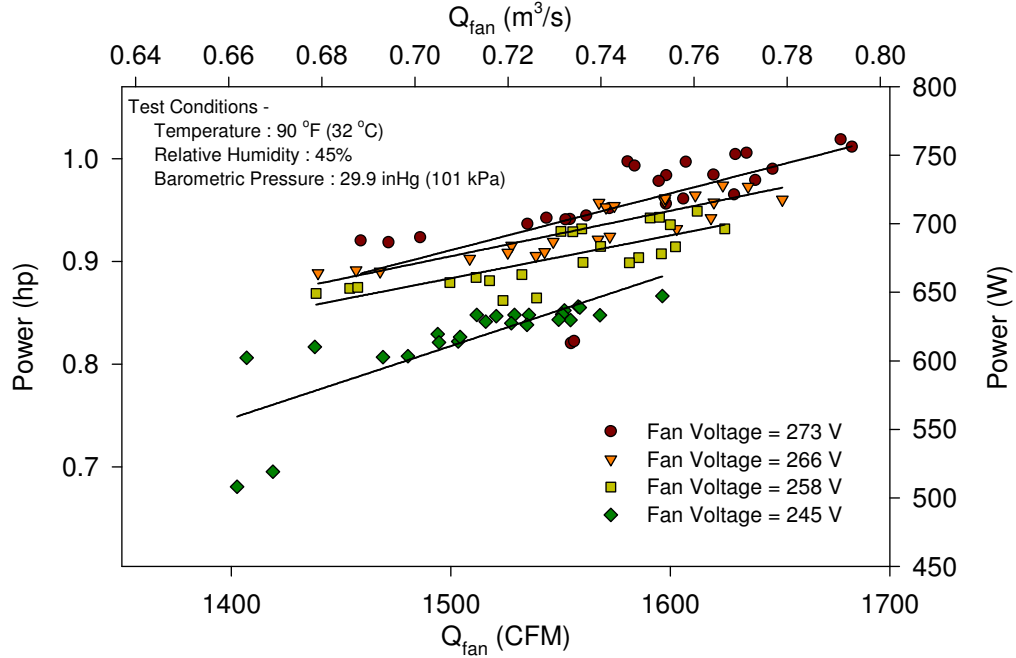


Figure 6-5: Fan Power for Series Terminal Unit S12B

6.2.2 Power Model

The fan power model for series fan terminal units, Eq (6.3), was a function of the SCR voltage and the rake pressure. The coefficients for the various sizes and groups are presented in Table 6-3.

$$Power_{fan} = C_1 + C_2 \cdot V^2 + C_3 \cdot V + C_4 \cdot P_{rake} \quad (6.3)$$

Table 6-3: Model Coefficients for Series Fan Power Model

Name	C₁[W]	C₂[^W/v²]	C₃[^W/v]	C₄[^W/in. w.g.]	R²_{adj}
S8A	-732.7	-0.0114	7.13	-2.12	0.989
S8B	-595.7	-0.0111	6.96	-13.25	0.983
S8C	-455.5	-0.00817	5.32	1.91	0.994
S12A	-269.4	0.00854	1.80	19.05	0.997
S12B	125.9	0.00534	0.736	-16.36	0.870
S12C	-917.0	-0.0129	9.86	97.73	0.990

Comparison of the R^2_{adj} statistics for each model shows that these models account for over 98% of the variation in power for five of the six fans. The lowest R^2_{adj} value of 0.870 was for the series S12B terminal unit, which also had the lowest R^2_{adj} for the airflow model. These model deficiencies were assumed to be due to the malfunctioning SCR on the terminal unit.

CHAPTER VII

SUMMARY AND CONCLUSIONS

VAV systems have proven themselves to be a very effective solution for reducing energy use in air distribution systems of commercial buildings. VAV fan powered terminal units can be either series or parallel configuration. The fan on a series VAV terminal unit runs continuously during the unit operation, while the fan on the parallel terminal unit operates intermittently. The purpose of this research was to characterize the airflow output and power consumption of both series and parallel fan powered terminal units.

An experimental setup was built to obtain data on fan powered terminal units from three different manufacturers and two different sizes. Data were collected for fan power and airflow as a function of several independent variables: the downstream and upstream static pressures, the setting of the SCR, the position of the primary airflow damper, and the amount of primary airflow. The models were derived from the experimental data. The statistical analysis for each model resulted in a single model form for which the different terminal units had different coefficients.

Three different models were developed for the parallel terminal units. A leakage model characterized the leakage along the terminal unit sheet metal seams and backdraft damper when the fan was off. The R^2_{adj} statistics for the leakage model indicated that four of the six terminal units had models that accounted for at least 95% of the variation in the leakage. The other two terminal units had models that accounted for 77% and 86% of the variation in the leakage. A second model characterized the fan airflow. The statistics for the parallel airflow model indicated that five of the six units had models that accounted for at least 93% of the variation in fan airflow. The sixth terminal unit appeared to have significant leakage while the fan was on, resulting in a model with an R^2 value of 81%. From the data that was collected, it was not possible to develop a model that could completely capture the effect of the air leakage. The third model for

the parallel terminal units characterized the power consumption of the terminal unit fan. The statistics for the parallel power model showed that all terminal unit models explained at least 91% of the variation in power.

Two models were developed for the series terminal units. The first model characterized the airflow of the terminal unit fan. The R^2_{adj} statistics indicated that the model could account for 99% of the variation in fan output in five of the six terminal units. The sixth unit was found to have a faulty or malfunctioning SCR because there was little variation in the RMS voltages for the various SCR settings. As a result of this faulty device, the airflow model did a very poor job in capturing the variation in the fan airflow, with an R^2 value of only 0.69. The second model characterized the power consumption of the series terminal unit fan. The R^2_{adj} statistics indicated that in five of the units 98% of the variation in power could be accounted for. The sixth unit, with the faulty SCR, had an R^2 value of 0.87.

The construction quality of these terminal units could be an item of concern. These units were obtained from several manufacturers and in different sizes in an effort to get a 'snapshot' of units typically installed in the field. However, this sample of twelve terminal units resulted in two (P8A and S12B) that would not meet system design requirements. There is potential for large energy costs in buildings simply from terminal units malfunctioning. For example, in unit P8A the air leakage from parallel terminal units can be interpreted as lost energy to the plenum space. This leakage can also result in control issues because the terminal unit controller adjusts the primary air damper position in order to provide a certain quantity of primary air, depending on the thermostat control signal. However, if a portion of this primary air is not being delivered to the space containing the thermostat, there is potential for control instability.

The leakage from the other terminal units when the terminal unit fan was off was strongly dependent upon the value of the downstream static pressure. Therefore, at a certain downstream static pressure the unit would leak the same amount of air regardless of the amount of primary being delivered to the unit. At lower primary air flow rates the amount of leakage averaged between 7 and 10 % of the primary airflow. Since this

leakage is the average from all of the parallel terminal units tested, it can be expected that the units installed in the field will maintain similar characteristics.

From the high R^2 values, it was concluded that these empirical models adequately characterize fan powered terminal units. Cases in which the models were not able to account for at least 90% of the variation in data was always due to what appeared to be an unanticipated defect in the unit.

There are several ways in which future work can supplement this research. These models can allow for the development of a model for an entire VAV system that will ultimately result in an energy comparison of systems of the two styles of terminal unit. In developing this model, the analyst will need to ‘balance’ the terminal units in the model. He will assign a specific SCR voltage to each terminal unit to set the fan airflow. For the calculations for all simulations, these voltages will remain the same. The other variables in the VAV terminal unit models can easily be applied from a simulation program. The downstream and upstream static pressures will be applied from the simulation calculations. For each step-iteration, most simulations calculate the primary airflow required to meet the space load. The rake pressure can be calculated using these primary airflow values and the table in Appendix C.

When using these models as a tool to predict performance, it is important to note that extrapolation of data points outside the range of experimentally determined values is not recommended. The response of the dependent variables, airflow and power, was only statistically determined within the ranges of independent variables as specified in Table 4-1.

There is another area in which future work can supplement this research. After completing the analysis of the data for parallel terminal unit P8A, it became apparent that there is a need to quantify the leakage experimentally. By using another airflow measuring means, either another airflow chamber or pitot tubes, at the induced air port the volumetric balance can be properly applied. This will allow for a determination of the air leakage and the fan airflow while the fan is on. This setup would also allow for a

verification of the assumption made on the other parallel terminal units, that air leakage was negligible.

REFERENCES

- AMCA. 1999. *ANSI/AMCA Standard 210-99, Laboratory Methods of Testing Fans for Aerodynamic Performance Rating*. Arlington Heights, IL: Air Movement and Control Association.
- Alexander, J. and D. Int-Hout. 1998. Assuring zone IAQ. White paper. Titus. Retrieved Sept. 15, 2005. http://www.titus-hvac.com/tech_papers.asp.
- Ardehali, M.M. and T.F. Smith. 1996. Evaluation of variable volume and temperature HVAC system for commercial and residential buildings. *Energy Conversion Management* 37(9): 1469-1479.
- ASHRAE. 1996. *ANSI/ASHRAE Standard 130, Methods of Testing for Rating Ducted Air Terminal Units*. Atlanta: American Society of Heating, Refrigerating and Air-Conditioning Engineers, Inc.
- ASHRAE. 2001. *ASHRAE Fundamentals Handbook*. Atlanta: American Society of Heating, Refrigerating and Air-Conditioning Engineers, Inc.
- ASHRAE. 2004. *ANSI/ASHRAE Standard 90.1-2004, Energy Standard for Buildings Except Low-rise Residential Buildings*. Atlanta: American Society of Heating, Refrigerating and Air-Conditioning Engineers, Inc.
- Chen, S.Y.S., and S.J. Demster. 1996. *Variable Air Volume Systems for Environmental Quality*. New York: McGraw-Hill.
- DOE 2.2: Building Energy Use and Cost Analysis Software. 1998. Lawrence Berkeley National Laboratory at the University of California and James J. Hirsch & Associates.
- Elleson, J.S. 1993. Energy use of fan-powered mixing boxes with cold air distribution. *ASHRAE Transactions* 99(1):1349-1358.
- HASP/ACLD 7101 [Computer Software]. 1971. Tokyo: Japan Building Mechanical Engineers Association.
- Hydeman, M., S. Taylor, and J. Stein. 2003. Advanced variable air volume system design guide. *Integrated Energy Systems: Productivity and Building Science*. 78-79. San Francisco: California Energy Commission.

- Inoue, U. and T. Matsumoto. 1979. A study on energy savings with variable air volume systems by simulation and field measurement. *Energy and Buildings* 2:27-36.
- Khoo, I., G.J. Levermore, and K.M. Letherman. 1998. Variable-air-volume terminal units I: steady state models. *Building Services Engineering Research & Technology* 19(3):155-162.
- Kolderup, E., T. Hong, M. Hydeman, S. Taylor, and J. Stein. 2003. Integrated design of large commercial HVAC systems. *Integrated Energy Systems: Productivity and Building Science*. San Francisco: California Energy Commission.
- Montgomery, D.C., E.A. Peck, G.G. Vining. 2001. *Introduction to Linear Regression Analysis: Third Edition*. New York: John Wiley & Sons, Inc.
- Mickey, R.M., O.J. Dunn, V.A. Clark. 2004. *Applied Statistics: Analysis of Variance and Regression*. Hoboken, NJ: John Wiley & Sons, Inc.
- Neter, J., M.H. Kutner, C.J. Nachtsheim, W. Wasserman. 1996. *Applied Linear Regression Models*. Chicago: Irwin, Inc.
- SAS System for Windows (Pre-Production Version 9.00) [Computer Software]. 2002. Cary, NC: SAS Institute Inc.
- Sekhar, S.C. 1997. A critical evaluation of variable air volume system in hot and humid climates. *Energy and Buildings* 26: 223-232.
- TRACE[®] 600: Load Design and Economics Simulation Program. 1993. La Cross, WI: The Trane Company, American Standard Company.
- U.S. Department of Energy. 1982. *DOE-2 Engineers Manual*, v 2.1A. Berkley, CA: U.S Department of Energy.
- Wendes, H. 1994. *Variable Air Volume Manual*. Lilburn, GA: The Fairmont Press, Inc.

APPENDIX A: EXPERIMENTAL DATA AND ANALYSIS

This appendix provides a complete set of figures showing the experimental data for the parallel and series fan terminal units.

A.1 PARALLEL FAN TERMINAL UNITS

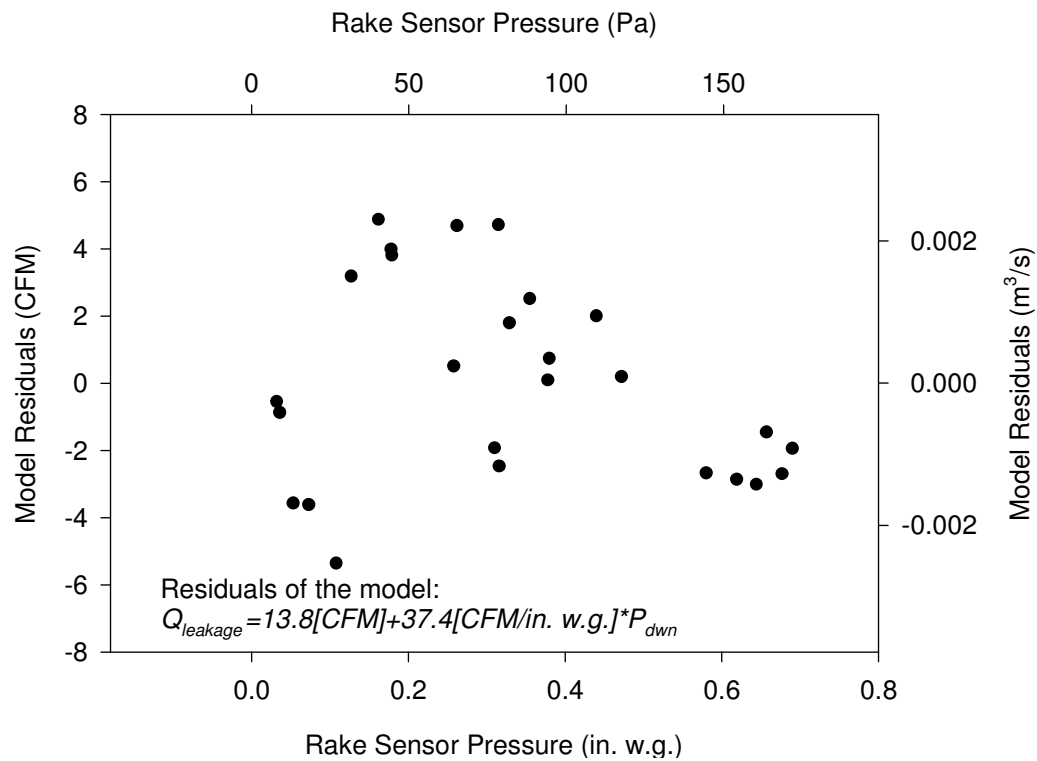


Figure A-1: Residuals Plot for Parallel Terminal Unit P8B

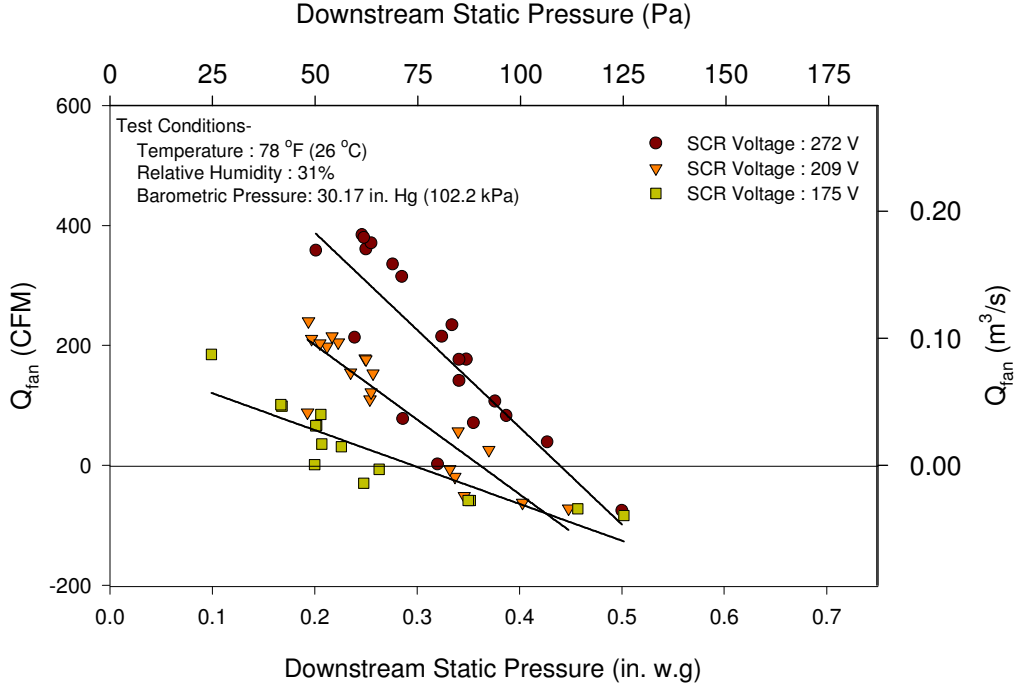


Figure A-2: Fan Airflow for Parallel Terminal Unit P8A

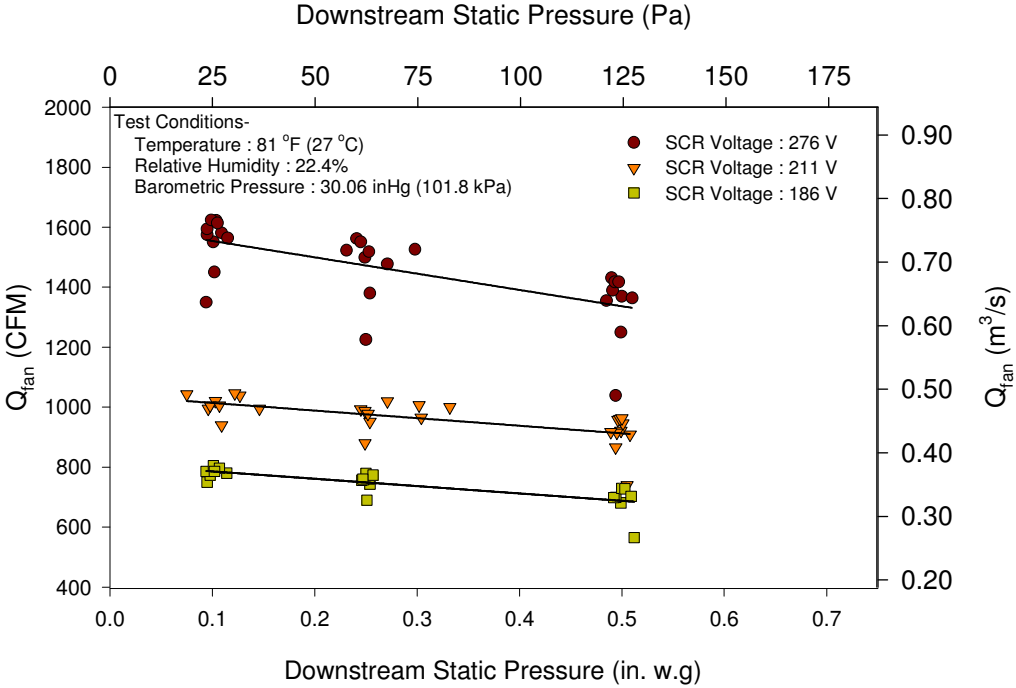


Figure A-3: Fan Airflow for Parallel Terminal Unit P12A

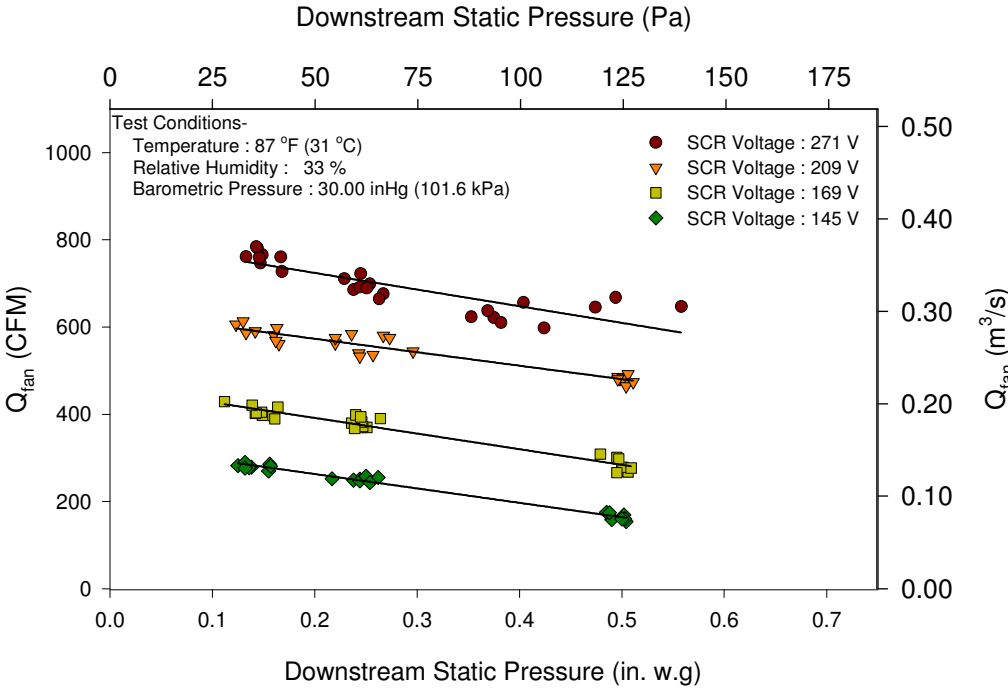


Figure A-4: Fan Airflow for Parallel Terminal Unit P8B

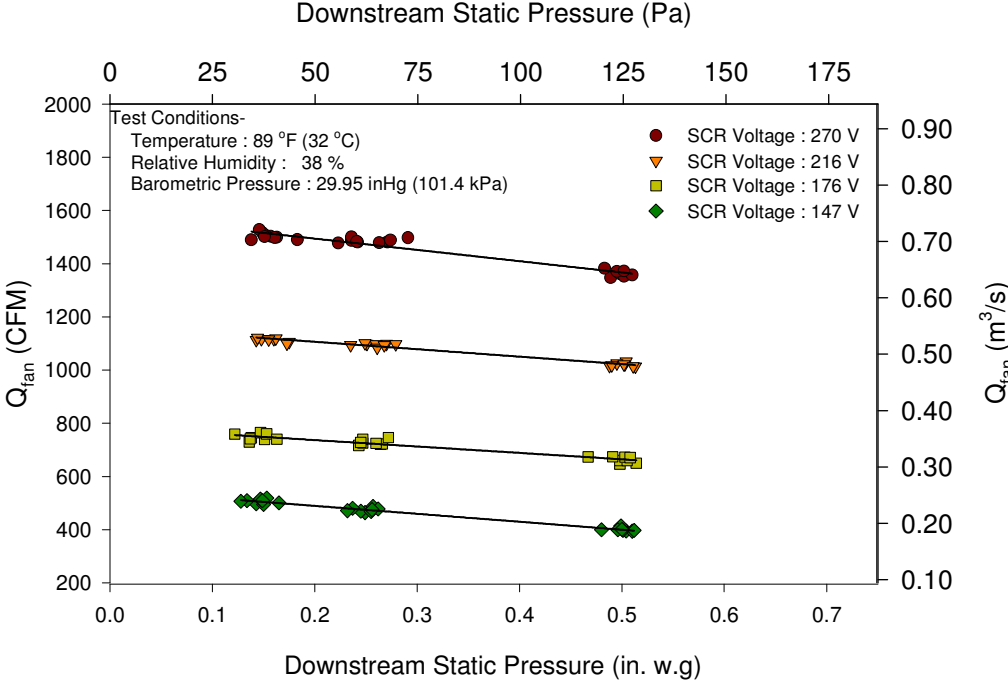


Figure A-5: Fan Airflow for Parallel Terminal Unit P12B

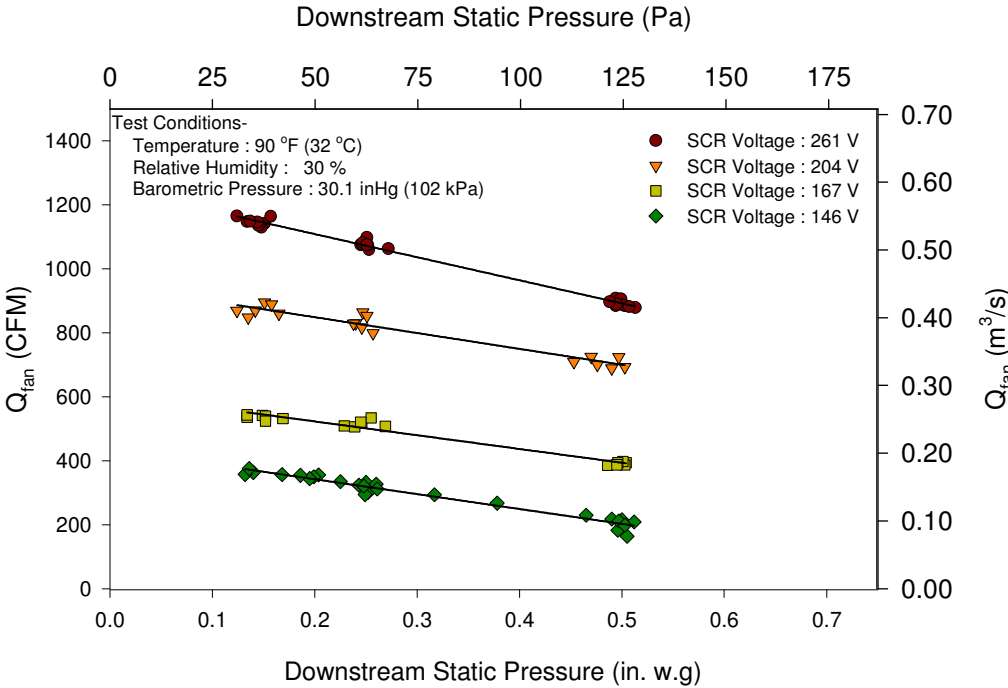


Figure A-6: Fan Airflow for Parallel Terminal Unit P8C

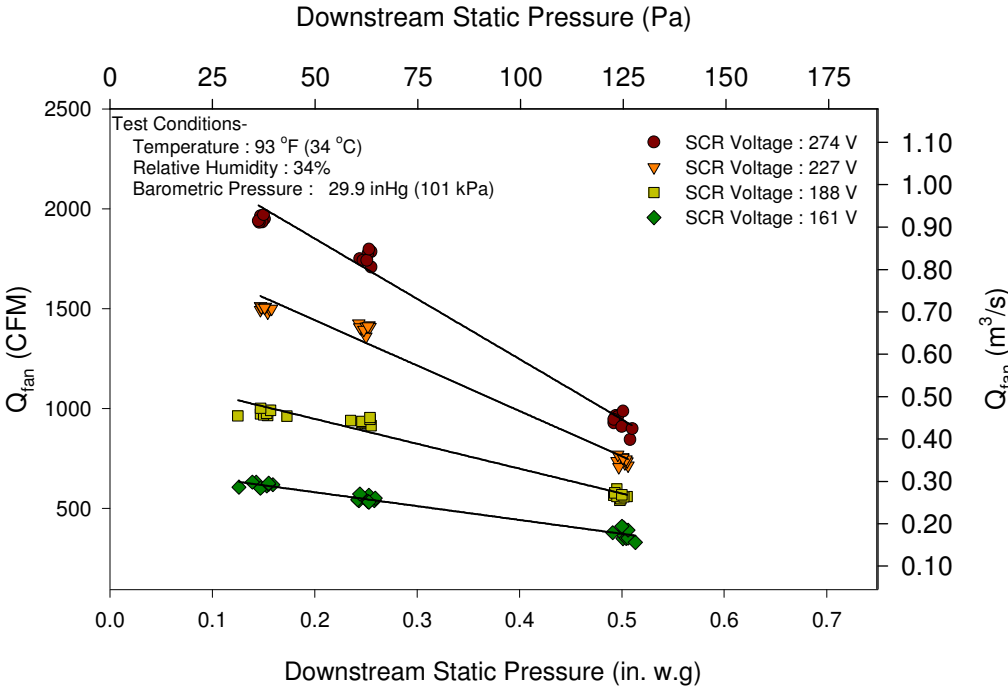


Figure A-7: Fan Airflow for Parallel Terminal Unit P12C

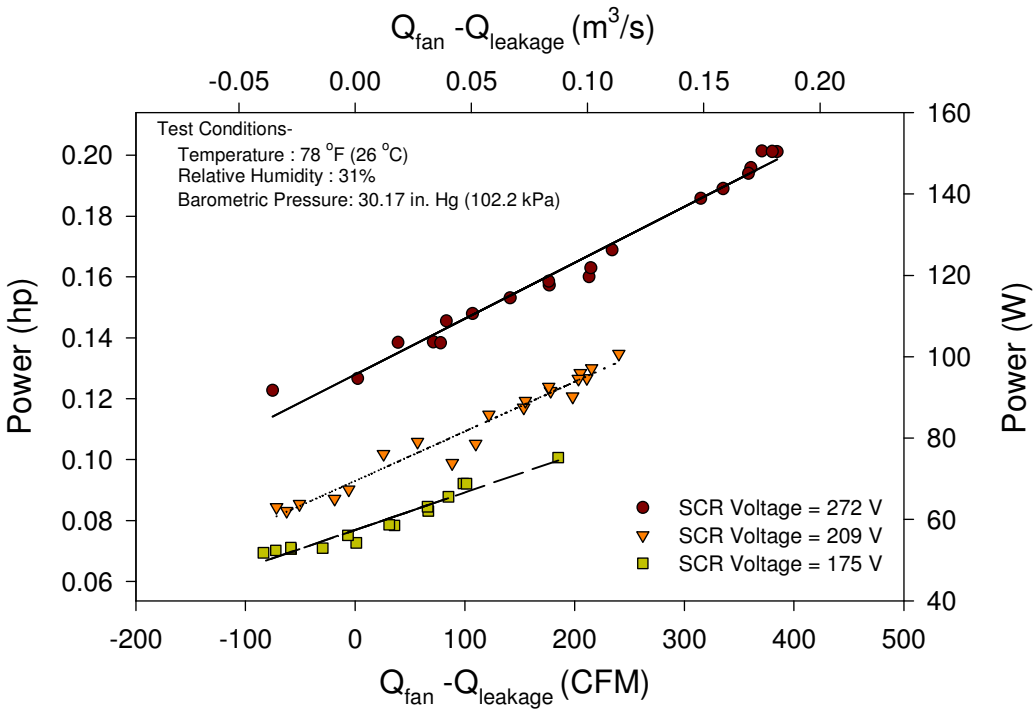


Figure A-8: Fan Power for Parallel Terminal Unit P8A

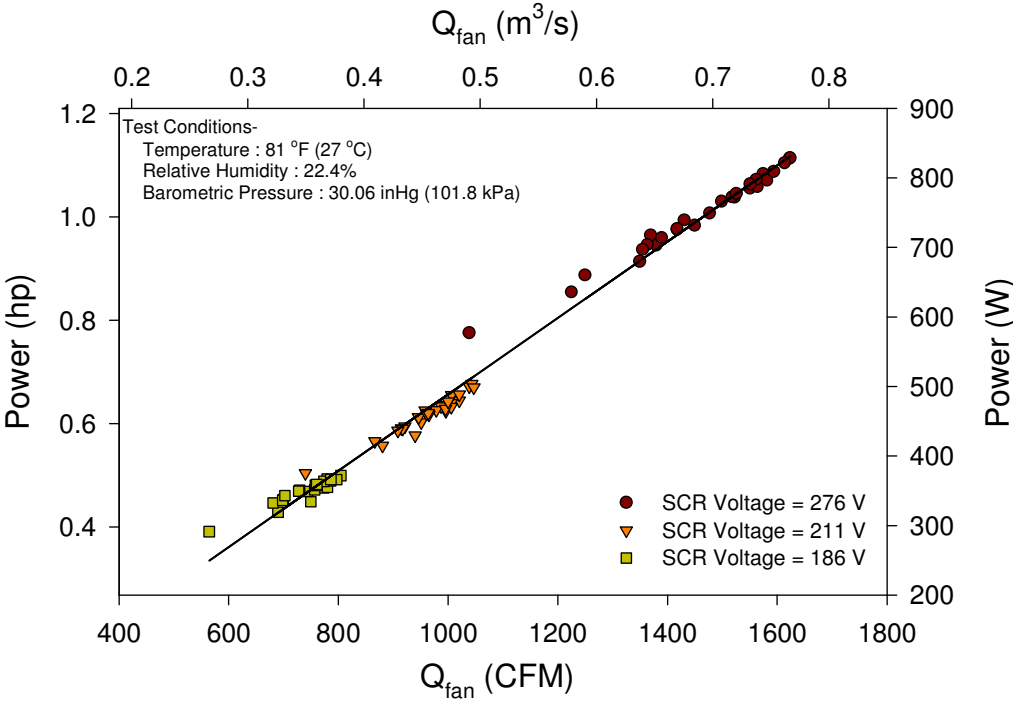


Figure A-9: Fan Power for Parallel Terminal Unit P12A

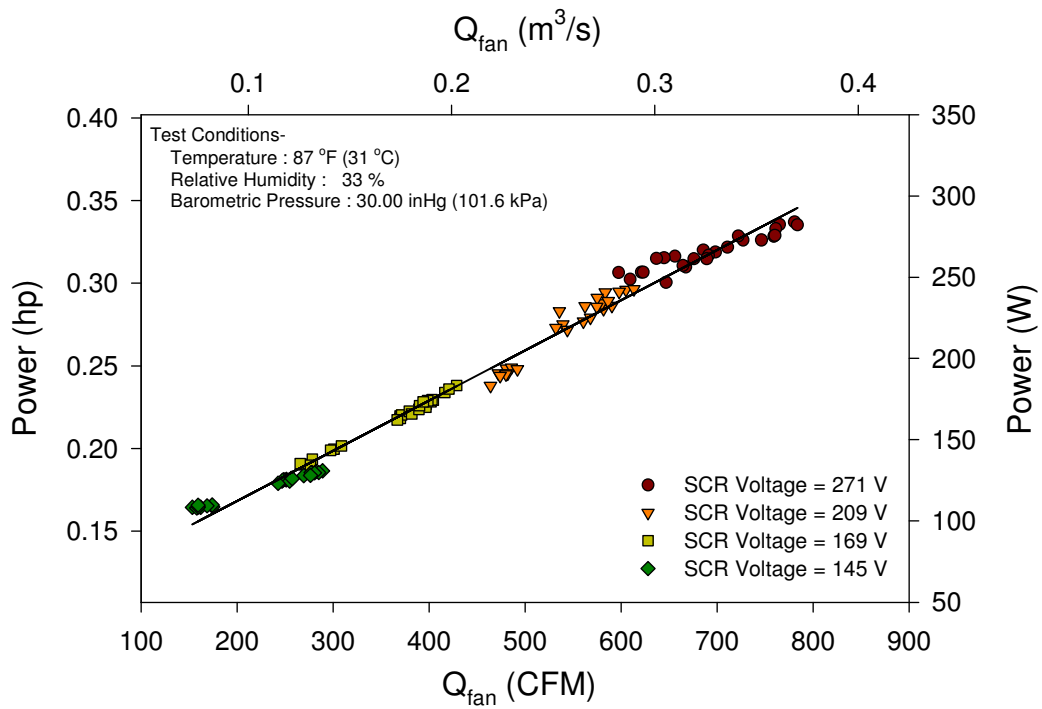


Figure A-10: Fan Power for Parallel Terminal Unit P8B

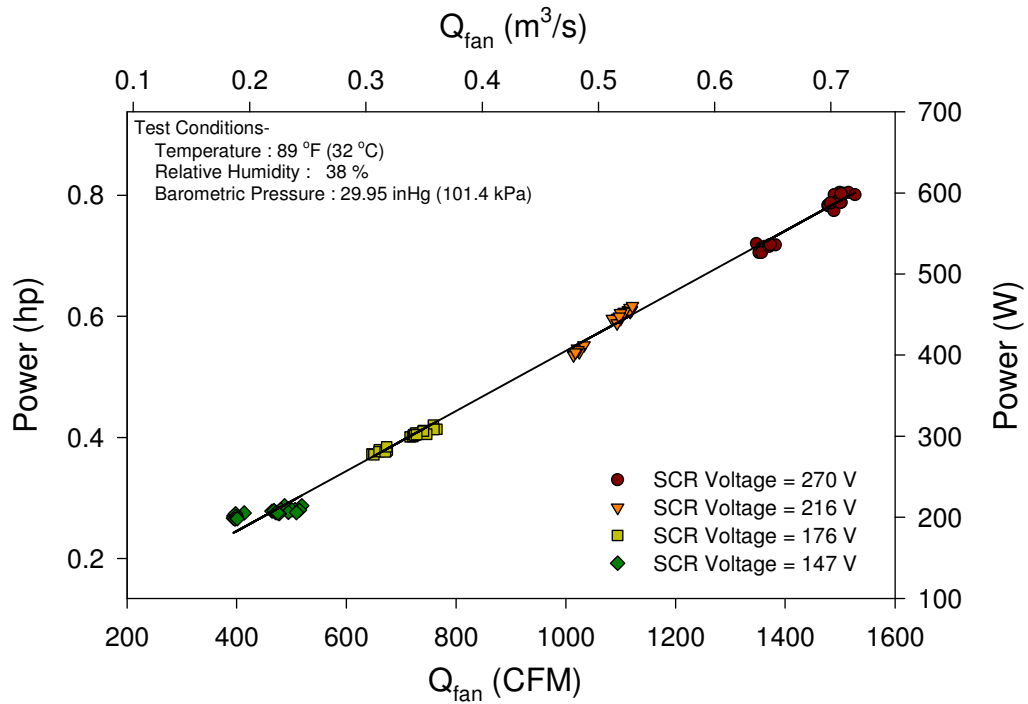


Figure A-11: Fan Power for Parallel Terminal Unit P12B

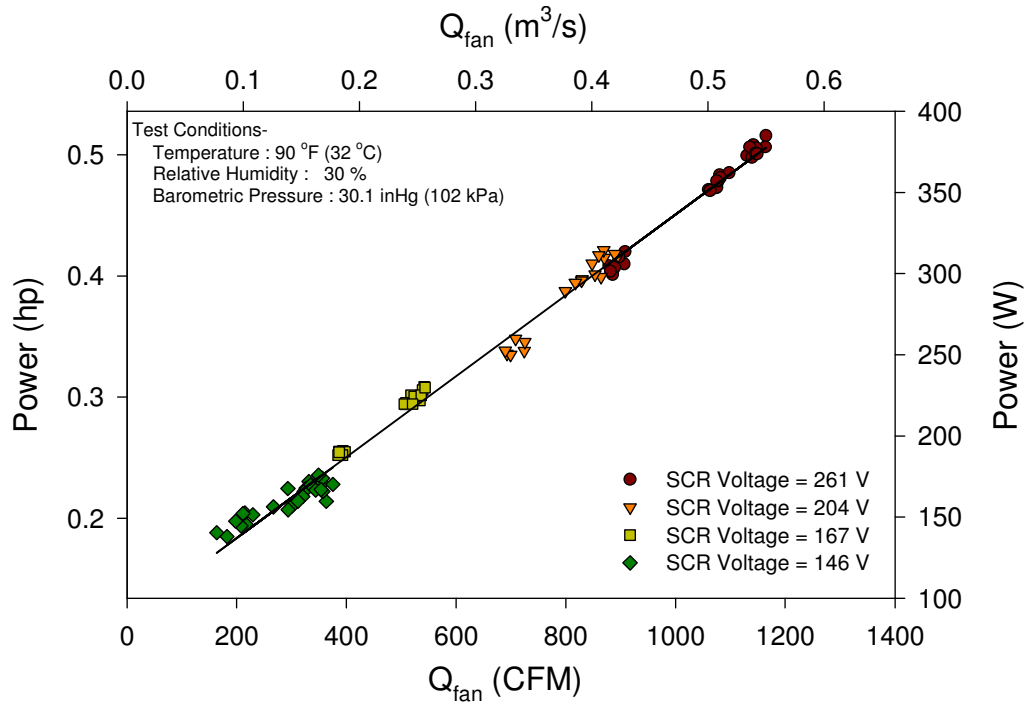


Figure A-12: Fan Power for Parallel Terminal Unit P8C

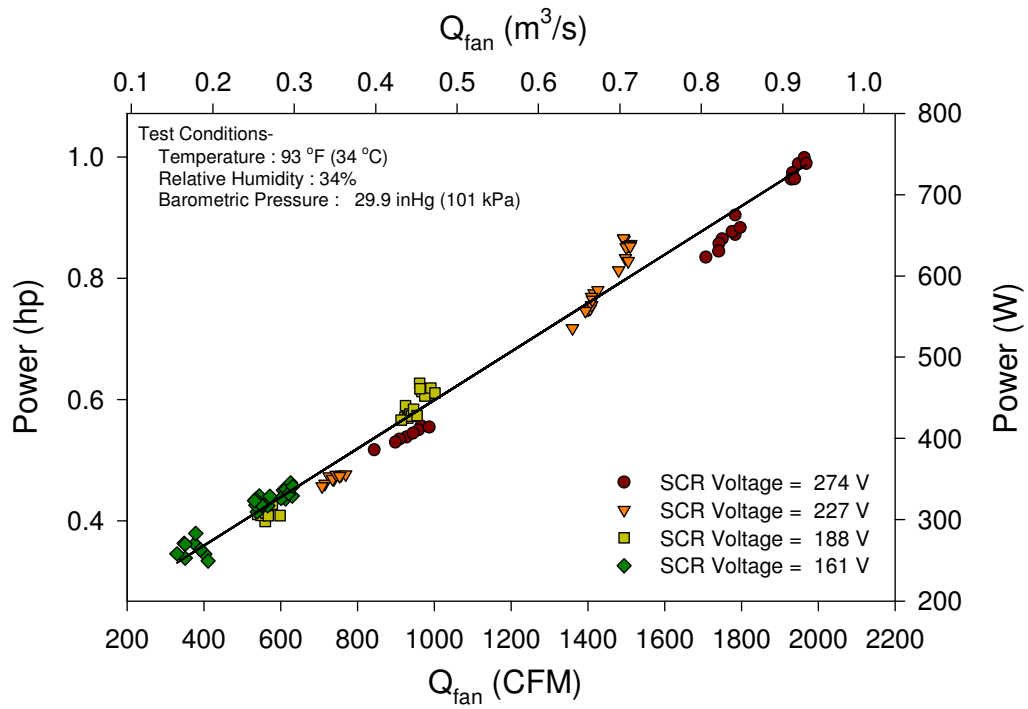


Figure A-13: Fan Power for Parallel Terminal Unit P12C

A.2 SERIES FAN TERMINAL UNITS

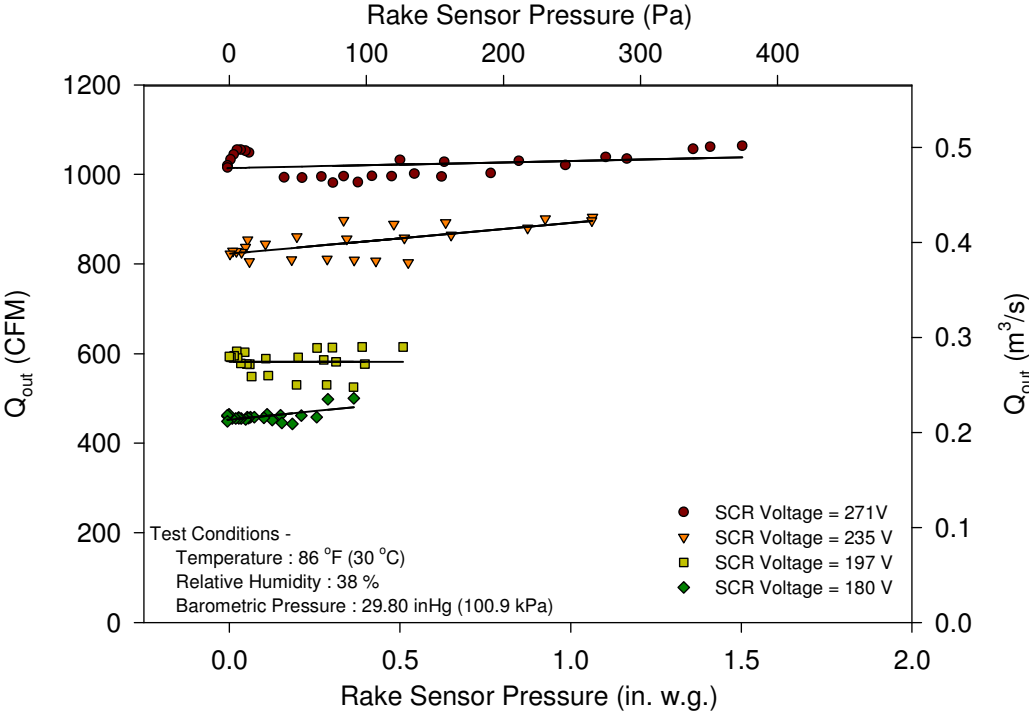


Figure A-14: Fan Airflow for Series Terminal Unit S8A

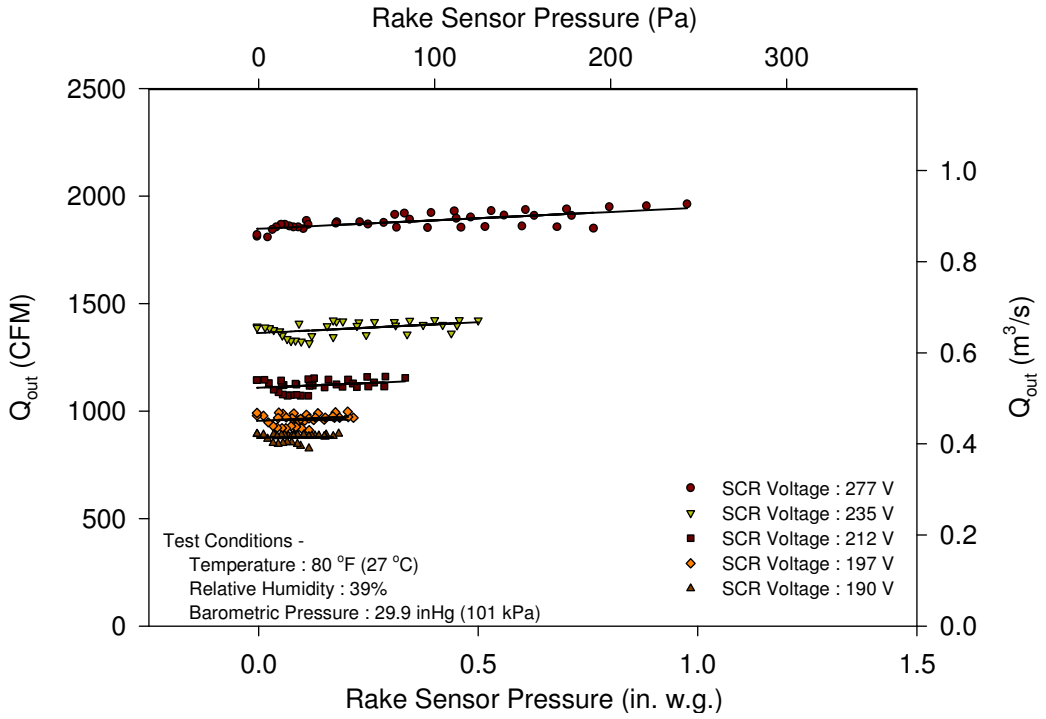


Figure A-15: Fan Airflow for Series Terminal Unit S12A

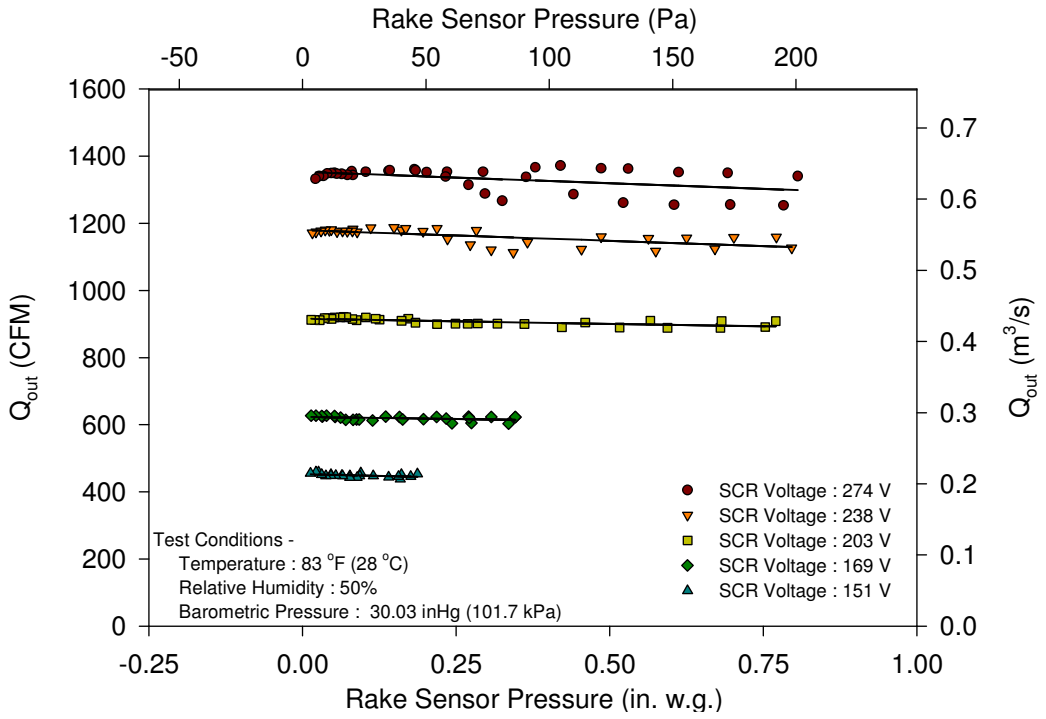


Figure A-16: Fan Airflow for Series Terminal Unit S8B

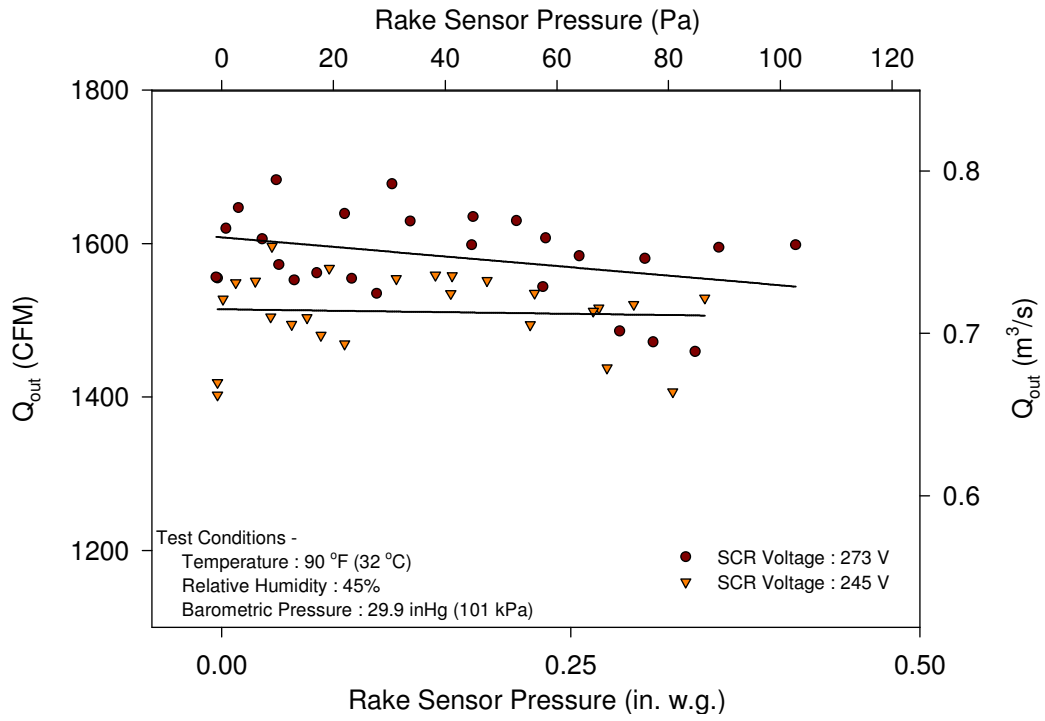


Figure A-17: Fan Airflow for Series Terminal Unit S12B

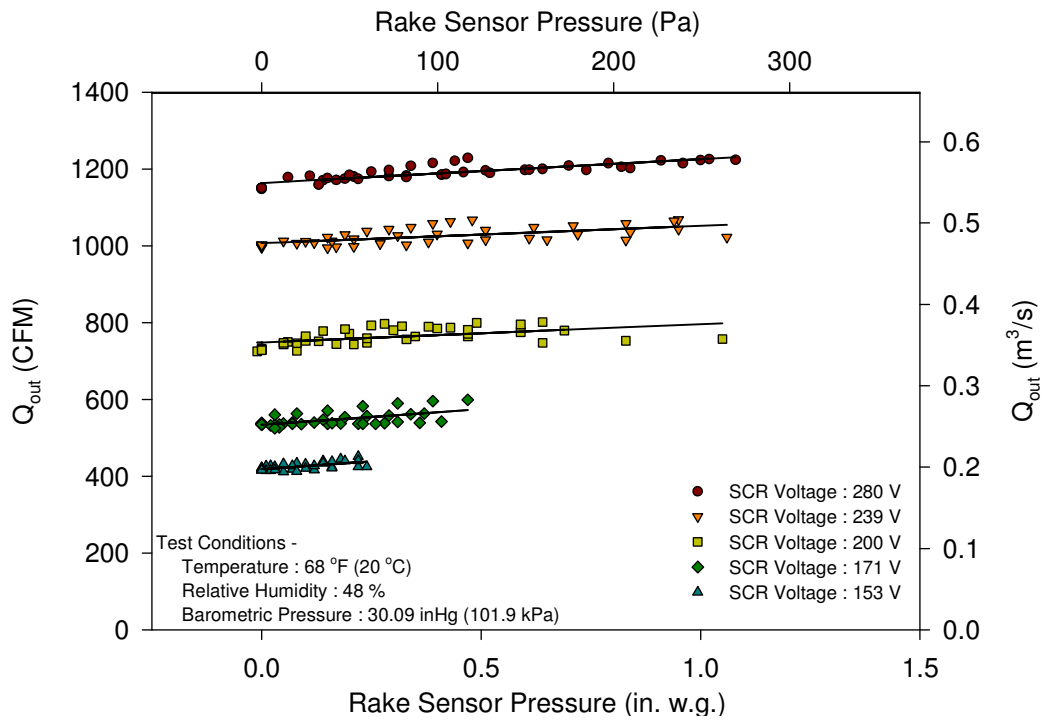


Figure A-18: Fan Airflow for Series Terminal Unit S8C

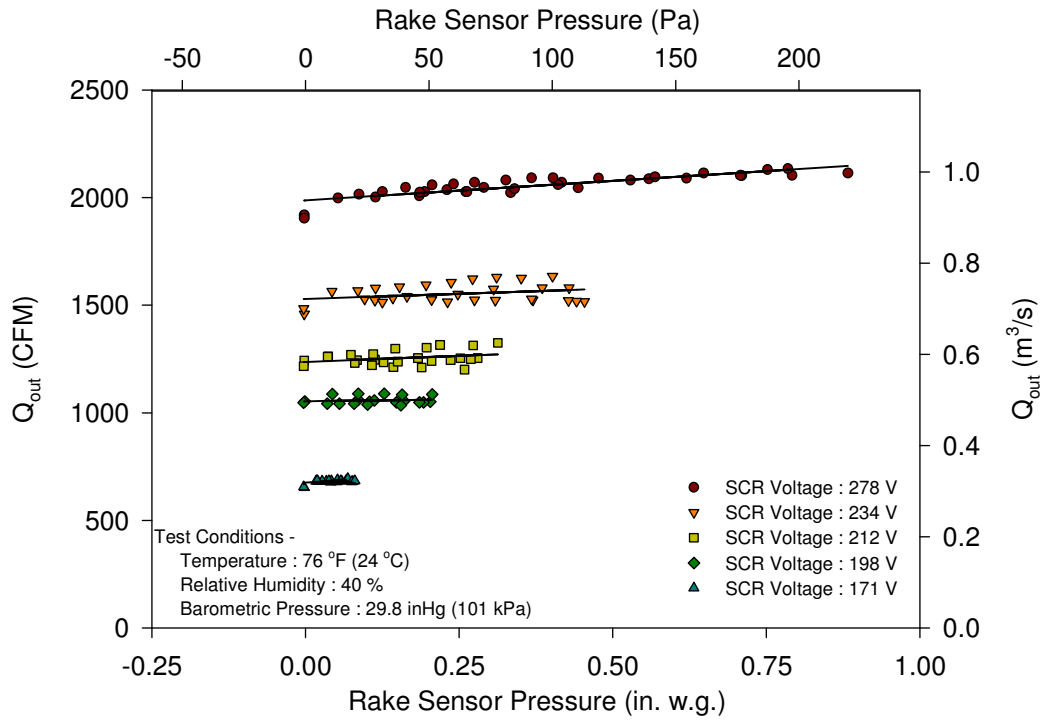


Figure A-19: Fan Airflow for Series Terminal Unit S12C

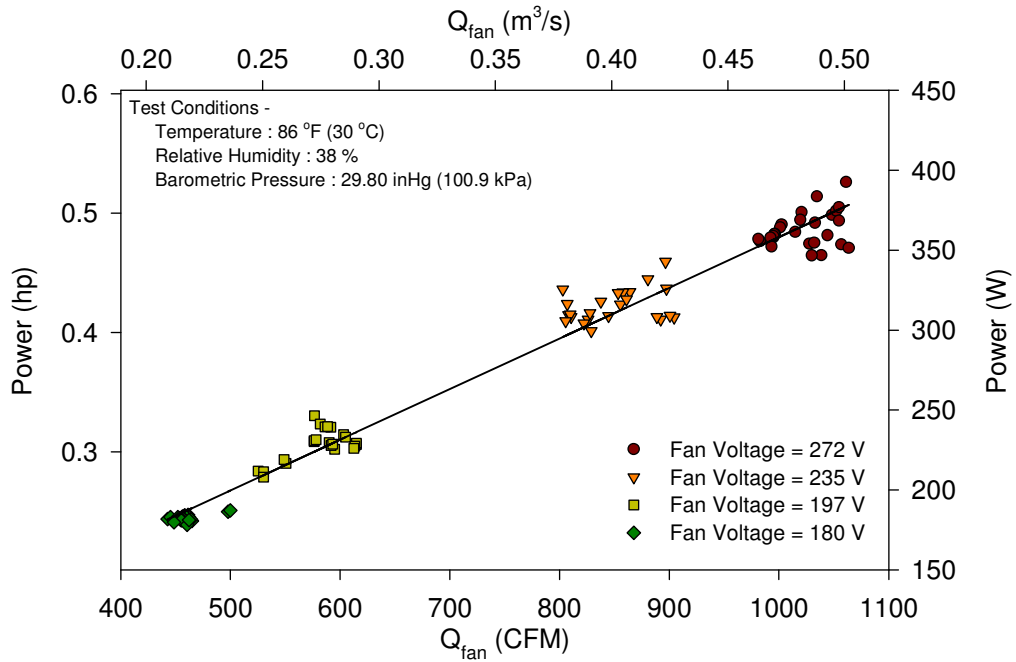


Figure A-20: Fan Power for Series Terminal Unit S8A

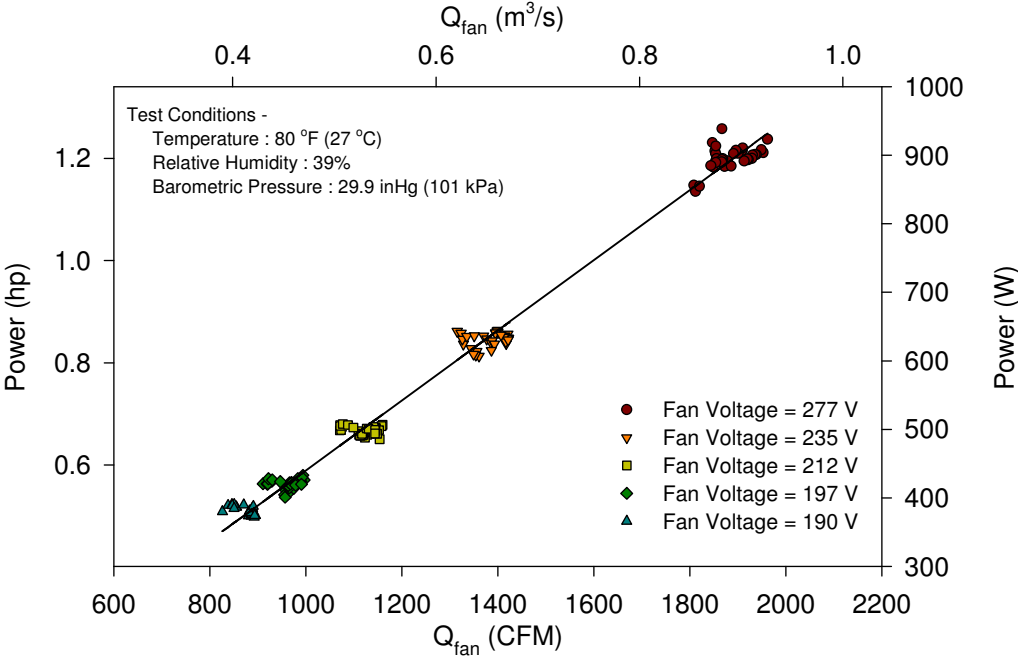


Figure A-21: Fan Power for Series Terminal Unit S12A

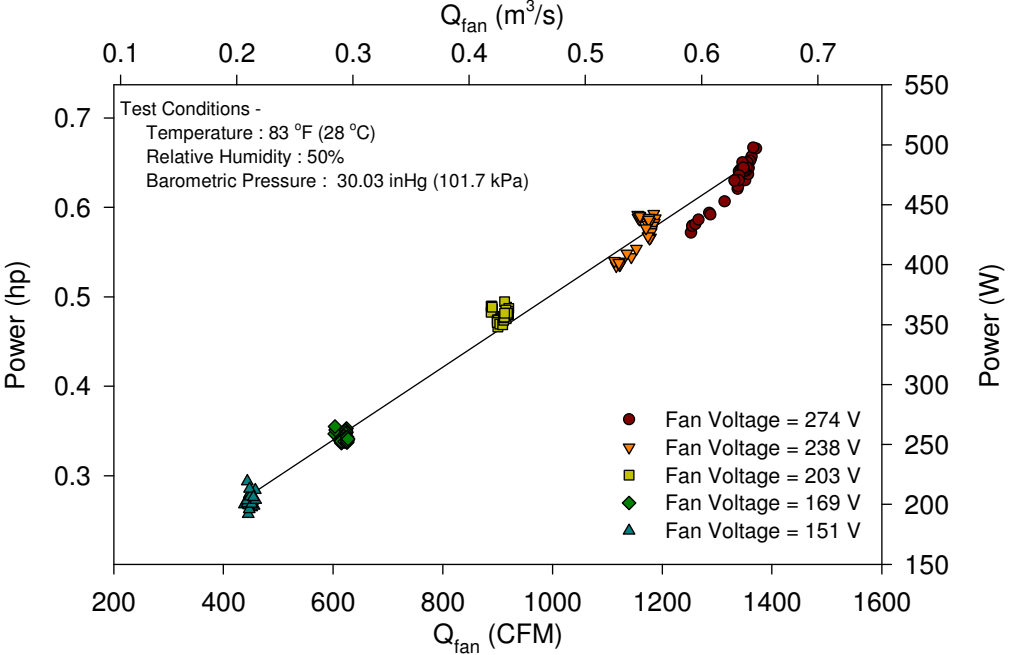


Figure A-22: Fan Power for Series Terminal Unit S8B

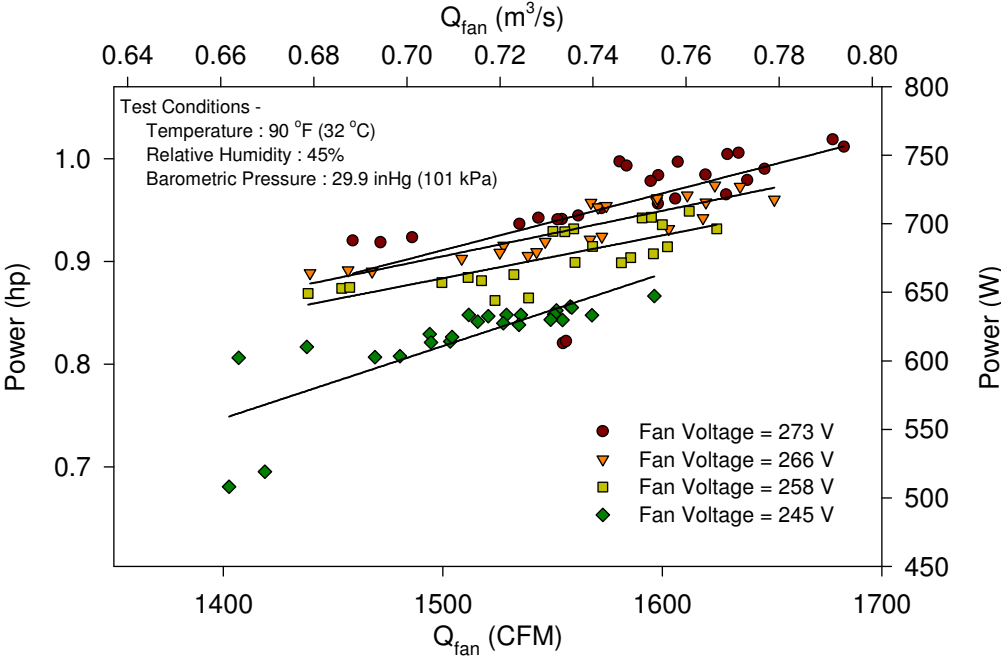


Figure A-23: Fan Power for Series Terminal Unit S12B

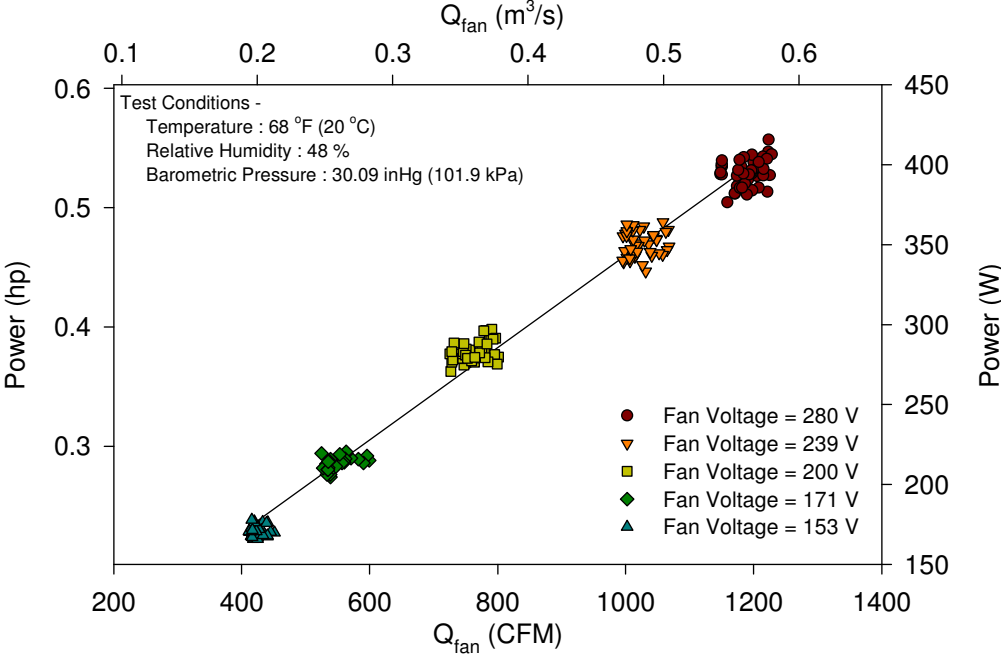


Figure A-24: Fan Power for Series Terminal Unit S8C

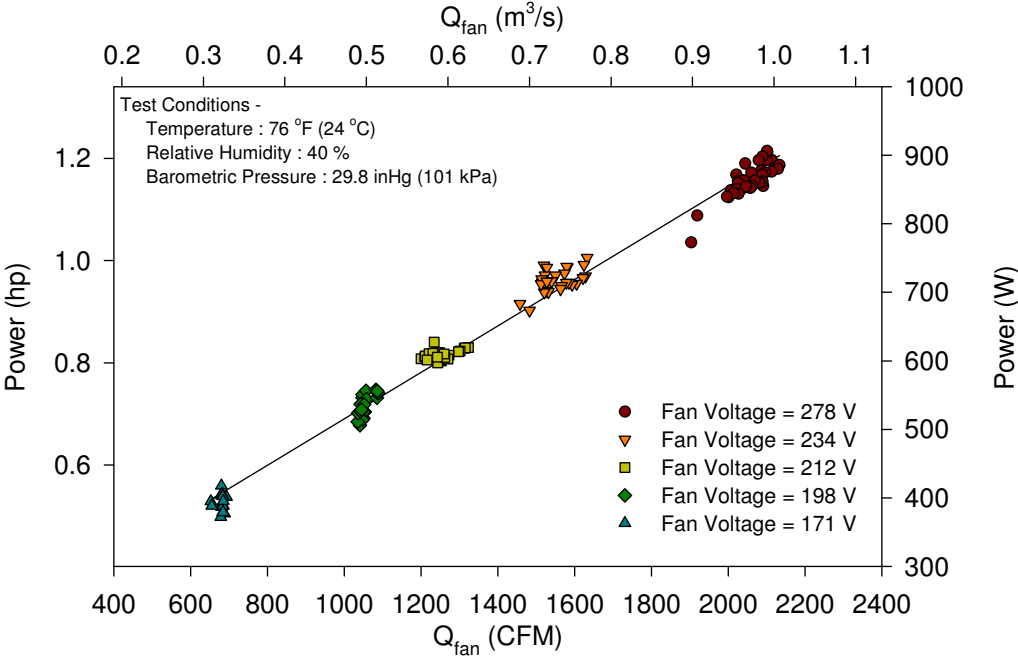


Figure A-25: Fan Power for Series Terminal Unit S12C

APPENDIX B: FAN PULSATION PROBLEM

There were some unexpected data obtained when testing the series S8A unit. Appendix B provides the details of what was discovered.

The occurrences were first noticed during some of the tests when adjusting the assist blower to a 0.25 in. w.g. (62 Pa) downstream static pressure. The pressure would approach the desired downstream static pressure and would suddenly jump past it. It would then fluctuate above and below the desired downstream static, quite erratically.

It was discovered that the fluctuations only occurred near the 0.25 in. w.g. (62 Pa) downstream static pressure. At other downstream static pressures, above and below 0.25 in. w.g. (62 Pa), the phenomenon could not be recreated. Other experimental variables, such as damper position, amount of primary airflow, SCR setting, and upstream static pressure were varied to see if they had any effect on the pulsations. After several tests, it was concluded that the only variable that had a significant effect on the pulsations was the downstream static pressure.

For several test runs, data were continuously obtained and saved to capture the time-variance of this pressure. Figure B-1 and Figure B-2 provide some of the results from this study. The downstream static pressure fluctuated from 0.2 in. w.g. (50 Pa) to 0.27 in. w.g. (67 Pa), at what seemed to be random intervals (Figure B-1). Figure B-2 shows the results from a tachometer that was instrumented to the fan motor.

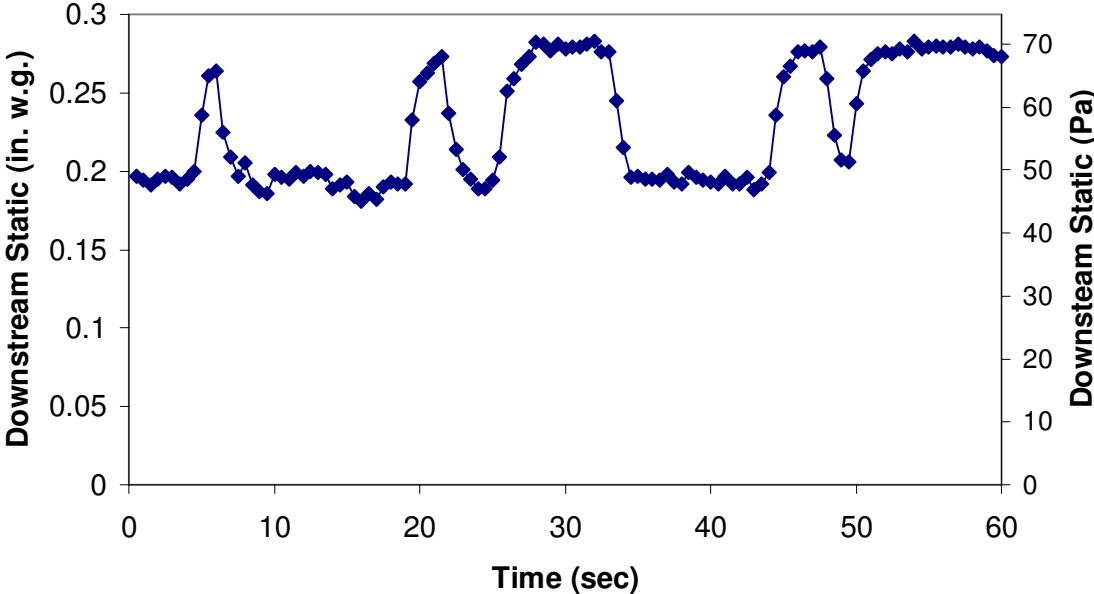


Figure B-1: Downstream Static Pressure During Pressure Fluctuations

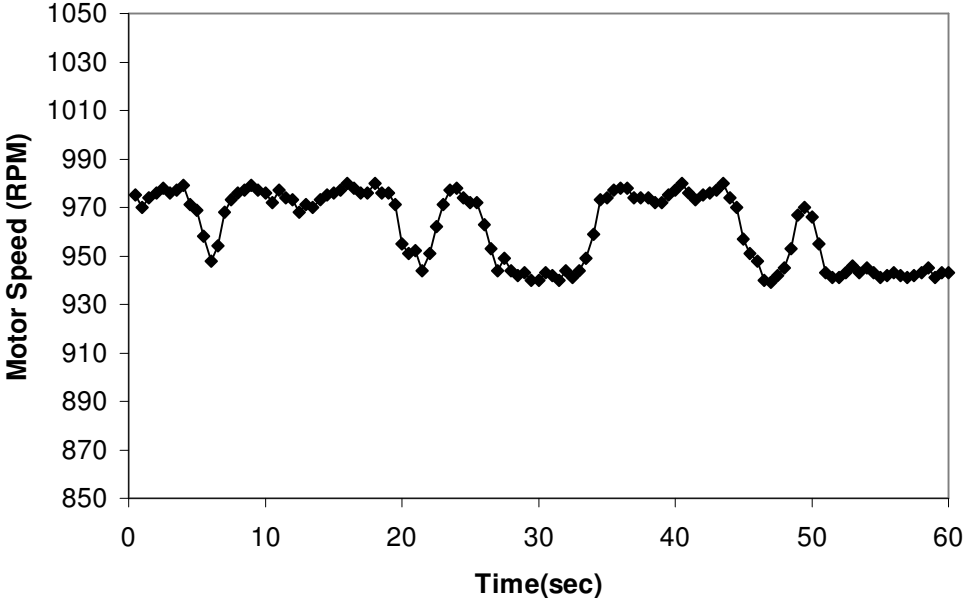


Figure B-2: Fan Motor Speed During Pressure Fluctuations

It was concluded that the fluctuations were caused by the fan motor. A new motor was obtained by the manufacturer and installed in the VAV terminal unit. Initially, this appeared to have solved the problem. However, further investigation found that the fluctuations still occurred but much less severe, being approximately ± 0.01 in w.g. (2.5 Pa). Because of these fluctuations, it was decided that in the data collection for the other terminal units, a longer sampling time of 20 seconds for pressure readings would be required. The averaging would minimize the effects of the fluctuations.

APPENDIX C: CONVERSION OF PRIMARY AIR TO RAKE PRESSURE

Each manufacturer claimed that there was a linear relationship between the rake pressure and the amount of primary air entering the terminal unit. The data obtained affirmed that a linear approximation was sufficient (Figure C-1).

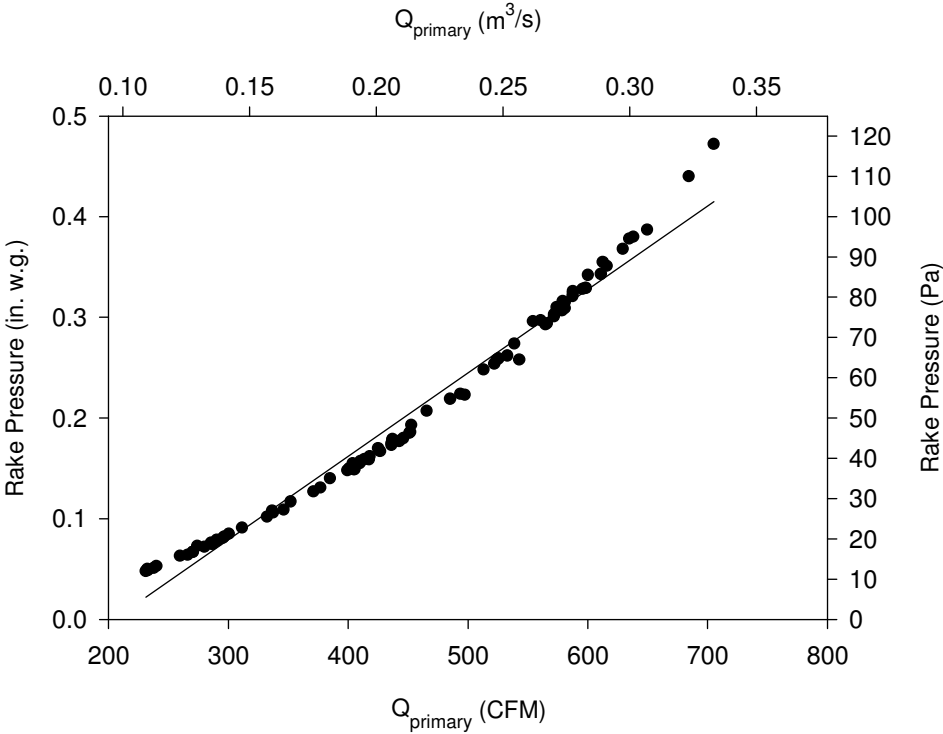


Figure C-1: Linear Approximation between Primary Airflow and Rake Pressure

This linear approximation is presented in Eq. (C.1), with the coefficients for each terminal unit presented in Table C-1.

$$P_{rake} = C_1 + C_2 \cdot Q_{primary} \quad (C.1)$$

Table C-1: Coefficients for Rake Sensor Approximation

Name	C₁[in. w.g.]	C₂[^{in. w.g.}/_{CFM}]	Name	C₁[in. w.g.]	C₂[^{in. w.g.}/_{CFM}]
S8A	-0.204	0.00111	P8A	-0.190	0.00109
S8B	-0.140	0.000776	P8B	-0.130	0.000749
S8C	-0.183	0.000922	P8C	-0.149	0.000816
S12A	-0.162	0.000409	P12A	-0.168	0.000438
S12B	-0.129	0.000306	P12B	-0.0991	0.000277
S12C	-0.158	0.000351	P12C	-0.109	0.000279

APPENDIX D: VERIFICATION ON TEST APPARATUS

The Figure 15 and Figure 12 airflow chambers were connected directly together, without the VAV terminal unit, in order to test the accuracy of the chambers against each other. The results of this test are presented below (Table D-1).

Table D-1: Verification of Test Apparatus

	Test Airflow, CFM (m ³ /s)								
Figure 15	1821 (51.6)	1655 (46.9)	1401 (39.7)	1117 (31.6)	752 (21.3)	642 (18.2)	533 (15.1)	463 (13.1)	280 (7.93)
Figure 12	1808 (51.2)	1601 (45.3)	1330 (37.7)	1065 (30.2)	742 (21.0)	628 (17.8)	513 (14.5)	441 (12.5)	272 (7.70)
Difference	-13 (-0.37)	-54 (-1.53)	-71 (-2.01)	-52 (-1.47)	-10 (-0.28)	-14 (-0.40)	-20 (-0.57)	-22 (-0.62)	-8 (-0.23)
% Diff.	0.7	3.2	5.1	4.7	1.4	2.3	3.9	4.8	3.0

VITA

James C. Furr Jr. was born in Arlington, Texas and graduated from Sam Houston High School in 1999. He graduated with a Bachelor of Science in Mechanical Engineering at Texas A&M University, College Station in December 2003. In January 2004 he enrolled in the Master of Science program in the Department of Mechanical Engineering at Texas A&M University. He received his Master of Science degree in May of 2006. He plans on gaining experience in the industry, and possibly pursuing a PhD in the future.

Mr. Furr can be contacted at Lockheed Martin Aeronautics Company, PO Box 748, Ft. Worth, TX 76101. His email address is james.c.furr@lmco.com